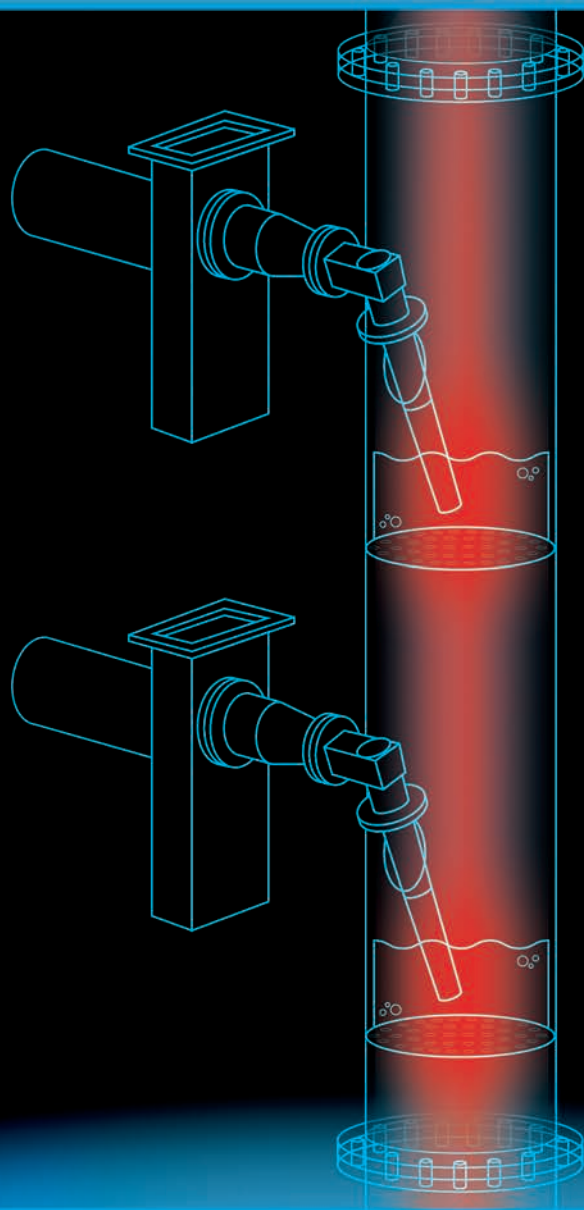


Microwave Enhanced Reactive Distillation



Ernesto Altman Restrepo

Microwave Enhanced Reactive Distillation

Proefschrift

ter verkrijging van de graad van doctor
aan de Technische Universiteit Delft,
op gezag van de Rector Magnificus prof. ir. K.C.A.M. Luyben,
voorzitter van het College voor Promoties,
in het openbaar te verdedigen op maandag 21 november 2011 om 10:00 uur

door

Ernesto ALTMAN RESTREPO

Chemisch ingenieur
geboren te Cali, Colombia

Dit proefschrift is goedgekeurd door de promotor:
Prof. dr. ir. A. I. Stankiewicz

Copromotor:

Dr. ir. G. D. Stefanidis

Samenstelling Promotiecommissie:

Rector Magnificus	Voorzitter
Prof. dr. ir. A. I. Stankiewicz	Technische Universiteit Delft, promotor
Dr. ir. G. D. Stefanidis	Technische Universiteit Delft, copromotor
Prof. dr. Tapio Salmi	Åbo Akademi
Prof. dr. ir. L.A.M. van der Wielen	Technische Universiteit Delft
Prof. dr. ir. A.B. de Haan	Technische Universiteit Eindhoven
Dr. ir. T. van Gerven	Katholieke Universiteit Leuven
Dr. ir. C. Almeida-Rivera	Unilever
Prof. dr. ir. G. J. Witkamp	Technische Universiteit Delft, reservelid

Dit werk is financieel ondersteund door Agentschap NL
(Ministerie van Economische Zaken, Nederland).

ISBN 978-94-6191-100-1

Copyright© 2011 by Ernesto Altman Restrepo, Delft

All rights reserved. No part of the material protected by this copyright notice may be reproduced or utilized in any form or by any means, electronic or mechanical, including photocopying, recording or by any information storage and retrieval system, without written permission from the author. An electronic version of this thesis is available at <http://www.library.tudelft.nl>

Published by Ernesto Altman Restrepo, Delft

Lay-out by In Zicht Grafisch Ontwerp, Arnhem, the Netherlands

Printed by Ipskamp Drukkers in the Netherlands

Dedicated with love
to my wife Natalia and
to my children Alejandro and Nicolas

Contents

Summary	11
Samenvatting	13
Part I Introductory Guideline and Data	17
Chapter 1 The Challenge of Microwave-Intensified Chemical Processes: Focus on Reactive Distillation	19
Chapter 2 The Synthesis of <i>n</i> -Propyl Propionate as Case System	41
Chapter 3 Thermo-Physical Data for Reactive Distillation	57
Part II Conventional Activation	77
Chapter 4 Feasibility Analysis Using Residue Curve Mapping in Reactive Distillation	79
Chapter 5 Experimental, Modeling and Simulation of Reactive Distillation	95
Part III Microwave Activation	119
Chapter 6 The Effects of Microwave Irradiation on Molecular Separation	121
Chapter 7 The Effects of Microwave Irradiation on the <i>n</i> -Propyl Propionate Esterification Reaction	139
Part IV Microwave Enhanced Reactive Distillation (MWeRD)	159
Chapter 8 Technology Integration: The Concept of Microwave Enhanced Reactive Distillation (MWeRD)	161
Chapter 9 Overview and Conclusions	175
Curriculum Vitae	187
Publications and Oral Presentations	189
Acknowledgements	191

“The future of humanity is uncertain, even in the most prosperous countries, and the quality of life deteriorates; and yet I believe that what is being discovered about the infinitely large and infinitely small is sufficient to absolve this end of the century and millennium. What a very few are acquiring in knowledge of the physical world will perhaps cause this period not to be judged as a pure return of barbarism.”

Primo Levi

Summary

The application of electromagnetic radiation in form of microwaves (MW) has gathered the attention of the scientific community in recent years. MW used as an alternative energy source for chemical syntheses (microwave chemistry) has been proven to provide clear advantages over conventional heating methods in terms of reaction time, yield and selectivity. Several applications using this technology have been effectively demonstrated in diverse scientific fields. In this thesis, the scope of microwave chemistry was further expanded to a reactive distillation (RD) process with the primary objective to evaluate its use in view of possible process intensification (PI). The ultimate goal was to conceptually address the novel concept of a MW enhanced RD process (MWeRD) based on demonstrated effects in partial processes namely; molecular separation and chemical reaction.

This thesis is divided in four main parts, each of them covering different aspects and experimental work of the research. Part I, comprises Chapters 1, 2 and 3, and presents the introductory guideline, the problem definition and the research questions. The synthesis of *n*-propyl propionate was chosen as case system due to the suitability of this esterification reaction for RD applications. The thermo-physical data required to accurately address RD design and operation, and the dielectric properties relevant for MW dielectric heating were experimentally determined. The thermodynamic behavior of the system was accurately predicted using a fitted UNIQUAC-HOC model, while experimental reaction kinetics data were used to fit parameters of a pseudo-homogenous model. The data presented in these chapters was necessary to develop the concepts in the subsequent parts of the thesis.

Part II of this dissertation comprises Chapters 4 and 5 dealing with the design, modeling, experimentation and simulation of conventional RD. The thermodynamic and kinetic models regressed in the previous part were used to conceptually design and determine feasibility of the conventional RD process using a practical method called Residue Curve Mapping (RCM) in combination with some heuristic rules. Given that the process was feasible, RD experimentation was implemented. Experiments performed in a conventionally heated pilot-scale column (DN-50) equipped with two types of structured packings (Sulzer BX and Katapak-SP 11) are reported. In addition, a non-equilibrium stage model (NEQ model) for the column was used. Model predictions were compared to experimental results showing good accuracy. Theoretical investigations of the most important operating parameters (total feed, molar feed ratio, reflux ratio and heat duty) and their effect on the overall process performance are presented.

Part III of this thesis includes the results of the fundamental research performed using microwave activation. The experimental work was divided in two parts. In the first part comprising Chapter 6, the influence of MW on molecular separation of the binary mixtures composing the quaternary case system is discussed based on experimental results conducted in a custom designed distillation head. Four of the six binary pairs constituting the quaternary case system were studied showing, in some cases, an enhanced separation of the components. Then in Chapter 7, the effects of MW radiation on the case reaction were studied comparing reaction conditions under MW and conventional heating using different homogenous and heterogeneous catalysts. From all the catalysts tested, Zn triflate proved to be more effective under microwave heating producing 40% more ester compared to the conventionally heated experiment.

With the results gathered in Parts II and III, the new concept of a microwave enhanced reactive distillation process is proposed in Part IV. The general benefits and barriers of the technology integration are discussed based on the results of the MW enhanced reaction and separation. The novel concept of a MWeRD process is presented using two different types of MW technology and giving a detailed discussion on hardware, operating conditions and up-scalability of the process. To conclude, an overview of the highlights of the thesis is included, giving recommendations for further research in terms of the fundamental mechanisms of how MW work at a molecular level, the energy efficiency of the proposed concept and other reaction systems that could potentially benefit from MWeRD.

Samenvatting

De laatste jaren is de toepassing van elektromagnetische straling in de vorm van microgolven (MG) een steeds groter onderdeel geworden van wetenschappelijk onderzoek. Het is gebleken dat het gebruik van MG voordelen biedt ten opzichte van conventionele verwarmingsmethoden op het gebied van reactietijd, rendement en selectiviteit. Verscheidene toepassingen op diverse wetenschappelijke terreinen hebben de werking van MG aangetoond. In dit proefschrift wordt het gebruik van MG verder uitgebreid naar de mogelijke toepassing in reactieve distillatie (RD) processen als mogelijk proces intensificatie (PI) concept. Het uiteindelijke doel is om het innovatieve concept van MG toegepast in RD te beschrijven op basis van aangetoonde effecten op de afzonderlijke processen, namelijk moleculaire scheiding en chemische reactie.

Dit proefschrift is onderverdeeld in vier delen, welke elk een afzonderlijk onderdeel van het onderzoek beslaat. Deel I bestaat uit de hoofdstukken 1,2 en 3 waarin het onderzoek wordt geïntroduceerd en de probleemstelling en onderzoeksvragen worden geformuleerd. De synthese van n-propyl propionaat is gebruikt als case-studie systeem vanwege het feit dat verestering reacties zeer geschikt zijn voor RD toepassingen. De benodigde thermo-fysische data voor het ontwerp en werking van het RD proces en de diëlektrische eigenschappen die relevant zijn voor verwarming door middel van MG zijn experimenteel bepaald. De thermodynamica van het systeem is voorspeld met het UNIQUAC-HOC model en de kinetiek van de reactie is beschreven met een pseudohomogeen model waarbij de verscheidene parameters zijn verkregen door regressie van experimentele data. Deze gegevens zijn essentieel voor de ontwikkeling van de concepten in de volgende delen van dit proefschrift.

Deel II van deze thesis bestaat uit de hoofdstukken 4 en 5 en behandelen het ontwerpen, modelleren, experimentatie en simulatie van conventionele RD. De thermodynamische en kinetische modellen uit deel I zijn gebruikt voor een conceptueel ontwerp van een conventioneel RD proces. Hierbij is de 'residue curve map (RCM)' methode in combinatie met heuristische regels gebruikt voor de haalbaarheidsanalyse van het systeem. Deze analyse heeft uitgewezen dat het systeem geschikt is voor RD waarna experimenten zijn uitgevoerd. De experimenten zijn uitgevoerd in een conventioneel verwarmde pilot schaal distillatie kolom (DN-50) uitgerust met twee type gestructureerde pakkingen (Sulzer BX and Katapak-SP11) en een 'non-equilibrium stage' model (NEQ model) is gebruikt om de kolom te modeleren. Het theoretisch model is in staat om de experimentele resultaten nauwkeurig te voorspellen. De meest belangrijke

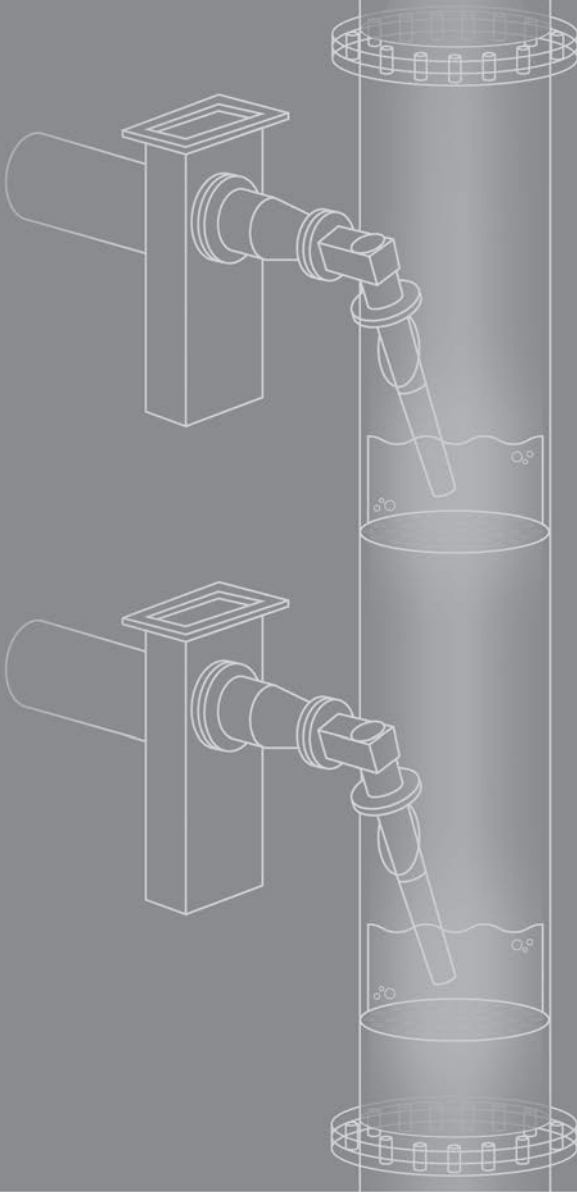
operationele parameters (totale feed, compositie van de feed, reflux ratio en benodigde energie) en hun invloed op de werking van het algehele proces zijn beschreven.

Deel III van dit proefschrift bevat the resultaten van het onderzoek naar de invloed van het gebruik van MG in RD. Het experimentele werk is onderverdeeld in twee delen. In het eerste gedeelte, hoofdstuk 6, wordt de invloed van MG op de moleculaire scheiding van de binaire mengsel beschreven, die voortkomen uit het vier componenten tellende systeem. Deze experimenten zijn uitgevoerd in een speciaal ontworpen distillatie unit. Vervolgens is in hoofdstuk 7 het effect van MG straling op de chemische reactie onderzocht. Hierbij zijn verscheidene homogene en heterogene katalysatoren met elkaar vergeleken waarbij is gekeken naar het verschil tussen conventionele verwarmingsmethoden en het gebruik van MG. Van alle katalysatoren blijkt Zn-triflaat het meest baat te hebben bij het gebruik van MG waarbij 40% meer ester wordt gevormd in vergelijking met conventionele verwarming.

De resultaten van deel II en III vormen de basis voor het nieuwe concept voor 'microwave enhanced reactive distillation process' (MWeRD) dat wordt beschreven in deel IV. De algemene voordelen en problemen van de technologie worden beschreven op basis van de resultaten van de experimenten waarbij MG zijn gebruikt in combinatie met reactie en scheiding. Het nieuwe concept van een MWeRD proces wordt gepresenteerd aan de hand van twee verschillende type MG technologieën waarbij een gedetailleerde bespreking van de hardware, de condities van het proces en de mogelijkheid to opschaling word gegeven. Tot slot is een overzicht van de meest belangrijke punten van het proefschrift opgenomen, zijn aanbevelingen voor verder onderzoek op het gebied van de fundamentele mechanismen hoe MG werken op een moleculaire schaal gegeven, is de energie efficiëntie van de voorgestelde concepten bepaald en worden mogelijke andere reactiesystemen die kunnen profiteren van MWeRD besproken.



Part I



Introductory Guideline and Data

1

The Challenge of Microwave-Intensified Chemical Processes: Focus on Reactive Distillation

“Mother Nature will teach us in a very hard way that money cannot be eaten and gasoline cannot be drunk”

Words of a Cree Indian while talking about the Athabasca oil sands exploitation

1.1 Challenges of the chemical industry in the 21st century¹

Chemicals play an increasingly vital role in 21st century lifestyles, consumption and free market economies. More than 98% of all goods manufactured today undergo some type of chemical processing.¹ Furthermore, the growth and wealth of the world's strongest economies (those based on manufacturing) are linked to the development of their chemical industries. For example, the Netherlands has one of the most dynamic chemical industries in the world, which accounts for approximately 15% of the country's GDP.² ² Huge manufacturing facilities are spread all over the country, and the companies rank among the world's largest. This situation, however, could change drastically in the years to come. An unprecedented amount of resources, particularly energy, will be needed to sustain this trend. In the Netherlands alone, the chemical industry consumes ca. 436 PJ energy per year, representing 15% of the total national energy consumption³, an amount comparable to that consumed by all Dutch households. Besides the considerable use of energy, transformation of raw materials into useful goods by the chemical industry has proven to be highly unproductive, producing almost four times more waste than the volume of goods it produces.⁴

The root of the problem may lie in the fundamentals of the industry itself. Most of the basic technology currently used by the chemical industry was developed in the mid-1900s. The scaling-up of such processes was proportional to market expansion, translating into vast production facilities that required massive capital investments. With the increase in the cost of energy, the industry

¹ In this thesis, the chemical industry refers to the cluster of industries involving chemical manufacturing, petroleum refining, iron and steel manufacturing, pulp and paper manufacturing, pharmaceuticals and cement.

² Including mining, gas and oil based on a GDP of \$770 billion US in 2009.

rushed to improve process efficiency³, which, together with the environmental burden, has been the driving force behind the advancement of the chemical industry for more than 40 years. If it hadn't been for that, developed countries would now be consuming at least two times more fossil fuels and raw materials to produce their current GDPs, at the 1970 level of resource expenditures.⁵ Traditional methods to improve efficiency currently used by the chemical industry include manipulation of processing conditions to optimize plant operation, retrofitting, improved controls, waste reutilization and reduction, heat recovery and improved catalysis. However, the core of the industry has remained practically unchanged, which is the main reason why it is still highly inefficient despite all the above mentioned improvements. If the technologies now used by the chemical industry are compared with those used in a different field of science, for example electronics, it would be as if today's computers would still be using technologies similar to transistors and vacuum tubes.

Two other increasingly important aspects, somewhat related to sustainable development, are risk minimization and safety at chemical plants. Dramatic incidents, with fatal outcomes, have occurred, even in large companies, despite the efforts made and the priority assigned to minimizing risks and improving safety standards. Well-known examples are those of a Nypro chemical plant in Flixborough, UK, in 1974; an AZF plant in Toulouse, France; and the incident that occurred in Bhopal, India, in 1984, considered by many as the biggest chemical disaster in human history, attributed to poor safety methods and the large volumes of deadly chemicals needed due to process inefficiencies. As a result, the chemical industry has a very poor public image, only preceded by the tobacco and nuclear industries. Public awareness about the importance of these issues has only awakened recently as the complex topics of material and energy availability, climate change and sustainability take the industry to the forefront of worldwide debate.

Only recently have numerous cutting-edge technologies with demonstrated feasibility become commercially available for the chemical industry, which could potentially improve production processes. These technologies can be divided in two major groups, one comprising novel equipment such as intensive mixers or intensive heat and mass-transfer devices (e.g. spinning disk reactor, micro-channel heat exchangers),^{6,7} and a second group including process-intensifying methods such as hybrid separations, integration of reaction and separation or heat exchange (e.g. reactive distillation, membrane reactors),^{8,9}

³ The term *efficiency* means that the same or more output of goods is produced using less energy and/or materials.

techniques using alternative energy sources (e.g. light and ultrasound)¹⁰ and new process-control methods (e.g. intentional unsteady-state operation).¹¹ The implementation of such technologies could improve process efficiency to levels that would allow sustained growth of the industry without using additional resources (or even less resources) than those used today, despite the increase in population and product demand. Furthermore, improved process efficiency will also reduce greenhouse gas emissions, alleviate the dependence on fossil fuels, and make production plants inherently safer.

The question is, given the evident benefits, what is hindering the prompt implementation of these technologies? Several obstacles have been identified and are summarized below:

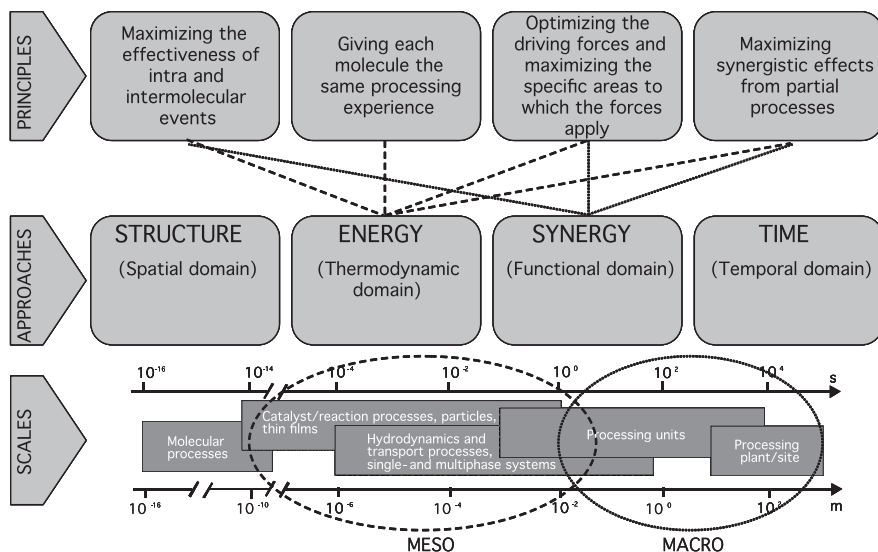
- a. The chemical industry, especially commodities producers, is subject to markets with small profit margins and strong competition, making them extremely conservative.
- b. New technologies pose technical risks such as production cuts or quality issues, even if they have been proven effective at the pilot scale.
- c. Management teams may not be aware of the potential benefits of the radically different technologies that are emerging.
- d. The chemical industry tends to be reactive instead of proactive. Investments in efficiency are usually made to comply with legislation, regulations, or consumer pressure.
- e. High energy prices force attention to be focused on efficiency and conservation, using traditional methods to gain efficiency.
- f. Innovation brings new know-how that has to undergo a learning/maturity curve—risk is therefore intrinsic.
- g. The tools and methodologies available to scale-up modern process development are still scarce.

1.2 Process intensification: A paradigm change for chemical industry innovation

As described in section 1.1, the fundamental problem of the chemical industry is that the current processes applied are still distant from achieving optimal operational efficiency. The future (perhaps only a generation ahead) of many chemical operations depends to a large extent on the creativity of engineers to generate solutions that produce MUCH more using a lot LESS⁴—a challenge for both academia and industry, taken over by chemical engineers who have been applying alternative process methodologies categorized by modern chemical engineering as *process intensification* (PI).¹²⁻¹⁴ This new area is characterized by innovative, radically different and revolutionary milestones exemplified in industrial demonstrations of striking impact on process and plant efficiencies. Important reference cases include the Eastman Chemical methyl acetate process using reactive distillation,¹⁵ the BASF BasilTM process using ionic liquids and the DSM Urea 2000 and Melamine processes.¹⁶ In its early stages, PI was simply considered a technological toolbox to replace existing processing units and gain efficiency. Recently, Van Gerven and Stankiewicz¹⁷ proposed a more fundamental approach based on four generic *principles* or *goals* to be achieved using four different *approaches*, applied at three different *scales*. This approach should be accompanied by a paradigm shift from the current “economies of scale” to the imminent “economies of efficiency”. To fully understand this approach to PI, Figure 1.1 presents a schematic representation of the methodology, describing principles, approaches, and scales. Currently available PI technologies can be classified based on this chart. Once the goals and approaches have been identified, PI technologies and methods can be selected as potential candidates for process improvement.

One major application of PI is the combination of several unit operations into multifunctional equipment, referred to as the synergy approach. The most common example is the integration of reaction and separation into the denominated multifunctional reactors. The goal is to integrate reaction with at least one more function, usually a unit operation (i.e. extraction, adsorption, absorption, chromatography, crystallization, distillation) that normally would have to be performed in a separate piece of equipment. Integrated reactive separation processes are increasingly applied in the chemical industry because of the: (i) economic benefits, such as lower energy consumption, capital investment and operational costs, (ii) reduced health, safety and environmental

⁴ MUCH means ten to thousands percent more; LESS means resources, energy, space, time, etc.

Figure 1.1 Fundamental approach to process intensification.¹⁷

risks, and (iii) robust and reliable modeling of such integrated operations, allowing for accurate design and scale-up. The main problem in such intensified units is the increased process complexity and the reduced operational feasibility window where the process is viable.

1.3 Reactive distillation

Reactive distillation (RD), where reaction, separation and enthalpy exchange take place in a single processing unit, best illustrates the multifunctional equipment concept previously discussed.¹⁴ RD processes used in esterification syntheses are among the most researched and cited examples of PI. Good reviews of current and potential applications of RD can be found in the literature.¹⁸⁻²² The concept of RD is not new, with the first pertinent patent dating back to 1921.²³ Some authors claim that the first undisclosed commercial applications of RD date from the late 1950s,¹⁸ while the best known commercial examples—the Eastman Chemical methyl acetate process and the MTBE process used by many companies—were made public in the 1980s.^{15,24} It was only then that RD gained importance as a suitable technology that could replace the conventional sequence of chemical reaction followed by distillation.

1.3.1 The unbeatable distillation

"I don't know what the future separation technologies will be, but I am sure they will look a lot like distillation" (Eastman Chemical Company)

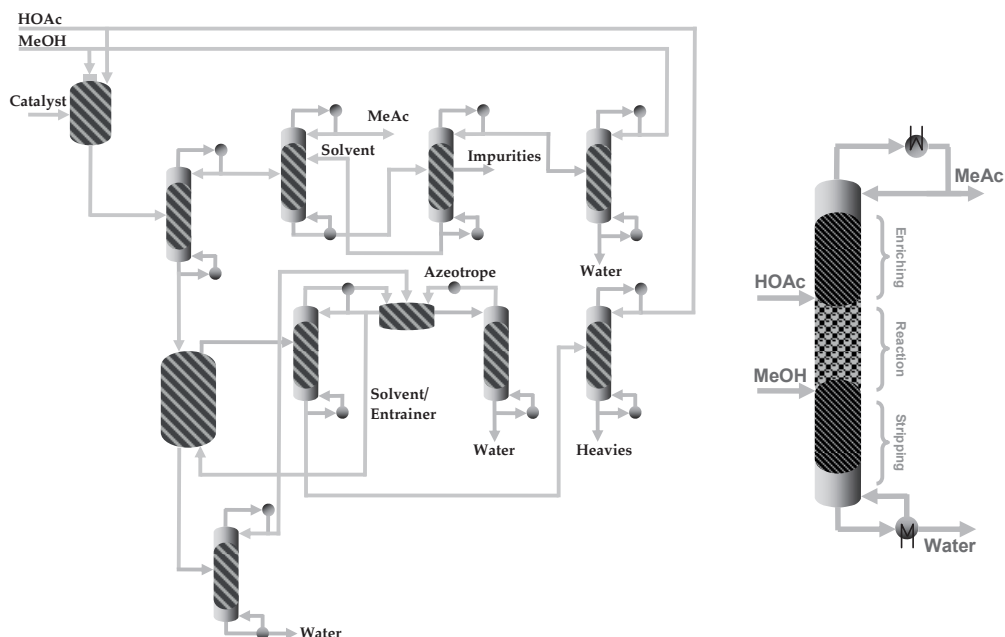
The above statement, taken from a presentation made by the Eastman Chemical Company, clearly illustrates the mindset of industry towards distillation. Coming from an innovation of the 1980s, it can now be argued that distillation is rather outdated from an academic perspective, but from an industrial point of view it is still the norm and will be for years to come. Without doubt, distillation is the separation technology most used in chemical facilities and by far the most energy-intensive. Approximately 80% of total energy consumed by the chemical industry is used in the form of heat,²⁵ with separation operations accounting for half this use. Distillation operations therefore account for a large fraction of total energy consumption. In some countries, distillation accounts for 6 to 8% of total energy consumed. It is hard to find another example of such a mature, stable, and energy-inefficient technology in the industry. If designed and operated correctly, distillation processes could run for years with extremely little maintenance. One of the keys to their success is the absence of moving and/or turning parts inside the equipment. The history of chemical engineering science is undeniably linked to distillation. The origins of distillation can be traced back to the early modern humanity when used to extract essential oils and alcoholic beverages. Modern distillation techniques started with the work of McCabe and Thiele, published in 1925, which used the graphical design of fractionating columns.²⁶

1.3.2 The Eastman example

The Eastman example shows clearly how effective and profitable a successful implementation of PI at a commercial scale can be. Figure 1.2 shows the drastic difference between the old conventional process and the new highly integrated reactive-separation unit. According to Eastman data, the new process allowed (i) an 80% reduction in capital expenditures due to the elimination in the number of units (from 28 to 1), (ii) a 50% decrease in conversion costs thanks to heat integration and (iii) reduced carbon footprint of the chemical plant. It took 1 year to design the concept, the scale-up effectiveness was 500:1, and the company was granted 2 patents. In brief, Eastman gained enormous prestige worldwide.

As described above, the integration of reaction and distillation brings important advantages in many aspects but especially regarding energy consumption when looking at the overall process performance. General advantages of RD include: (i) improved reaction yield/selectivity via equilibrium

Figure 1.2 Process integration for methyl acetate production: (Left) Process used prior to 1980, excluding details such as the impurity removal/recovery systems; (Right) Intensified reactive distillation unit, where MeOH = methanol, HOAc = acetic acid, and MeAc = methyl acetate.



shift due to in-situ product removal; (ii) improved energy use due to the compact, integrated design (e.g. reaction heat can be used for distillation); (iii) lower investment costs (less processing units); (iv) improved separation efficiency (e.g. reaction eliminates the separation of azeotropes); (v) avoided use of other chemicals (e.g. entrainers); (vi) minimized risk (e.g. by using less chemicals and less possible failure points).

1.3.3 Recent developments

The last two decades have been particularly important for RD. The learning curve in the understanding of the process matured particularly fast. Tools were quickly designed,²⁷⁻²⁹ scaled-up methodologies implemented,^{8, 30} and modelling and simulation programs developed.^{31, 32} As a result, RD was quickly introduced into industrial practice worldwide, starting with esterification reactions and later expanding to other chemical processes.

According to different authors,^{14, 18, 19, 21, 22} RD can be used in processes like: (i) esterification (e.g. acetates, propionates, lactates); (ii) etherification (e.g. TAME, ETBE, MTBE, DIPE); (iii) transesterification (e.g. stearic acid from acetic acid and vinyl stearate); (iv) ester hydrolysis; (v) dehydration of ethers to alcohols; (vi) hydrodesulfurization; (vii) alkylation of aromatics and aliphatics (e.g. ethylbenzene from ethylene and benzene); (viii) isomerization (e.g. butene); (ix) hydrogenations/oxidative dehydrogenation; (x) dimerization (e.g. oligomerization of C₄ olefins); (xi) carbonylation; (xii) amination; (xiii) nitration; (xiv) Fischer-Tropsch, among many others. This study focused on esterification reactions because of the amount and clarity of scientific information available and the moderate operating conditions required in most cases for experimentation.

The previous statements do not imply that there is no room for further improvement. RD is still based on the old fashioned and energy-inefficient concept of adiabatic distillation. Major improvements can be achieved by using efficient design concepts including diabatic columns with heat pumps, Hi-Gee distillation, HiDiC columns and microchannel distillation, to mention only a few examples. Further research is needed, targeted specifically to minimizing the energy expenditure of distillation.

1.3.4 Reactive distillation hurdles

There are a number of obstacles that prevent the widespread application of RD, which could be further improved by different methodologies using PI.

a) Fewer degrees of freedom

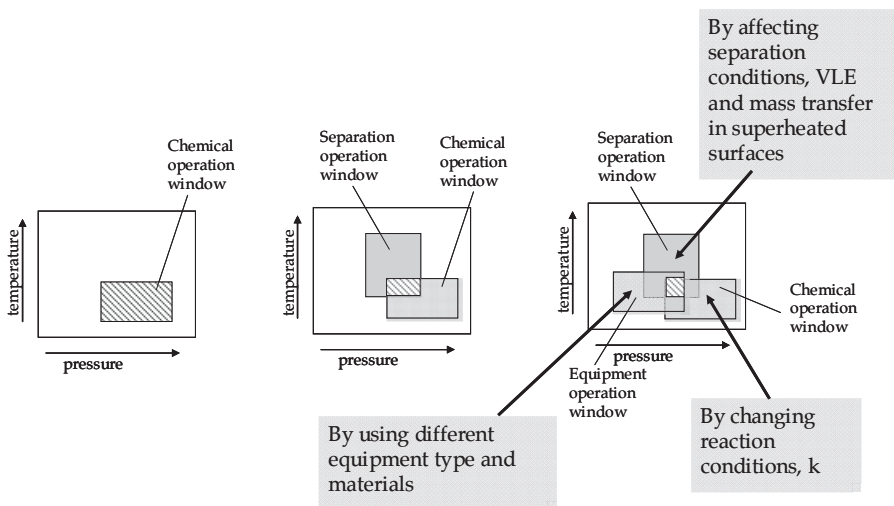
The deliberate integration of several functions into one process may imply that the degrees of freedom would be higher than in the conventionally activated reaction followed by downstream separation. However, the opposite occurs. The degrees of freedom are lowered by shifting from sequential processing units into integrated reaction and separation processes, thus making the “optimal” design and operation of RD processes a complex task. Integration should be considered as a phase addition into the known Gibb’s phase rule. The nonlinear coupling of reaction, transport phenomena and thermodynamic parameters gives rise to highly system-dependent elements, meaning that if one operational variable is chosen, all others are fixed.

b) Reduced operational feasibility window

Since both operations (reaction and distillation) are conducted simultaneously, overlapping of the operational window for reaction, distillation and equipment design occurs. Therefore, the temperatures and pressures of both

processes must match, depending on a given hardware (column) configuration. Figure 1.3 schematically illustrates this problem.³³ In the case of RD, the operational window for separation in pressure-temperature coordinates is usually limited by the thermodynamic properties (e.g. boiling points) of the components involved. On the other hand, the window in which the reaction (catalytic) delivers acceptable yields/selectivities to the required product often has a limited overlap with the separation window. This overlap may be decreased further by the feasibility window for equipment design (e.g. structured packings with highly viscous materials). The above specifications usually lead to a very small, restricted area in which the process is technically and economically feasible. In some cases no such area can be found.

Figure 1.3 Superposition of operational windows reducing the process feasibility area (adapted from Schembecker and Tlatlik).³³



c) Slow rate of partial processes (reaction, separation, or both)

With slow reaction rates, expensive, large, and energy-inefficient equipment must be used (e.g. complex columns with side-reactors in heterogeneous systems) to provide sufficient residence time for the reaction to be completed. The same holds for difficult separations, such as in binary mixtures with a relative volatility close to unity. If rates could be enhanced (i.e. quicker reactions or increased molecular separation), then equipment size could be reduced.

d) Optimal reaction conditions mean non-optimal separation conditions

Process conditions at which the reaction optima or process feasibility occur will probably not correspond to the same conditions for optimum separation. The process is restricted by this mismatch in the thermodynamic domain. Endothermic reactions are an example of such a divergence. Integration of product purification in high-temperature processes makes product recovery very difficult.

One way of overcoming these obstacles would be to apply the PI approach to the thermodynamic domain (energy), using alternative forms of energy that work at a meso-scale (Figure 1.1). The most important alternative sources include energy from electric, acoustic, and electromagnetic (MW and light) fields.³⁴ Of these, the academia has paid special attention to the application of MW (dielectric) heating to improve yield and selectivity in chemical syntheses. Conditions for separation, mass transfer, heat transfer and reaction rate can be drastically different than those in conventional processes, possibly enlarging the operational feasibility windows and thereby augmenting the superposition area where the process is only possible.

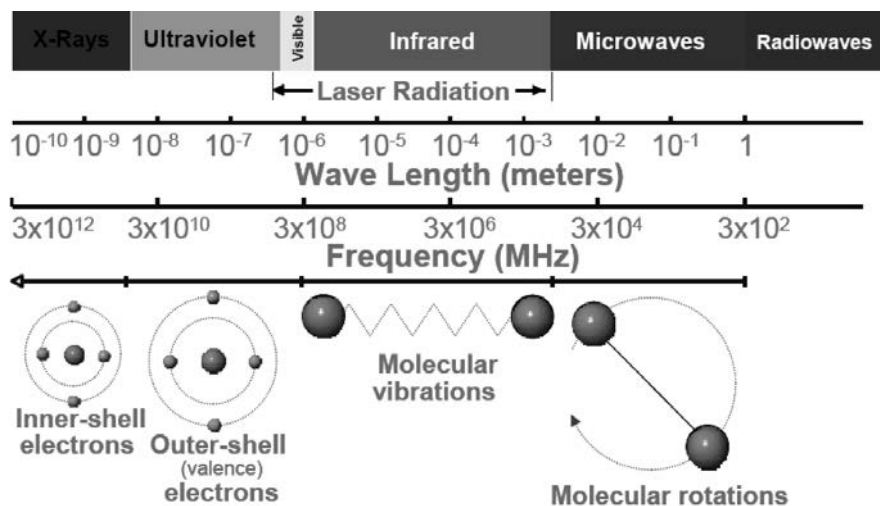
1.4 Microwaves: fundamentals, drivers, and challenges

Microwaves (MW) are a form of electromagnetic energy consisting of a magnetic field and an electric field that move at the speed of light. They operate at frequencies ranging from 0.3 to 300 GHz, corresponding to wavelengths of approximately 1 mm to 1 m (Figure 1.4) in the electromagnetic spectrum. Almost the entire range is occupied by radar and telecommunication applications and, to avoid interference, there are laws that require industrial and domestic microwave equipment to operate at several standard allocated frequencies. In the Netherlands, for example, allowed frequencies are 0.43, 2.45, 3.39, 5.80, 6.78 and 24.15 GHz.³⁵ Throughout this thesis, all experiments were performed with equipment operating at 2.45 GHz, which corresponds to a 12.2 cm wavelength.

Under MW activation conditions, only molecular movement (rotation, ionization) is affected, not molecular structure. The quantum energy of microwaves at the given frequency of 2.45 GHz is 0.037 kcal/mol, which is unable to break chemical bonds. Hydrogen bonds, for example, need approximately 4.8 kcal/mol. Therefore, the microwave effect on the excitation of molecules is purely kinetic. There are two fundamental mechanisms of transforming electromagnetic energy from microwaves into heat that operate

for liquids and gases: (i) *dipole rotation*, which is the alignment of polar molecules to the alternating electric field, and (ii) *ionic conduction*, where free ions or ionic species move as the molecules direct themselves to the electric field.

Figure 1.4 Electromagnetic spectrum.³⁶



These phenomena create a very different environment for energy transfer and activation of the reacting mixtures, as compared with the conventional way, which depends completely on the thermal conductivity of the materials involved. Several distinctive features of MW activation are: (i) direct coupling of energy (internal heating), (ii) volumetric heating and (iii) very rapid, selective absorption of radiation by dielectric substances at a nano-scale.

Over the last decades, the application of electromagnetic radiation in the form of microwaves for chemical syntheses (microwave chemistry) has been slowly pushing its way into academic research, laboratory analyses and industrial operations. Microwave technology has been used in different applications, including organic, inorganic, biochemistry, medicinal chemistry, drug discovery, synthesis of polymers and ionic liquids, as well as in material sciences with a proven intensification outcome, which is extensively reported in literature. In 2010 alone, microwave technology was addressed by more than 800 articles published in peer reviewed journals, books³⁶⁻⁴⁰ and review articles⁴¹⁻⁴⁷. Results

showed that MW are not only capable of reducing reaction times from several hours to a few minutes but also of increasing overall reaction yields by a factor two or even more. And yet, no commercial microwave-enhanced chemical processes have been discussed in open literature.

The real challenge is to bring the aforementioned MW benefits into industrial practice. Despite demonstrated benefits, the extensive use of MW has been hindered by the poor understanding of the interaction mechanisms between chemical media and electromagnetic waves at the molecular scale,^{48, 49} the on-going debate on thermal and non-thermal effects posed by microwaves, and the biases and contradictions found when comparing operating conditions to conventional activation. Moreover, the most relevant results have been published by chemists and physicists, who paid little attention to important chemical engineering aspects, such as measurement and control of reaction parameters (e.g. pressure and temperature). Beyond doubt, two of the main obstacles to the industrial application of microwave reactors have been the reliable scale-up of laboratory results⁵⁰⁻⁵² and the design of microwave equipment that could fit conventional chemical apparatuses.⁵³⁻⁵⁸

1.5 Problem statement and research questions

This study aims to evaluate the use of MW as an alternative energy source to intensify reactive distillation processes. The ultimate goal is to explore a novel concept of microwave-enhanced reactive distillation (MWeRD) based on demonstrated effects in partial processes (reaction and separation) and taking into account engineering challenges to achieve technology integration. To this end, the following research questions have been formulated and addressed in this thesis:

- Question 1. *What are the effects of applying microwave irradiation to a distillation process, if any? Can molecular separation be improved?*
- Question 2. *Can microwave irradiation affect heterogeneous and homogenous liquid phase esterification reactions? Are there any benefits in terms of yield, selectivity and operating conditions?*
- Question 3. *Is it possible to enlarge the operational feasibility window of reactive distillation processes heated with microwaves?*

Question 4. *How can the conventional reactive distillation technology be integrated with current microwave hardware?*

The research was divided into four major parts, which are discussed in depth in the chapters of this thesis.

1.6 Originality of research and thesis outline

To the best of knowledge, this thesis is the first attempt to investigate MW irradiation as a means to intensify reactive distillation processes. The nine chapters of the dissertation are compiled in four parts, each of which covers fundamental aspects of conventional RD processes and the effects of MW radiation on partial processes comprising RD, namely molecular separation and chemical reaction.

Chapters 1 to 3 (Part I) form a comprehensive introduction to the thesis.

Chapter 1 addresses the challenges currently faced by the chemical industry and how PI can potentially change the current paradigm by implementing alternative technologies that could drastically enhance process efficiency. The strengths and weaknesses of RD as a PI example are discussed as well as the research questions that arise about the novel concept of a MW-heated RD process. In *Chapter 2*, the esterification synthesis of *n*-propyl propionate is presented as the case system. The basic data relevant for RD application of this ester and the dielectric properties of the system are also explained in detail. *Chapter 3* contains the thermo-physical data required to accurately address RD process design. A UNIQUAC-HOC model is used to predict the thermodynamic behavior of the case system, while reaction kinetics is modeled via a pseudo-homogenous approach.

Chapters 4 and 5 (Part II) cover state-of-the-art experimentation and modeling of conventional RD processes.

Chapter 4 focuses on the design of RD processes using physicochemical fundamentals. The thermo-physical data gathered in Chapter 3 are used to build the residue curve maps of the case system. A detailed explanation of the technique and a feasibility analysis of the process are presented in this chapter. Because the process was viable, a pilot-scale set-up was assembled for laboratory experimentation. The conventional process was further improved by using a

decanter on the column top. The details of these experiments and the use of a non-equilibrium model to generate process data and avoid expensive, time-consuming experimentation are presented in *Chapter 5*.

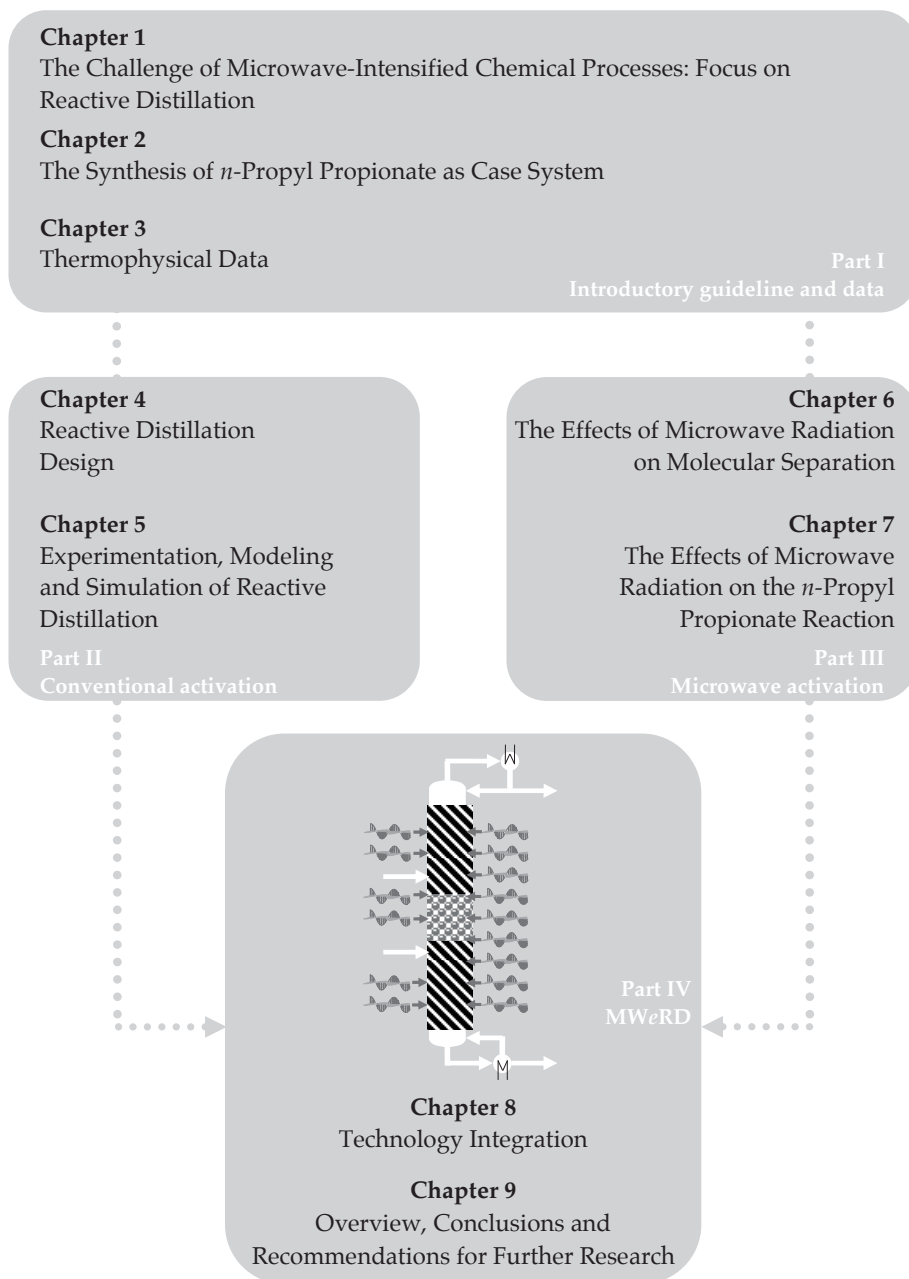
Subsequently, in Part III, the effects of MW radiation on the two fundamental functions of RD, namely separation (chapter 6) and reaction (chapter 7), are studied separately.

In *Chapter 6*, the influence of MW on molecular separation of the binary mixtures composing the quaternary case system is discussed based on experimental results. Four binary pairs were studied showing, in some cases, an enhanced separation of the components. *Chapter 7* deals with the effect of MW radiation on the esterification reaction. Interactions of different homogenous and heterogeneous catalysts with the electromagnetic field are studied.

The last two chapters (Part IV) bring together the proposed concept of a microwave-enhanced reactive distillation (MWeRD) process.

The information generated in parts II and III of the thesis are used to discuss the general benefits of technology integration in *Chapter 8*. This chapter outlines the steps for further research and the type of hardware needed for the integration of both technologies. *Chapter 9* summarizes the highlights of the work and presents recommendations for follow-up research.

The thesis layout is schematically presented in Figure 1.5.

Figure 1.5 Schematic representation of the thesis.

1.7 References

1. Durbin M. *Statement before the U.S. House of Representatives. Energy and Commerce Committee, Subcommittee on Environmental and Hazardous Materials.* Legislative Hearing on H.R. 5533. **2008**.
2. IMF. *World Economic Outlook.* **2010**.
3. Spoelstra S. *Nederlandse en industriële energiehuishouding.* ECN-I-05-004. **2005**.
4. *World Resources Institute.* Available from: www.wri.org.
5. Lave L.B. *The Potential of Energy Efficiency: An Overview.* The Bridge. **2009**, National Academy of Sciences. Washington, DC.
6. Hessel V., Löwe H., Schönfeld F., Micromixers—A review on passive and active mixing principles. *Chemical Engineering Science.* **2005**. 60: 2479-2501.
7. Oxley P., Brechtelsbauer C., Ricard F., Ramshaw C., Evaluation of spinning disk reactor technology for the manufacture of pharmaceuticals. *Industrial and Engineering Chemistry Research.* **2000**. 39: 2175-2182.
8. Hoffmann A., Górak A., Catalytic distillation in structured packings. *AIChE Journal.* **2001**. 47(5): 1067-1076.
9. Schmitt M., Hasse H., Althaus K., Schoenmakers H., Götze L., Moritz P., Synthesis of n-hexyl acetate by reactive distillation. *Chemical Engineering and Processing.* **2004**. 43: 397-409.
10. Toukoniitty B., Mikkola J.P., Salmi T., Utilization of electromagnetic and acoustic irradiation in enhancing heterogeneous catalytic reactions. *Applied Catalysis A: General.* **2005**. 279: 1-22.
11. DSM. *Process Intensification Information Sheets.* D.R.B. V. **2000**, DSM Research B. V.
12. Becht S., Franke R., Hahn H., An industrial view of process intensification. *Chemical Engineering and Processing.* **2009**. 48: 329-332.
13. Stankiewicz A., Moulijn J.A., Process intensification: Transforming chemical engineering. *Chemical Engineering Progress.* **2000**. 96(1): 22-34.
14. Stankiewicz A., Reactive separations for process intensification: An industrial perspective. *Chemical Engineering and Processing.* **2003**. 42: 137-144.
15. Agreda V.H., High-purity methyl acetate via reactive distillation. *Chemical Engineering Progress.* **1990**. 86(2): 40-46.
16. Stankiewicz A., Moulijn J.A., *Re-engineering the chemical processing plant: process intensification.* Chemical Engineering Progress. **2004**, New York: Marcel Dekker.
17. Van Gerven T., Stankiewicz A., Structure, energy, synergy, time— The fundamentals of process intensification. *Industrial & Engineering Chemistry Research.* **2009**. 48: 2465-2474.
18. Harmsen G.J., Reactive distillation: The front-runner of industrial process intensification A full review of commercial applications, research, scale-up, design and operation. *Chemical Engineering and Processing.* **2007**. 46: 774-780.
19. Hiwale R.S., Mahajan, Y. S., Bhat, N. V., Mahajani, S. M., Industrial applications of reactive distillation: Recent trends. *International Journal of Chemical Reactor Engineering.* **2004**. 2: 1-52.
20. Kiss A., Omota F., Dimian A., C., Rothenberg G., The heterogeneous advantage: biodiesel by catalytic reactive distillation. *Topics in Catalysis.* **2006**. 40(141-150).
21. Srinivas S., Malik R., K., Mahajani S. M., Feasibility of reactive distillation for Fischer-Tropsch synthesis. *Industrial & Engineering Chemistry Research.* **2008**. 47: 889-899.
22. Sundmacher K., Kienle A., *Reactive Distillation.* **2003**, Weinheim: Wiley-VCH.
23. Backhaus A.A., Continuous process for the manufacture of esters. *US Patent 1,400,849.* **1921**.
24. Siirola J.J., An industrial perspective on process synthesis. *AIChE. Symp. Ser.* **1995**. 94(304): 222-233.
25. Jansens P.J., *Ingenieus Onderscheid.* Inaugurele Rede. **2001**: TU Delft.
26. McCabe W.L., Thiele E.W., Graphical design of fractionating columns. *Industrial & Engineering Chemistry Research.* **1925**. 17(6): 605-611.
27. Doherty M.F., Buzad G., Reactive distillation by design. *ICHEME Transactions.* **1992**. Part A: 448-458.

28. Fien G.J.A.F., Liu Y.A., Heuristic synthesis and shortcut design of separation processes using residue curve maps: A review. *Industrial & Engineering Chemistry Research*. **1994**. 33: 2505-2522.
29. Song W., Venimadhavan G., Manning J.M., Malone M.F., Doherty M.F., Measurement of residue curve maps and heterogeneous kinetics in methyl acetate synthesis. *Industrial & Engineering Chemistry Research*. **1998**. 37: 1917-1928.
30. Hoffmann A., Noeres C., Górak A., Scale-up of reactive distillation columns with catalytic packings. *Chemical Engineering and Processing*. **2004**. 43: 383-395.
31. Klöcker M., Kenig E.Y., Hoffmann A., Kreis P., Górak A., Rate-based modelling and simulation of reactive separations in gas/vapour-liquid systems. *Chemical Engineering and Processing*. **2005**. 44: 617-629.
32. Taylor R., Krishna R., Modelling reactive distillation. *Chemical Engineering Science*. **2000**. 55: 5183-5229.
33. Schembecker G., Tlatlik S., Process synthesis for reactive separations. *Chemical Engineering and Processing*. **2003**. 42: 179-189.
34. Stankiewicz A., Energy matters alternative sources and forms of energy for intensification of chemical and biochemical processes. *Chemical Engineering Research & Design*. **2006**. 84(7): 511-521.
35. Metaxas A.C., Meredith R.J., *Industrial microwave heating*. **1993**, London: Peter Peregrinus.
36. Hayes L.B., *Microwave Synthesis. Chemistry at the Speed of Light*. **2002**, Matthews, NC.: CEM Publishing.
37. Bogdal D., *Microwave-assisted Organic Synthesis, One Hundred Reaction Procedures*. **2005**, Oxford: Elsevier.
38. Kappe C.O.D., D.; Murphree S., *Practical Microwave Synthesis for Organic Chemists: Strategies, Instruments, and Protocols*. **2009**, Weinheim: Wiley-VCH.
39. Leadbeater N.E., *Microwave Heating as a Tool for Sustainable Chemistry (Sustainability)*. **2010**, Boca Raton: CRC Press.
40. Roussy G., *Foundations and Industrial Applications of Microwave and Radio Frequency Fields; Physical and Chemical Processes*, ed. Wiley-WCH. **1995**, Sussex: Wiley-WCH.
41. Caddick S.F., R., Microwave enhanced synthesis. *Tetrahedron*. **2009**. 65: 3325-3355.
42. De la Hoz A.D.-O., A.; Moreno A., Microwaves in organic synthesis. Thermal and non-thermal microwave effects. *Chemical Society Reviews*. **2005**. 34: 164-178.
43. Kappe C.O., Controlled microwave heating in modern organic synthesis. *Angewandte Chemie International Edition*. **2004**. 43: 6250-6284.
44. Kappe C.O., Dallinger D., Controlled microwave heating in modern organic synthesis: Highlights from the 2004-2008 literature. *Molecular Diversity*. **2009**. 13: 71-193.
45. Martínez-Palou R., Microwave-assisted synthesis using ionic liquids. *Molecular Diversity*. **2010**. 14: 3-25.
46. Nüchter M.O., B., Bonrathb W., Gumb A., Microwave assisted synthesis - A critical technology overview. *Green Chemistry*. **2004**. 6: 128-141.
47. Strauss C.R.R., D.W., Accounting for clean, fast and high yielding reactions under microwave conditions. *Green Chemistry*. **2010**. 12: 1340-1344.
48. Conner W.C., Tompsett G.A., How could and do microwaves influence chemistry at interfaces? *The Journal of Physical Chemistry B*. **2008**. 112: 2110-2118.
49. Perreux L.L., A., A tentative rationalization of microwave effects in organic synthesis according to the reaction medium, and mechanistic considerations *Tetrahedron*. **2001**. 57(45): 9199-9223
50. Damm M.G., T.N., Kappe C.O., Translating high-temperature microwave chemistry to scalable continuous flow processes. *Organic Process Research & Development*. **2010**. 14: 215-224.
51. Leonelli C.M., T.J., Microwave and ultrasonic processing: Now a realistic option for industry. *Chemical Engineering and Processing*. **2010**. 49: 885-900.

52. Strauss C.R., On scale up of organic reactions in closed vessel microwave systems. *Organic Process Research & Development*. **2009**. 13: 915–923.
53. *Sairem*. Available from: www.sairem.com.
54. *Fricke und Mallah*. Available from: www.microwaveheating.net.
55. *Microwave TM*. Available from: www.radiofrequency.com.
56. *Industrial Microwave Systems, L.L.C.*; Available from: www.industrialmicrowave.com.
57. *C-Tech Innovation*. Available from: www.ctechinnovation.com.
58. *Püschner*. Available from: www.pueschner.com.

The Synthesis of *n*-Propyl Propionate as Case System

*Some of the most prominent examples of process intensification (PI) in the chemical industry are reactive distillation (RD) processes used in esterification syntheses. In the previous chapter, the suitability of these reactions for RD research was discussed and therefore an esterification was chosen as exemplifying reaction. The present chapter describes general aspects of the acid catalyzed reaction to produce *n*-propyl propionate (ProPro) from 1-propanol (ProOH) and propionic acid (ProAc). The synthesis is thoroughly described, including relevant thermo-physical parameters of reagents and products, the main and side reactions and the reaction scheme. Furthermore, the state-of-the-art industrial production process is illustrated, including a proper column layout. Finally, experimental results of the dielectric properties of reagents and products are included and their importance for microwave chemistry discussed. This information will be used in the following chapters for further process development.*

The contents of this chapter were adapted from the work published in:

E. Altman, G. D. Stefanidis, T. van Gerven, A. Stankiewicz
“Microwave-Promoted Synthesis of *n*-Propyl Propionate using Homogeneous Zinc Triflate Catalyst.”

Ind. Eng. Chem. Res., Nigam Issue (2011); DOI: 10.1021/ie200687m
© 2011 American Chemical Society. Reprinted with permission.

“Karl Marx, a visionary, figured out that you can control a slave much better by convincing him he is an employee.”

Nassim N. Taleb

2.1 *n*-Propyl propionate synthesis

Esterification processes are in general, good test systems to prove concepts in RD. Most of the RD knowledge and design tools were developed for production of acetates after the introduction of the Eastman process in 1980. Thermo-physical data including thermodynamic equilibria and kinetic models are easily available for such systems. Esterification reactions are suitable for RD processes because:

- (i) As both operations are conducted simultaneously in a RD column, an overlap between the operational windows for reaction and distillation exists and consequently the process conditions are required to match. In many esterifications, the reaction temperature coincides with the distillation temperatures.
- (ii) As the esterification reaction is reversible, the simultaneous withdrawal of the products shifts the equilibrium to the product side thus improving product formation.
- (iii) The possibility of RD to overcome azeotropes and avoid expensive downstream processing.

Moreover, since the early stages of microwave chemistry when household equipment was used, esterification reactions were chosen as test systems. Motives for this include:

- (i) Esters are very important products in the chemical industry accounting for a large production volume. Any improvement could have a direct impact in industrial operations.
- (ii) The time for the reactions to reach equilibrium could take several hours; large energy savings could be obtained if this time is drastically shortened.
- (iii) Alcohols are very good microwave absorbing materials.
- (iv) Reactions usually take place in excess of one reactant that has to be separated downstream.

- (v) The reagents and products present in esterification reactions form highly non-ideal systems with several azeotropes present and by-product formation, causing difficult and expensive separation. This may be avoided by targeted selectivity.

One of the first papers on MW chemistry by Gedye et al.¹ reported increased reaction rates using benzoic acid with different alcohols in sealed Teflon vessels under MW activation conditions. In that case, the comparison with conventional heating was not fair since under conventional heating, reactions were performed in open reflux and the temperature was not recorded. The only process parameter compared was time. Nonetheless, this opened at the time a new research field that grew exponentially until this day.

In this work, the esterification reaction for the synthesis of the *n*-propyl propionate (ProPro) has been chosen as the exemplifying system.

2.1.1 Reaction scheme

ProPro is an important solvent for the chemical industry. It is considered a non-hazardous air pollutant by the U.S. Environmental Protection Agency which makes it an attractive option in many applications to replace harmful aromatic solvents like toluene. It can be found in diverse products ranging from paints, coatings and inks to cleaners and food flavors proving its versatility and market significance. Although the reaction occurs under acidic conditions, it is not self-catalyzed and addition of a strong acid catalyst, either homogeneous or heterogeneous, is needed. The ester is obtained from the esterification reaction of propionic acid (ProAc) and 1-propanol (ProOH) according to Equation 2.1. Key property parameters of the reactants and products are given in Table 2.1.

Industrial production is performed via a reactive distillation process using acidic surface-sulfonated ion exchange resins as catalysts.^{6,7} In this process, the purity of the product relies on achieving a high acid conversion and consequently excess of alcohol is usually used.



Table 2.1 Pure components property data

Property	Propionic acid	1-Propanol	<i>n</i> -Propyl propionate	Water
MW (g/mol) ^a	74.08	60.10	116.16	18.01
T_b (1.013 bar) (°C) ^a	141.16	97.78	122.49	100.00
ΔH_v (20°C) (kJ/mol) ^a	31.14	41.44	35.54	40.66
ΔH_f^0 (kJ/mol) ^b	-508.8	-302.6	-527.5	-285.8
ϵ' (20°C) (-)	3.18 ^c	20.10 ^d	5.25 ^c	80.40 ^d
ϵ'' (20°C) (-) ^d	NA	15.216	NA	9.889
$\tan \delta$ (-)	NA	0.757	NA	0.123

^a from ref. ², ^b from ref. ³, ^c from ref. ⁴, ^d from ref. ⁵. (NA= not available)

Under normal reaction conditions, (temperature range from 90 to 120°C and 1 bar of pressure) ion exchange resins are the preferred catalysts because important side reactions can be suppressed including:

- (i) The dehydration of the alcohol leading to propene production



- (ii) The self-condensation of the alcohol into the corresponding ether, di-*n*-propyl ether



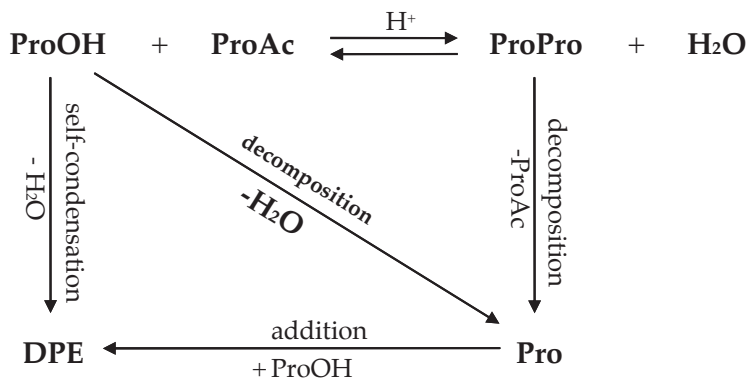
- (iii) The ester decomposition into propene and propionic acid



- (iv) The etherification of the alcohol



The complete reaction scheme is depicted in Figure 2.1 and described by Equations 2.1 to 2.5.

Figure 2.1 Reaction scheme of *n*-propyl propionate synthesis.

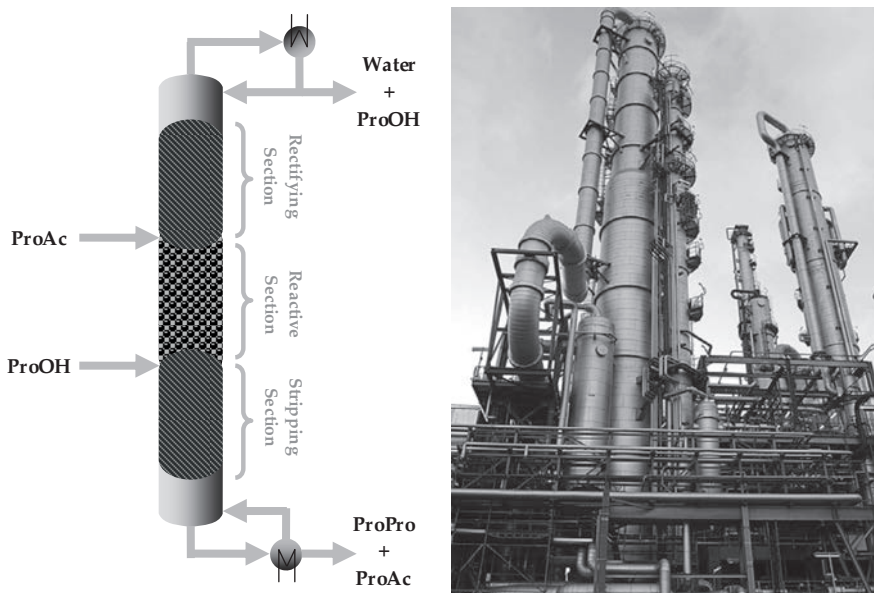
According to Ali *et al.*,⁸ the standard enthalpy change of reaction, ΔH_{R}^0 was determined experimentally to be -6.4 kJ/mol. They concluded that the reaction is exothermic and that the equilibrium constant has a weak dependence on temperature.

2.1 State-of-the-art production

The state-of-the-art industrial scale production of ProPro comprises the use of a RD process as the core of the system with two downstream units for reactant recovery and product purification. The RD column is equipped with structured packings, with the reactive section in the middle. The reactants are fed separately in countercurrent, the ProOH in the bottom of the reactive section and the ProAc fed at the top of the reactive section as seen in Figure 2.2 (left). Since ProAc is the heavy boiler, the unreacted acid will fall to the bottom of the column and exit along with the product of interest ProPro. For this reason an excess of alcohol is used at expense of hard azeotropic purification from the products exiting at the column top; the excess of alcohol with the reaction product water and some ProPro that may be distilled according to process conditions. Buchaly *et al.*⁹ studied in a pilot scale column the effect that various process parameters like *distillate to feed ratio*, *reflux ratio*, *molar feed ratio* and *column load* had on product yield. Molar fractions ($x_{\text{ProPro, bottom}}$) in the bottom stream of more than 0.95 were possible to achieve with a molar excess of 2:1 ProOH/ProAc and enough catalyst (low feed) to achieve high acid conversion. Figure 2.2 (right) depicts how the real

RD column looks clearly showing not many differences from any normal adiabatic distillation column.

Figure 2.2 State-of-the-art production of *n*-propyl propionate using RD.



2.2 Dielectric properties relevant to microwave chemistry

2.2.1 Fundamentals of dielectric properties

Understanding the way in which matter interacts with an electromagnetic field is of primary importance in microwave chemistry. The fundamental mechanisms occurring during heating of irradiated solutions at molecular scale can lead to better interpretation of observed reaction phenomena, more accurate modeling, and estimation of important parameters, such as penetration depth and absorbed energy.¹⁰⁻¹⁴ However, it is still very unusual in microwave chemistry literature to find reports of dielectric properties of reagents, catalysts and products taking part in reactions. In addition, the variation of these parameters with temperature and frequency is usually neglected and readers are often referred to data obtained at standard conditions (2.45 GHz, 1 bar and 20-25°C).

The opposite occurs in other scientific areas, where microwaves are used to heat as in food applications, where a lot of effort has been given to accurately determine these properties.^{15, 16} Microwave absorption and propagation is only possible in materials that are dielectric. The latter meet two conditions when applying an electric current through them; they will: (i) act as capacitors, storing energy, and (ii) have very little conductivity. This storing ability can be quantified with the absolute permittivity, ϵ . In radio frequency heating, time harmonic discontinuous electric and magnetic fields are used to transmit energy into materials. When the alternating fields are applied to dielectric materials in frequencies corresponding to the electromagnetic region (109 – 1012 Hz), polarization occurs. Two main mechanisms account for this phenomena at molecular level; dipole orientation (physical rotation of dipoles) and ionic conduction (distortion of the electron cloud). The periodic variation of these fields has an angular frequency and is accounted for with the complex permittivity ϵ^* , related to the electric field, and the complex permeability μ^* , related to the magnetic field. For heating applications, the complex permeability μ^* is generally not considered. The complex permittivity ϵ^* is the permittivity of the material ϵ relative to that of free space ϵ_0 ($1/36\pi \cdot 10^{-9}$ F/m) as seen in Equation 2.6.

$$\epsilon^* = \frac{\epsilon}{\epsilon_0} \quad (2.6)$$

$$\epsilon^* = \epsilon' - j\epsilon'' \quad (2.7)$$

$$\tan \delta = \frac{\epsilon''}{\epsilon'} \quad (2.8)$$

The complex permittivity parameter ϵ^* has two parts associated in a complex number as shown in Equation 2.7. The real part ϵ' is the dielectric constant and the imaginary part ϵ'' is the dielectric loss. Both parameters have physical meanings and are temperature and frequency dependant. ϵ' is a measure of how much energy from an external electric field is stored and ϵ'' is a measure of how dissipative (electromagnetic energy transformed to heat) a material is. Consequently, ϵ'' is a more important parameter to account for and use to compare materials employed in dielectric heating. The latter, however, is not sufficient to describe the ability of a material to convert electromagnetic energy into heat and a third parameter, known as loss tangent $\tan \delta$, is introduced. The loss tangent is expressed as a quotient shown in Equation 2.8. At standard conditions, water is an example of an inefficient dielectric material ($\epsilon' = 80.4$, $\epsilon'' = 9.889$, $\tan \delta = 0.123$) and DMSO an example of an efficient one ($\epsilon' = 45.0$, $\epsilon'' = 37.125$, $\tan \delta = 0.825$). In microwave chemistry literature, solvents are usually

classified as good ($\epsilon'' > 10$, $\tan \delta > 0.5$), medium ($\epsilon'' = 1-5$, $\tan \delta = 0.1-0.5$) and low microwave-absorbing ($\epsilon'' < 1$, $\tan \delta < 0.1$). Another important parameter to consider is the penetration depth d_p . It is defined as the maximum distance that a wave can penetrate into a sample where its power has dropped to 37% of its original transmitted value. There are several expressions found in literature to calculate this parameter. In this study, we have used the formula shown in Equation 2.9, where c is the speed of light ($3 \cdot 10^8$ m/s) and f is the frequency in (Hz).

$$d_p = \frac{c}{2\pi f \sqrt{2\epsilon' \sqrt{1 + \left(\frac{\epsilon''}{\epsilon'}\right)^2 - 1}}} \quad (2.9)$$

As a general statement, the use of microwave activation to heat chemical reactions should only be considered if at least one of the components in the reacting mixture (reagents/catalysts) couples strongly with the electromagnetic field and possible localized superheating can be achieved (e.g. heterogeneous gas phase reactions). Achieving this targeted heating in liquid phase reactions is more difficult especially if various components are good absorbers.

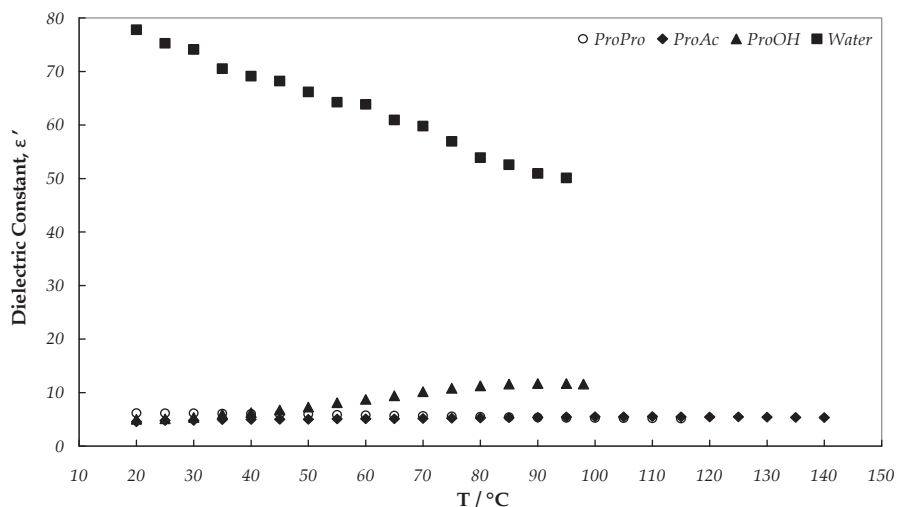
2.2.2 Measurements of dielectric properties

Dielectric properties of catalysts, reagents, products and the reacting system were determined over a frequency range of 200 MHz to 20 GHz using a high temperature dielectric probe (85070D, Agilent) connected to a network analyzer (E5062A, Agilent). Prior to each measurement, the equipment was calibrated following the standard procedure using air, water at 20°C and the shorting block. The dielectric constant ϵ' and the dielectric loss ϵ'' values were determined as a function of temperature ramping from 20°C to the boiling point or the reacting temperature with 5°C increments. The temperature was kept constant using an oil bath. A especially designed liquid holder was used to minimize any air gaps existing between the samples and the probe. Three measurements were carried out at each temperature over the frequency range.

2.3 System dielectrics

According to literature data, an equimolar reacting system consisting of ProOH and ProAc should be a good microwave absorbing mixture. From the ϵ' and ϵ'' values, presented in Table 2.1, it can be inferred that most of the energy put into the system at the beginning of the reaction and without catalyst will come from the high dielectric material (in this case the alcohol) and that the acid will account for very little heat input.

Figure 2.3 Dielectric constant ϵ' of reactants and products involved in the synthesis of ProPro as a function of temperature.



Since the dependence of the dielectric parameters with temperature was not known, the properties of the pure components were determined experimentally and are presented in Figures 2.2 to 2.5. Measurements started at the temperature of 20°C and ended before reaching the boiling point of the liquids. It is clear that in this esterification system, water and alcohol are the energy dissipating components, whereas the acid and the ester contributions to dielectric heating are very low. As compared to literature data reported at 20°C, we found the following values for the dielectric properties of the system components: ProOH ($\epsilon' = 5.02$, $\epsilon'' = 3.31$, $\tan \delta = 0.660$), ProAc ($\epsilon' = 4.54$, $\epsilon'' = 0.15$, $\tan \delta = 0.033$), ProPro ($\epsilon' = 6.17$, $\epsilon'' = 0.11$, $\tan \delta = 0.017$) and water ($\epsilon' = 77.80$, $\epsilon'' = 9.64$, $\tan \delta = 0.124$). Most

of the experimental data agree with literature values except for the dielectric constant of ProOH. The alcohol was expected to be a better absorbing material despite its high efficiency recorded in the loss tangent value which is in the same order of magnitude with values already published. However, it is better to consider as a comparison parameter the dielectric loss ϵ'' since we are interested in the capacity of a substance to transform electromagnetic energy into heat irrespective of the efficiency of the process. The plot of ϵ'' vs. T in Figure 2.3 shows clearly the dependence of the dielectric properties with temperature. It should not be generalized that with a temperature increase the values for ϵ' and ϵ'' will drop. Close to the boiling points, water and ProPro values descended to ($\epsilon' = 50.10$, $\epsilon'' = 2.78$, $\tan \delta = 0.055$) at $T = 95^\circ\text{C}$ and ($\epsilon' = 5.12$, $\epsilon'' = 0.04$, $\tan \delta = 0.008$) at $T = 115^\circ\text{C}$, respectively, while ProAc and ProOH registered an increase to ($\epsilon' = 5.32$, $\epsilon'' = 0.21$, $\tan \delta = 0.039$) at $T = 140^\circ\text{C}$ and ($\epsilon' = 11.58$, $\epsilon'' = 3.32$, $\tan \delta = 0.287$) at $T = 98^\circ\text{C}$, respectively. For practical purposes, the increase in the ProAc properties is marginal because the alcohol dictates the dielectric behavior of the binary system and the efficiency of ProOH drops significantly.

Figure 2.4 Dielectric loss ϵ'' of reactants and products involved in the synthesis of ProPro as a function of temperature.

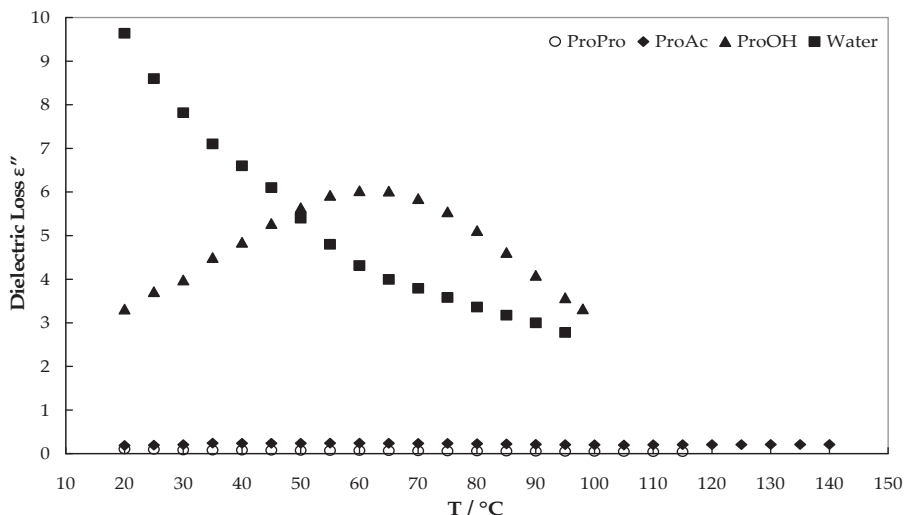
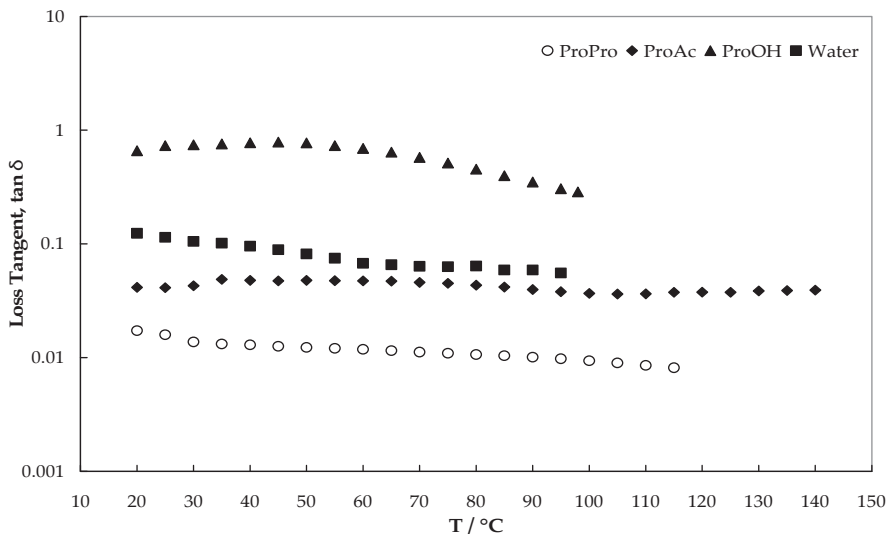


Figure 2.5 Loss tangent $\tan \delta$ of reactants and products involved in the synthesis of ProPro as a function of temperature.



Dielectric properties increase with temperature due to a change in the relaxation time (τ) response of the solvents.¹⁰ In the case of alcohol, there is an optimum $\epsilon'' = 6.03$ occurring at $T = 60^\circ\text{C}$ and an optimum $\tan \delta = 0.786$ occurring at $T = 45^\circ\text{C}$. At higher temperatures τ goes down as the molecules will return faster to a random state when the electric field is off. At the temperature optima, the relaxation time will drop below the angular frequency of the electromagnetic radiation $\tau = 1/\omega$ and a decay in the values occur.

Nomenclature

d_p penetration depth (m)

Greek letters

ε permittivity of the material

ε^* complex permittivity

ε' dielectric constant

ε'' dielectric loss

ε_0 free space permittivity

τ relaxation time

μ^* complex permeability

$\tan \delta$ loss tangent

Subscripts

ProAC propionic acid

ProOH 1-propanol

ProPro *n*-propyl propionate

2.4 References

1. Gedye R., Smith F., Rousell J., The Use of Microwave Ovens for Rapid Organic Synthesis. *Tetrahedron Letters*. **1986**. 27(3): 279-282.
2. Poling B.E., Prausnitz J. M., O'Connell J. P., *The Properties of Gases and Liquids*. 5th ed, ed. McGraw-Hill. **2001**: McGraw-Hill.
3. Duarte C. *Production of TAME and n-Propyl Propionate by Reactive Distillation*. Department of Chemical Engineering, Ph.D. thesis. **2006**, Univerisity of Porto.
4. Wohlfahrt C., *Landolt-Börnstein - Group IV Physical Chemistry Numerical Data and Functional Relationships in Science and Technology*. Vol. 6: Static Dielectric Constants of Pure Liquids and Binary Liquid Mixtures. **1991**: Springer.
5. Hayes L.B., *Microwave Synthesis. Chemistry at the Speed of Light*. **2002**, Matthews, NC.: CEM Publishing.
6. Altman E., Kreis P., Stefanidis G. D., Stankiewicz A., Górak A., Pilot plant synthesis of n-propyl propionate via reactive distillation with decanter separator for reactant recovery. Experimental model validation and simulation studies. *Chemical Engineering and Processing*. **2010**. 49: 965-972.
7. Buchaly C., Kreis P., Górak A., Hybrid separation processes-Combination of reactive distillation with membrane separation. *Chemical Engineering and Processing*. **2007**. 46: 790-799.
8. Ali S.H.T. A., Al-Sahhaf T., Synthesis of esters: Development of the rate expression for the Dowex 50 Wx8-400 catalyzed esterification of propionic acid with 1-propanol. *Chemical Engineering Science*. **2007**. 62: 3197-3217.
9. Buchaly C. *Experimental Investigation, Analysis and Optimisation of Hybrid Separation Processes*. Lehrstuhl für Fluidverfahrenstechnik **2008**, Dissertation Technische Universität Dortmund
10. Gabriel C., Gabriel S., Grant E. H., Halstead B. S. J., Mingos D. M. P., Dielectric parameters relevant to microwave dielectric heating. *Chemical Society Reviews*. **1998**. 27: 213-223.
11. Heng P.W.S.L., Lee C.C., Dielectric Properties of Pharmaceutical Materials Relevant to Microwave Processing: Effects of Field Frequency, Material Density, and Moisture Content. *Journal of Pharmaceutical Sciences*. **2010**. 99: 941-956.
12. Holtz E.A., Rasmuson A., Influence of dielectric and sorption properties on drying behaviour and energy efficiency during microwave convective drying of selected food and non-food inorganic materials. *Journal of Food Engineering*. **2010**. 97: 144-153.
13. Horikoshi S.I., Serpone N. Chemical Reactions with a Novel 5.8-GHz Microwave Apparatus. 1. Characterization of Properties of Common Solvents and Application in a Diels-Alder Organic Synthesis. *Organic Process Research & Development*. **2008**. 12: 257-263.
14. Kaatze U.B., von Roden K., Structural aspects in the dielectric properties of pentyl alcohols. *The Journal of Chemical Physics*. **2010**. 133: 094508.
15. Sosa-Morales M.E.V.-J., García H. S. Dielectric properties of foods: Reported data in the 21st Century and their potential applications. *LWT - Food Science and Technology*. **2010**. 43: 1169e1179.
16. Wang Y.W., Hallberg L. M. Dielectric properties of foods relevant to RF and microwave pasteurization and sterilization. *Journal of Food Engineering*. **2003**. 57: 257-268.

Thermo-Physical Data for Reactive Distillation

In the previous chapter, the esterification reaction of ProPro was introduced as the case system including the relevant parameters and the reaction scheme with the side reactions occurring. In this chapter the most important data needed for proper RD design and modeling are presented; namely the thermodynamics of the system and the kinetics of the reaction. Isobaric vapor–liquid equilibrium (VLE) data were measured for various binary systems at 101.3 kPa. Isothermal liquid-liquid equilibrium (LLE) data were measured for the ternary system ProOH + water + ProPro at 288.15 K. VLE and LLE data were fitted using the UNIQUAC model to account for non idealities in the liquid phase while the Hayden O’Connell (HOC) equation of state was used to account for non idealities in the vapour phase. The regressed models are in good agreement with the experimental data. With the UNIQUAC parameters obtained from the data regression, the thermodynamic behaviour of the quaternary mixture was predicted and the equilibrium constant in the reaction kinetics calculated.

The contents of this chapter were adapted from the work published in:

Ernesto Altman, Georgios D. Stefanidis, Thomas van Gerven,
Andrzej I. Stankiewicz

**“Phase Equilibria for Reactive Distillation of Propyl Propionate.
Pure Component Property Data, Vapor-Liquid Equilibria and Liquid-Liquid
Equilibria.”**

J. Chem. Eng. Data, **56** (2011) 2322-2328; DOI: 10.1021/je101302p

© 2011 American Chemical Society. Reprinted with permission.

“Thoroughly conscious ignorance is the prelude to every real advance in science.”

James Clerk Maxwell

3.1 Process development

In the present chapter, thermodynamic equilibrium and kinetic data needed for the synthesis of ProPro in a RD process are presented. This system, as other esterification reactions used in RD processes¹⁻³, is characterized by strong liquid and vapour phase non-idealities with several azeotropes present. The azeotropic data at the corresponding temperature and compositions are shown in Table 3.1.

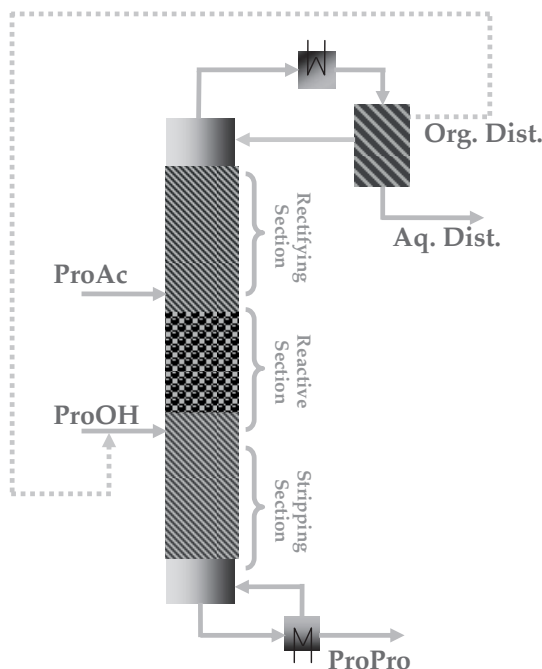
In esterification reactions performed in RD processes, one of the reactants is often fed in excess (in this case ProOH) in order to achieve the maximum conversion of the other. As a result, the distillate product is a mixture of the water produced, the excess of ProOH that does not react and some ProPro. An easy way to separate this mixture (as compared to distillation or membrane processes) is to take advantage of the phase split by coupling the column with a liquid-liquid separator and reflux back, part of the organic phase rich in ProOH and ProPro. The rest can be mixed with the ProOH feed. The schematic representation of the process can be seen in Figure 3.1. ProPro is collected at the bottom of the column together with the acid that did not react.

Table 3.1 Azeotropic data

Type of azeotrope	Temperature (°C)	Mass fraction (g/g)			
		ProOH	ProAc	ProPro	Water
Homogeneous	87.6	0.432	-	-	0.568
Homogeneous	99.9	-	0.050	-	0.950
Heterogeneous	90.0	-	-	0.350	0.650
Heterogeneous	86.2	0.350	-	0.130	0.520

For accurate process design, reliable kinetic and thermodynamic data are needed. In the case of thermo-physical data, the behaviour of the quaternary mixture can be built on the information of the six constituent binary systems. Buchaly et al.⁴ presented a set of UNIQUAC binary interaction parameters for the quaternary VLE calculation based on data extracted from ASPEN Properties PlusTM and data predicted using the UNIFAC-Dortmund method.⁵ Limited experimental data is available for some of the constituent binary pairs (Dortmund Data Bank (DDB2000)), these being predominantly not up to date. In addition, large differences in concentrations and temperatures are found among data sets of the same system. Consequently, more recent experimental data is needed for comparison. The experimental data found comprise: one data set⁶ for the binary system ProOH + ProAc, two data sets^{7,8} for the binary ProOH + ProPro, two data sets^{7,9} for water + ProPro, 66 data sets^{10,11} for ProOH + water and 31 data sets^{12,13} for the system water + ProAc. No experimental data was found for the system

Figure 3.1 Schematic representation of the proposed reactive distillation process for the synthesis of propyl propionate with a decanter separator on top for reactant and product recovery.



ProAc + ProPro. Finally, only one data set¹⁴ is available for the ternary system ProOH + water + ProPro. In this chapter, we present experimental vapour-liquid equilibrium data for the constituent binary systems, where scarce or no data is available and liquid-liquid equilibrium data of the ternary system that condensates at the column top. The experimental data were regressed using the tool built in ASPEN Properties PlusTM to describe the phase behaviour of the quaternary system inside the column and to predict the phase behaviour of the ternary mixture after phase split in a decanter.

3.2 Experimental

3.2.1 Chemicals

ProOH, ProAc and ProPro were purchased from Sigma-Aldrich. The purities of these components were reported to be more than $w = 0.995$ for ProOH and more than $w = 0.990$ for ProAc and ProPro. The reagents were degassed with an ultrasonic bath and dried over molecular sieve pellets from Sigma-Aldrich. Water used was bidistilled and deionized with an HPLC (Elgastat Maxima from Elga). The reagents were used without further treatment after being analyzed by gas chromatography. The densities were measured at 298.15 K using a density meter DMA 5000 (Anton Paar) with a reported uncertainty of $\pm 0.000005 \text{ g}\cdot\text{cm}^{-3}$. Boiling points of pure components were determined with the VLE apparatus. The pure component experimental values were compared with literature data showing good agreement and are presented in Table 3.2.

Table 3.2 Comparison of the Boiling Points T_B and Density ρ at 298.15 K of the Pure components with Literature Data

Component	T_B/K		$\rho/\text{g}\cdot\text{cm}^{-3}$	
	experimental	literature ^a	experimental	literature
1-propanol	370.29	370.93	0.80427	0.78102 ^b
propionic acid	414.53	414.31	0.99372	0.988797 ^b
propyl propionate	395.10	395.64	0.88162	0.8755 ^c
water	373.26	373.15	0.99822	0.98803 ^d

^a from ref. ¹⁵, ^b from ref. ¹⁶, ^c from ref. ¹⁷, ^d from ref. ¹⁸.

3.2.2 Apparatus and procedure

A glass Fischer LABODEST vapour-liquid equilibrium apparatus model 602/D, (Fischer Labor) was used in the VLE determinations. The apparatus is a dynamic recirculating still equipped with a Cottrell circulation pump. The pure component boiling points as well as the equilibrium temperatures were measured with a digital thermometer (Yokogawa model 7563) with an accuracy of ± 0.01 K. When the temperature remained constant for 30 min or longer, thermodynamic equilibrium was assumed and liquid and condensed vapour samples were taken for analysis. Liquid-liquid equilibrium measurements for the ternary mixture were performed at constant temperature. Mixtures of a known composition in the immiscibility region were prepared, poured inside glass vials with a magnetic stirrer and then placed in an isothermal bath with built in temperature control. The bath temperature was kept at 288.15 ± 0.02 K. The samples were stirred for 1 hour and then set for 24 hours. At this point, thermodynamic equilibrium was assumed and samples from both phases were taken with a syringe for analysis. Preliminary experiments were performed to establish the time to achieve equilibrium (no variation of composition in time).

3.2.3 Analysis

Vapor and liquid phases obtained in the experimental determination of binary VLE and ternary LLE were measured by gas chromatography with a Varian 3900GC instrument equipped with a flame ionization detector. The column used was a CP-Wax 58 FFAP CB (50m, 0.25mm, $0.2\mu\text{m}$ / CP7727) and helium was used as carrier gas. Injector, detectors and oven temperature were set at 473.15, 503.15 and 423.15 K, respectively. The column temperature profile started at 80°C , kept constant for 5 min, followed by a $60^\circ\text{C}/\text{min}$ ramp to 130°C , where it remained constant for an additional 15 min. A good peak separation was achieved under these conditions for all components. Samples were analyzed in triplicate. The reproducibility of the measurements was determined by doing repetitive analyses of the same sample using the calibrated GC. The standard deviation of the measurements (mole fraction) in the GC was ± 0.0015 . The quality of the calibration was evaluated by measuring several samples of known compositions three times and calculating the standard deviations between the known compositions and the GC measurements. The estimated uncertainty in the mole fraction of liquid and vapor compositions was 0.0045. For the systems containing water, data from the GC measurements (calculated by subtraction) was compared with results obtained from Karl-Fischer (KF) titration using a 756 KF Coulometer from Metrohm. The difference between KF and GC results was not greater than 0.0005 (mole fraction).

3.3 Thermodynamic equilibrium

3.3.1 Binary VLE measurements

Vapor-liquid equilibrium data for the binary systems were obtained under isobaric conditions at 101.3 kPa. When possible, experimental data from this work was compared to experimental data presented in literature to prove the correct operation of the equilibrium apparatus and the methods employed. For comparison, the UNIFAC-Dortmund group contribution method⁵ was used to generate data. All concentrations are expressed in mole fractions. The experimental data for the system ProOH (1) + ProAc (2) is presented in Figure 3.2. The experimental results from this binary pair, presented in this work, exhibit the largest deviation from data found in literature⁶ as can be seen in the graph where the x_1, y_1 and T, x_1, y_1 plots are shown. Since there was only one data set available for comparison, the UNIFAC-Dortmund group contribution method was used to predict the VLE behavior of the system. It can be seen that the experimental data from this work agree with the predicted values in both diagrams. Experimental data for the system ProOH (1) + ProPro (2) is presented in Figure 3.3 in terms of x_1, y_1 and T, x_1, y_1 diagrams. The x_1, y_1 diagram shows that our experimental data coincide very well with the data from Ortega et al.⁸ and the data from the UNIFAC-Dortmund model. Experimental data for the system ProPro (1) + ProAc (2) is presented in Figure 3.4. For this system, no literature data was available for comparison. The experimental data coincide well with the predicted UNIFAC-Dortmund model values in both x_1, y_1 and T, x_1, y_1 diagrams. Finally, the experimental data for the system water (1) + ProPro (2) is presented in Figure 3.5. This system shows an azeotrope determined in our experiments to be at $x_{\text{water}} = 0.6480$ and $T = 363.15$ K, which is in good agreement with previously reported data.^{4,19} The data from Mozzhukhin et al.⁷ deviate considerably at low water concentrations. Data predicted with the UNIFAC-Dortmund model follow well the experimental points in the x_1, y_1 diagram but fails in predicting the azeotrope temperature and composition.

3.3.2 Ternary LLE measurements

Liquid-liquid equilibrium data for the ternary system ProOH (1) + water (2) + ProPro (3) was obtained under isobaric conditions at 101.3 kPa and at a temperature of 288.15 K. Experimental data (tie lines) is presented in the published paper. The experimental data agree with the trend of data presented by Mozzhukhin et al.¹⁴ with experiments performed at 293.15 K. In Figure 3.6, the ternary diagram with the experimental tie line concentrations and the binodal curve is depicted. In this case, as the temperature is decreased, the immiscibility gap is reduced. To check the data consistency, the method of

Othmer-Tobias²⁰ was used. A linear relation from tie line concentrations was obtained with a squared regression value of 0.9797.

3.3.3 Model parameters

VLE experimental data were correlated using the UNIQUAC activity coefficient model in combination with the Hayden-O'Connell (HOC) equation of state.²¹ In this way liquid and vapor phase non-idealities are taken into account, incorporating the chemical theory of dimerization necessary due to the presence of ProAc. The starting relationship for calculating equilibrium at low or moderate pressures P , and temperatures T , of a given mixture is shown in Equation 3.1, where γ_i is the activity coefficient of component i , ϕ_i is the fugacity coefficient and x_i and y_i are the compositions of component i in the liquid and vapor phases, respectively.

$$y_i \phi_i(T, P, y) \cdot P = x_i \gamma_i(T, P, x) \cdot P_i^{sat}(T) \quad (3.1)$$

The vapor pressures of pure components at the given temperatures $P_i^{sat}(T)$ were calculated using the extended Antoine equation. Values of the surface area q and the molecular volume r were used in the UNIQUAC model. The pure component parameters used are available in the ASPEN Properties PlusTM library and are listed in Table 3.3. The thermodynamic behavior of the quaternary mixture can be built on the information of the six constituent binary systems by regressing separately each experimental data set finding the corresponding binary interaction parameters a_{ij} and $b_{ij}(T)$. The regression algorithm was calculated by minimizing the differences between estimated and experimental values considering the errors in the determination of all variables using the following objective function F_{VLE} :

$$F_{VLE} = \sum_{i=1}^{NP} \left[\left(\frac{T_{est,i} - T_{exp,i}}{\sigma_{T,i}} \right)^2 + \left(\frac{P_{est,i} - P_{exp,i}}{\sigma_{P,i}} \right)^2 + \sum_{j=1}^{NC-1} \left(\frac{x_{est,i,j} - x_{exp,i,j}}{\sigma_{x,i,j}} \right)^2 + \sum_{j=1}^{NC-1} \left(\frac{y_{est,i,j} - y_{exp,i,j}}{\sigma_{y,i,j}} \right)^2 \right] \quad (3.2)$$

Figure 3.2 Binary system 1-propanol (1) + propionic acid (2) at 101.3 kPa. ■ experimental data from this work; Δ , experimental data from ref 6; ---, data predicted using UNIFAC-Dortmund; —, data calculated using the regressed parameters with the UNIQUAC-HOC model.

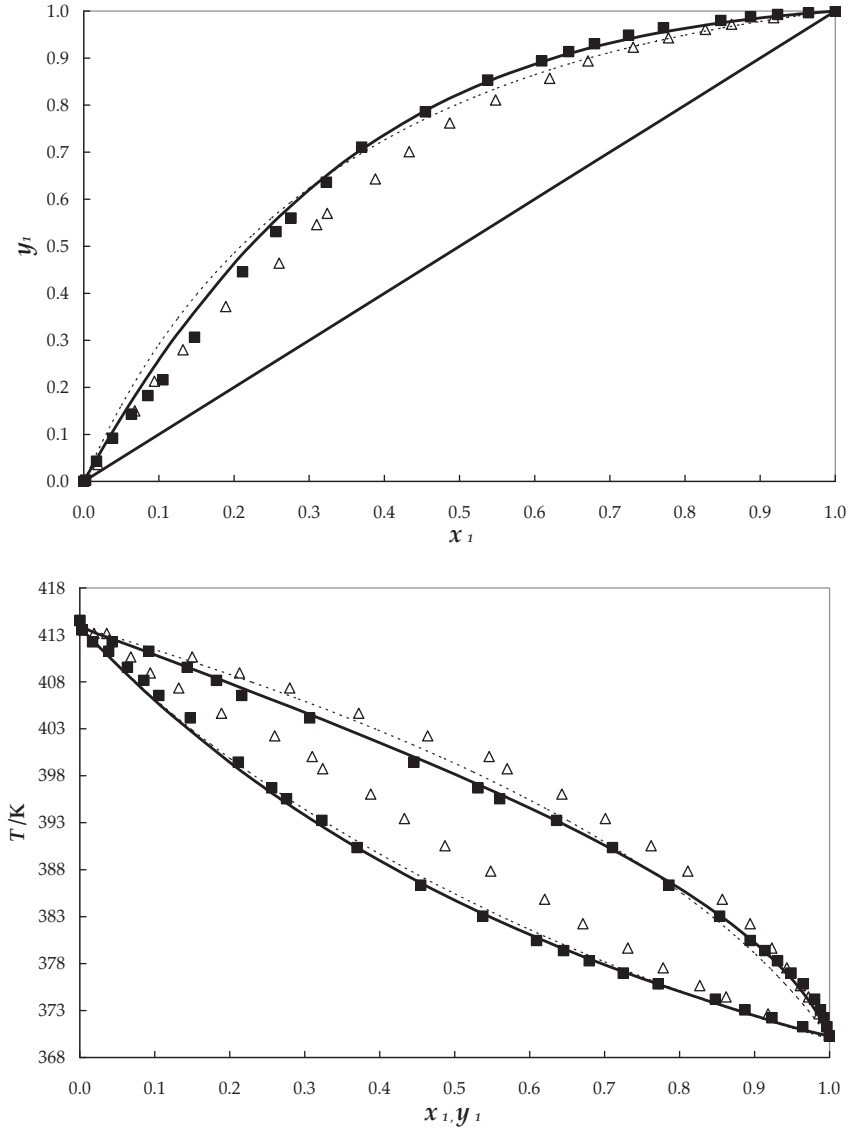


Figure 3.3 Binary system 1-propanol (1) + propyl propionate (2) at 101.3 kPa. ■ experimental data from this work; Δ , experimental data from ref ⁸; ---, data predicted using UNIFAC-Dortmund; —, data calculated using the regressed parameters with the UNIQUAC-HOC model.

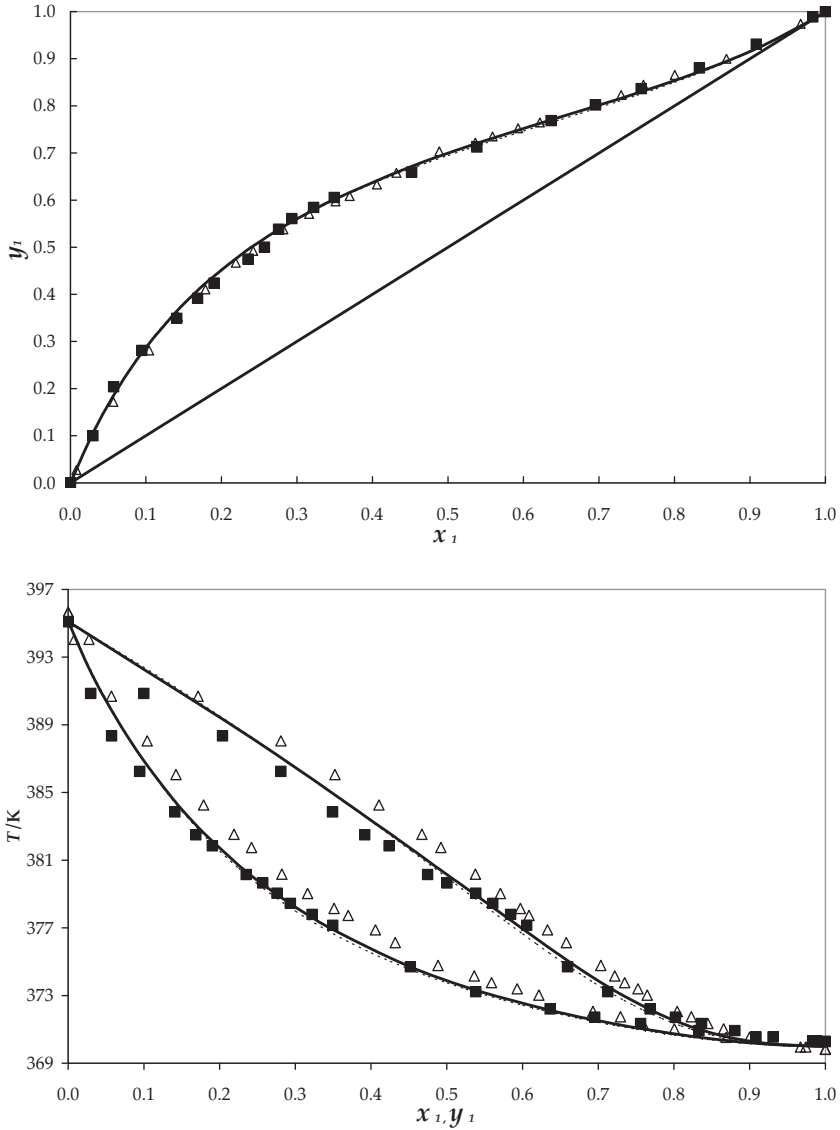


Figure 3.4 Binary system propyl propionate (1) + propionic acid (2) at 101.3 kPa.
■ experimental data from this work; ---, data predicted using UNI-FAC-Dortmund; —, data calculated using the regressed parameters with the UNIQUAC-HOC model.

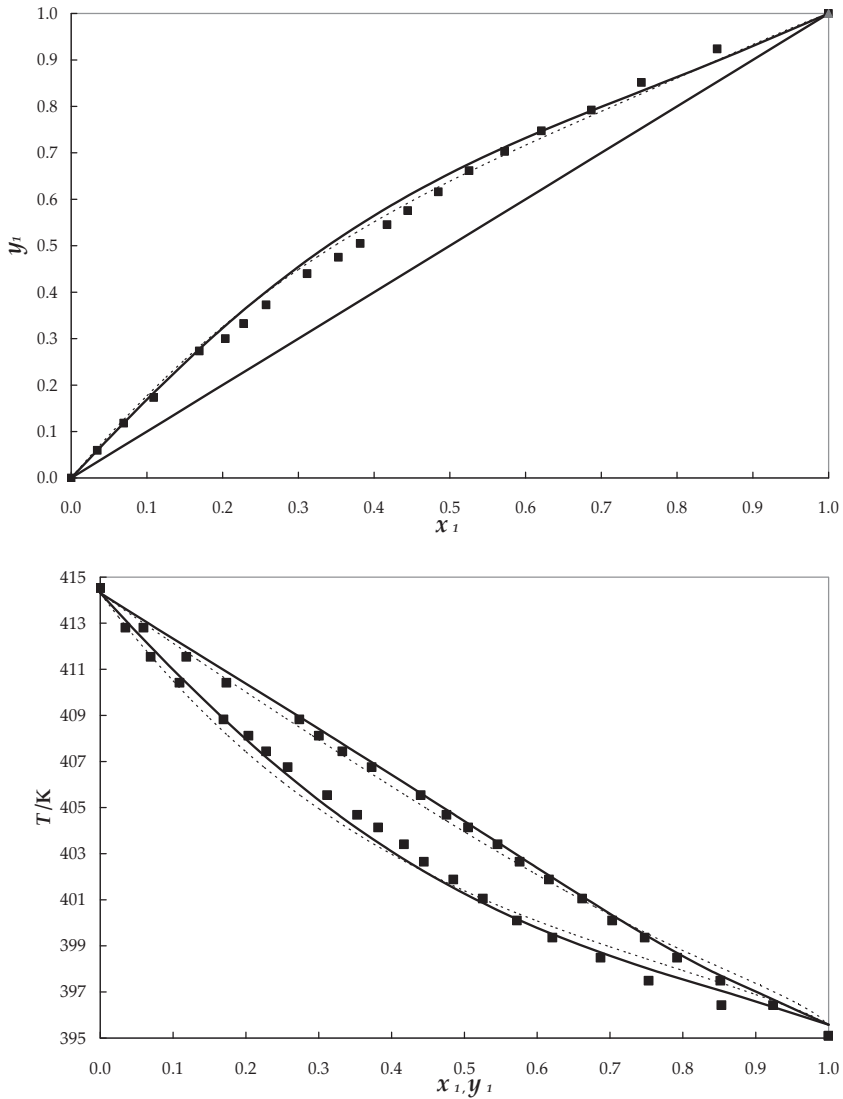


Figure 3.5 Binary system water (1) + propyl propionate (2) at 101.3 kPa.
■ experimental data from this work; Δ , experimental data from ref⁷; ---, data predicted using UNIFAC-Dortmund; —, data calculated using the regressed parameters with the UNIQUAC-HOC model.

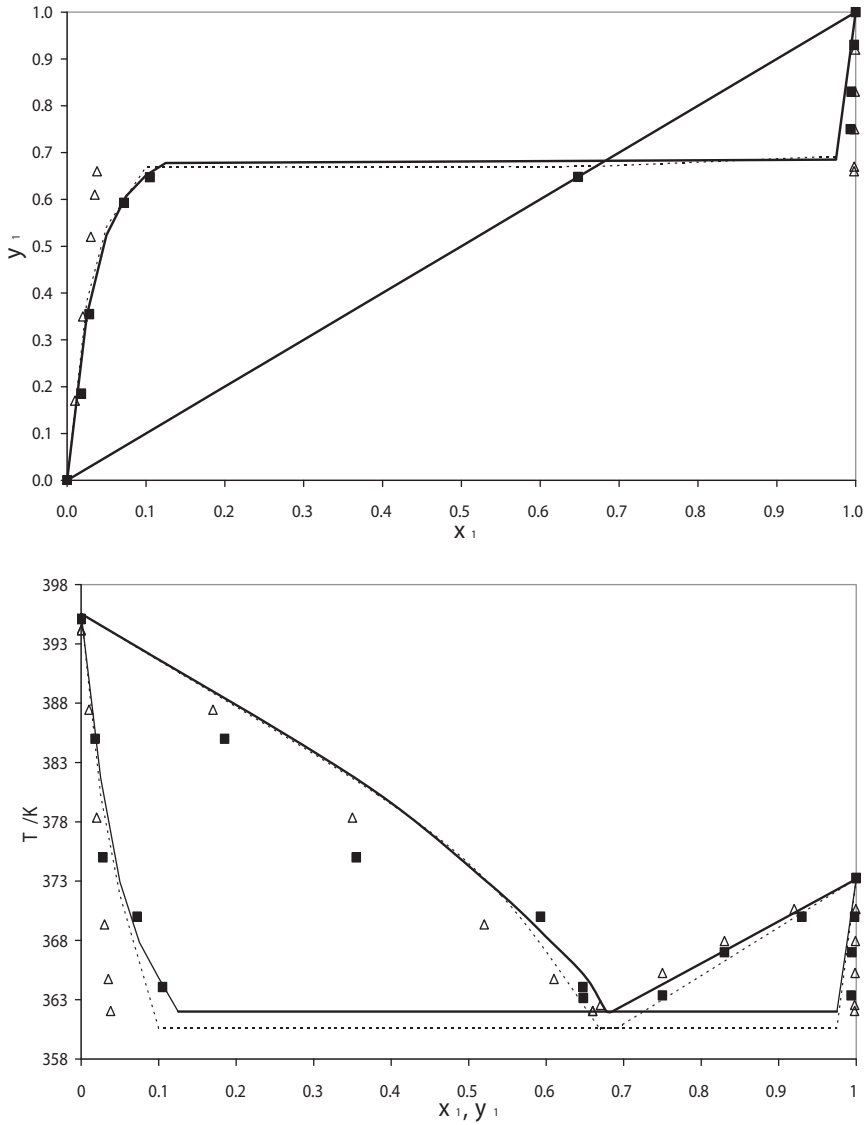
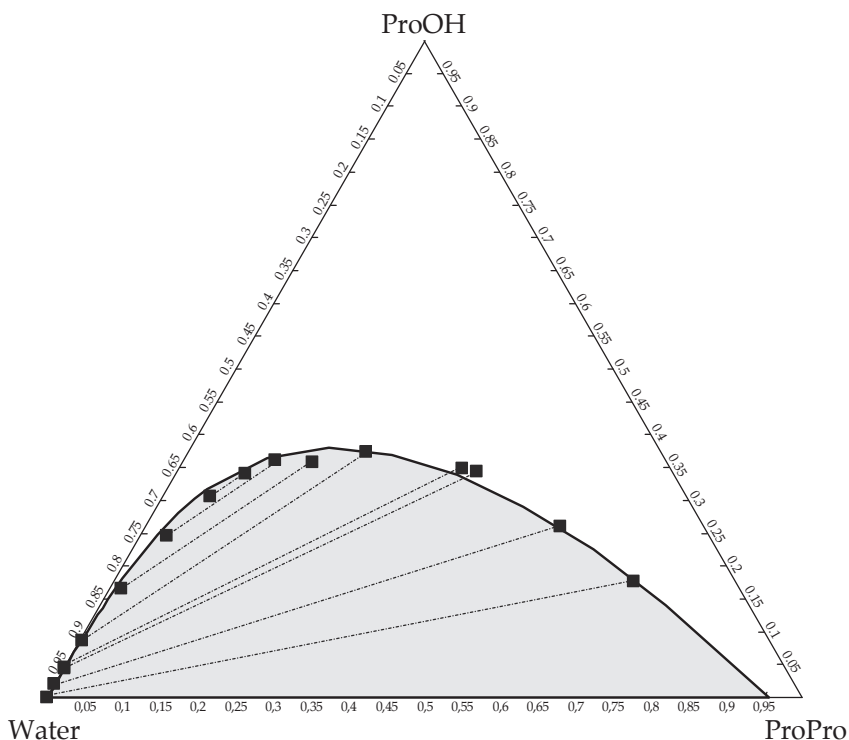


Figure 3.6 Ternary diagram for the system 1-propanol + water + propyl propionate at 101.3 kPa and 288.15 K with the binodal curve and experimental tie lines used for the prediction of phase split. ■, experimental data from this work; —, data calculated using the regressed parameters with the UNIQUAC model.



As seen in Figures 3.2 to 3.5, the UNIQUAC-HOC model is able to effectively describe the experimental data. The list of regressed binary interaction parameters along with the average mean deviations of temperature (ΔT) and vapor molar fractions (Δy) for the VLE data can be seen in Table 3.4. Binary parameters from the remaining two binary pairs ProOH + water and water + ProAc that were not measured experimentally in this work were extracted from Ref ⁴ and have been included in Table 3.4 as well. From the deviation values it is clear that the best fitted binary pair is the system ProOH (1) + ProAc (2) followed by ProPro (1) + ProAc (2). The non-ideal system of water (1) + ProPro (2) show minor deviations in temperature, clearly denoted in Figure 3.5.

Table 3.3 Physical Properties and Parameters for the Constituent Components^a

	water	1-propanol	propionic acid	propyl propionate
T_c /K	647.10	536.80	600.81	568.60
P_c /kPa	22064	5169	4617	3060
ω	0.345	0.620	0.574	0.449
$\mu \cdot 10^{-30}$ /C·m	6.163	5.596	5.836	5.963
r	0.92	2.78	2.86	4.83
q	1.40	2.51	2.61	4.20
C_1^b	73.65	94.13	54.55	78.32
C_2^b	-7258.2	-8604.8	-7149.4	-7256.9
C_3^b	0	0	0	0
C_4^b	0	0	0	0
C_5^b	-7.3037	-10.1100	-4.2769	-8.2280
C_6^b	4.17E-06	3.13E-06	1.18E-18	4.86E-06
C_7^b	2	2	6	2
C_8^b	273.16	146.95	252.45	197.25
C_9^b	647.1	536.8	600.8	568.6

^a Taken from Aspen Properties 2006 data bank: Critical Temperature T_c , Critical Pressure P_c , Acentric Factor ω , Dipole Moment μ , Surface Area r and Volume Parameter q Used in the UNIQUAC Model and parameters C_i for the Extended Antoine Equation with ^b
 $\ln(P^s) = C_1 + \frac{C_2}{T + C_3} + C_4 \cdot T + C_5 \cdot \ln(T) + C_6 \cdot T^{C_7}$ for $C_8 < T < C_9$ where P^s is in kPa and T in K.

Since the regressed UNIQUAC-HOC parameters were not able to satisfactorily represent the LLE behavior of the ternary system, a separate model was calculated with the experimental data obtained for the ternary mixture. The starting relationship for calculating LLE is shown in Equation 3.3, where $x_i^{(\text{Org})}$ is the composition of component i in the organic phase, $\gamma_i^{(\text{Org})}$ is the activity coefficient of component i in the organic phase and $x_i^{(\text{Aq})}$ and $\gamma_i^{(\text{Aq})}$ are the composition and activity coefficient of component i , respectively, in the aqueous phase.

$$x_i^{(\text{Org})} \cdot \gamma_i^{(\text{Org})} = x_i^{(\text{Aq})} \cdot \gamma_i^{(\text{Aq})} \quad (3.3)$$

Table 3.4 UNIQUAC Binary Interaction Parameters a_{ij} and b_{ij} Obtained from VLE Data and Average Mean Deviation of Temperature (ΔT) and Vapor Molar Fraction (Δy) Measured

component 1	component 2	i	j	a_{ij}	b_{ij}/K	ΔT	Δy
1-propanol	propionic acid	1	2	0.00	-281.0260	0.0067	0.0043
		2	1	0.00	195.6222		
1-propanol	propyl propionate	1	2	0.00	17.3160	0.2232	0.0032
		2	1	0.00	-122.7789		
propyl propionate	propionic acid	1	2	0.00	-413.3753	0.0928	0.0042
		2	1	0.00	204.9204		
water	propyl propionate	1	2	-4.47	1688.5940	1.2610	0.0194
		2	1	6.75	-3212.2200		
water	propionic acid	1	2	0.00	-244.8000	-	-
		2	1	0.00	73.80000		
1-propanol	water	1	2	1.84	-669.0000	-	-
		2	1	-2.41	620.8000		

The experimental data for the ternary mixture available was correlated using the UNIQUAC activity coefficient model to estimate the corresponding binary interaction parameters a_{ij} and $b_{ij}(T)$. The regression algorithm was calculated by minimizing the differences between estimated and experimental values considering the errors in the determination of all variables using the following objective function F_{LLE} :

$$F_{LLE} = \sum_{i=1}^{NP} \left[\left(\frac{T_{est,i} - T_{exp,i}}{\sigma_{T,i}} \right)^2 + \sum_{j=1}^{NC-1} \left(\frac{x_{est,i,j}^{Aq} - x_{exp,i,j}^{Aq}}{\sigma_{x,i,j}} \right)^2 + \sum_{j=1}^{NC-1} \left(\frac{x_{est,i,j}^{Org} - x_{exp,i,j}^{Org}}{\sigma_{x,i,j}} \right)^2 \right] \quad (3.4)$$

As seen in Figure 3.6, the UNIQUAC model with the regressed parameters is able to predict with good agreement the phase behavior of the ternary mixture at 288.15 K. The experimental tie lines agree with the calculated binodal curve; thus, the model can be used to predict phase split in a decanter and calculate the concentrations of the organic phase that will be recycled back to the column. The regressed parameters to model the phase behavior of the ternary mixture can be seen in Table 3.5.

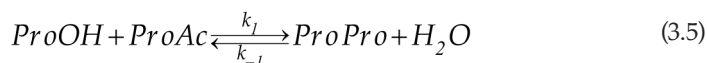
Table 3.5 UNIQUAC Binary Interaction Parameters a_{ij} and b_{ij} Obtained from LLE Data

component 1	component 2	i	j	a_{ij}	b_{ij}/K
1-propanol	water	1	2	0.0000	124.380
		2	1	0.0000	-310.440
water	propyl propionate	1	2	1.4741	-587.796
		2	1	1.3415	-928.157
1-propanol	propyl propionate	1	2	0.0000	131.270
		2	1	0.0000	-212.480

3.4 Reaction kinetics

The reaction scheme was described thoroughly in Chapter 2 in Figure 2.1 and by Equations 2.1 to 2.5. Duarte et al.²² studied extensively this reaction comparing various ion-exchange resins focusing specially on Amberlyst 15 and Amberlyst 46. He concluded that Amberlyst 46 was a more suitable catalyst than other counterparts due to the specificity towards ProPro avoiding DPE formation. In this research we used several experimental results from²² and performed the data regression to determine the equilibrium constants and the reaction rate needed for proper process design and modeling.

To model the synthesis of ProPro, a pseudo-homogeneous approach formulated in activities is proposed to calculate the reaction rate. Since the catalyst has the reactive sites (in this case sulfonic groups) only at the surface, it is reasonable to assume that the mixture will behave as if it was in the presence of a homogeneous catalyst. Thereby, it is not necessary to account in the model for the physical-chemical processes associated with adsorption and desorption mechanisms. Due to the strong liquid phase non-ideality of the mixture which include several azeotropes, a correction factor of the molar fractions is introduced with the activity coefficient calculated with the UNIQUAC model derived in section 3.3. The reversible reaction is described in Equation 3.5 with the rate constants k_1 for the forward and k_{-1} for the backward reaction.



At any given time, the rate of formation of a product and disappearance of a reactant is:

$$r_i = v_i \cdot \left(k_f(T) \cdot a_{ProAc} \cdot a_{ProOH} - k_{-f}(T) \cdot a_{ProPro} \cdot a_{H_2O} \right) \quad (3.6)$$

$$i = 1, \dots, n_c$$

At equilibrium, the rate of production is equal to zero:

$$k_f(T) \cdot a_{ProAc} \cdot a_{ProOH} = k_{-f}(T) \cdot a_{ProPro} \cdot a_{H_2O} \quad (3.7)$$

With:

$$K_{eq}(T) = \frac{k_f(T)}{k_{-f}(T)} = \frac{a_{ProPro} \cdot a_{H_2O}}{a_{ProAc} \cdot a_{ProOH}} \quad (3.8)$$

Rearranging equations 3.8 and 3.6 the following expression is obtained:

$$r_i = v_i \cdot \left(k_f(T) \cdot a_{ProAc} \cdot a_{ProOH} - \frac{k_f(T)}{K_{eq}(T)} \cdot a_{ProPro} \cdot a_{H_2O} \right) \quad (3.9)$$

$$i = 1, \dots, n_c$$

The temperature dependence of the equilibrium constant K_{eq} and the rate constant k_f was modeled via the Arrhenius approach.

$$k_f(T) = 4.28 \cdot 10^7 \exp\left(\frac{-5.78 \cdot 10^4}{R \cdot T}\right) \quad (3.10)$$

$$K_{eq}(T) = 3.49 \exp\left(\frac{-1.732 \cdot 10^4}{R \cdot T}\right) \quad (3.11)$$

The model is built using equations 3.9 through 3.11 and the thermodynamic parameters from table 3.4. As seen in Figures 3.7 and 3.8 the model is able to predict the experimental data with good agreement.

Figure 3.7 Experimental results and predicted data from the kinetic model.
Reaction conditions $T = 343.15\text{K}$, $m_{\text{cat}} = 10\text{g}$, $N_{\text{T}} = 9.7\text{ mol}$.

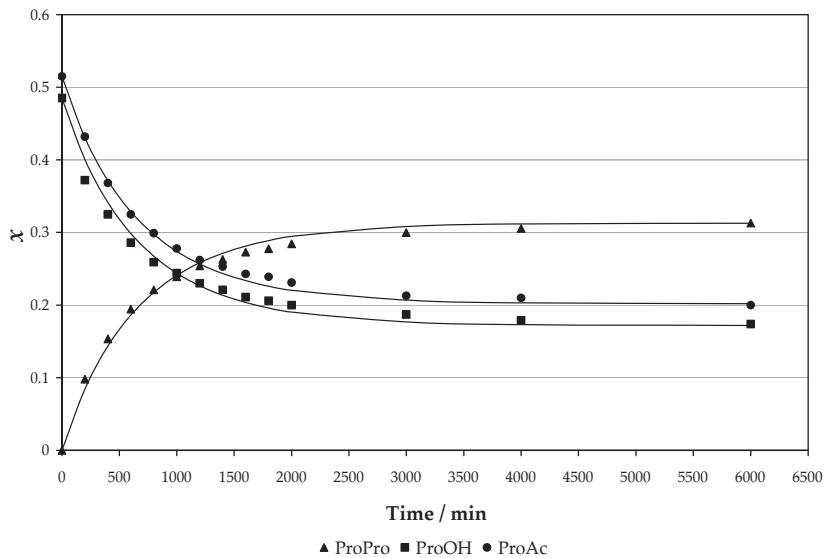
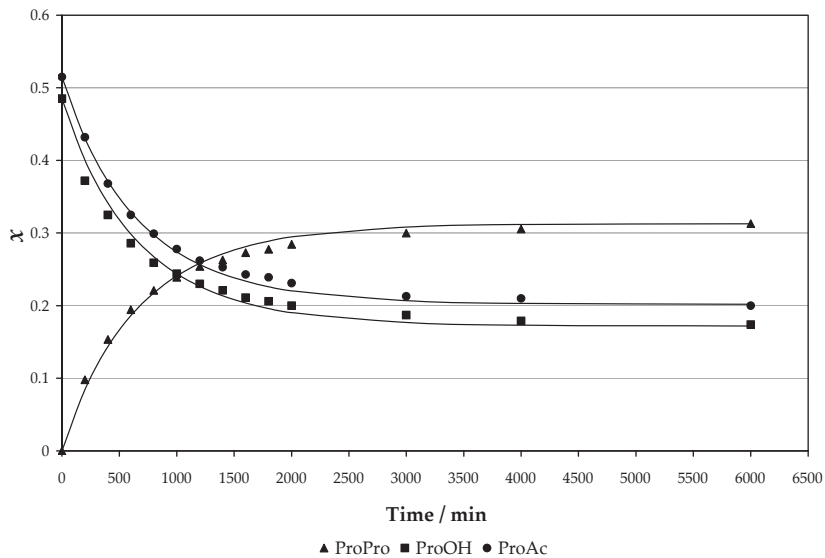


Figure 3.8 Experimental results and predicted data from the kinetic model.
Reaction conditions $T = 353.15\text{K}$, $m_{\text{cat}} = 10\text{g}$, $N_{\text{T}} = 9.27\text{ mol}$.

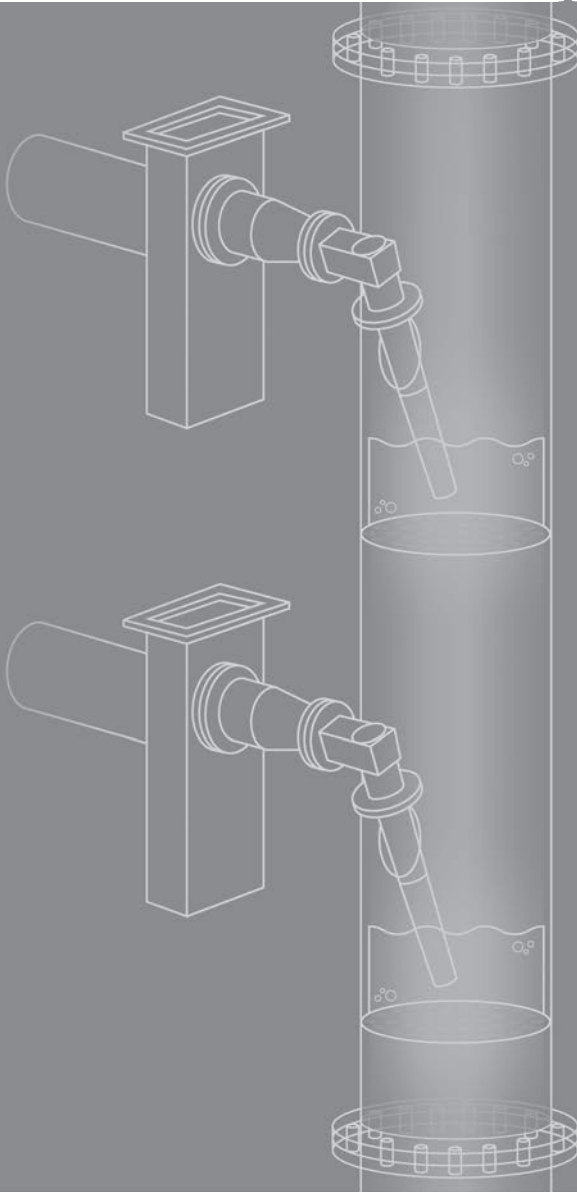


3.5 References

1. Calvar N., Dominguez A., Tojo J., Vapor-liquid equilibria for the quaternary reactive system ethyl acetate + ethanol + water + acetic acid and some of the constituent binary systems at 101.3 kPa. *Fluid Phase Equilibria*. **2005**. 235: 215-222.
2. Delgado P., Sanz M. T., Beltran, S., Isobaric vapor-liquid equilibria for the quaternary reactive system: Ethanol + water + ethyl lactate + lactic acid at 101.33 kPa. *Fluid Phase Equilibria*. **2007**. 255: 17-23.
3. Schmitt M., Hasse H., Phase Equilibria for Hexyl Acetate Reactive Distillation. *J. Chem. Eng. Data*. **2005**. 50: 1677-1683.
4. Buchaly C., Kreis P., Górak A., Hybrid separation processes-Combination of reactive distillation with membrane separation. *Chemical Engineering and Processing*. **2007**. 46: 790-799.
5. Gmehling J., Li J., Schiller M., A Modified UNIFAC (Dortmund) Model. 2. Present parameter matrix and results for different thermodynamic properties. *Ind. Eng. Chem. Res.* **1993**. 32: 178-193.
6. Amer Amezaga S., *Anal. Quim.* **1975**. 71: 117-126.
7. Mozzhukhin A.S., Mitropolskaya V. A., Serafimov, L. A., Torubarov, A. I., Rudakovskaya, T.S., Liquid - vapour and liquid-liquid phase equilibria in the 1-propanol-water-propyl propionate system at 760 mmHg. *Zh. Fiz. Khim.* **1967**. 41(1): 116-119.
8. Ortega J., Galvan S., Vapor-Liquid Equilibria of Propyl Propionate with 1-Alkanols at 101.32 kPa of Pressure. *J. Chem. Eng. Data*. **1994**. 39(4): 907-910.
9. Bomshtein A.L., Trofimov A. N., Kudakina E. N., Serafimov L.A., *Oniitekhim*. **1983**. Code 336 KHP - D83: 1-12.
10. Gabaldon C., Marzal P., Monton J. B., Rodrigo M.A., Isobaric vapor - liquid equilibria of the water + 1-propanol system at 30, 60 and 100 kPa. . *J. Chem. Eng. Data*. **1996**. 41(5): 1176-1180.
11. Vercher E., Rojo F. J., Martinez-Andreu A., Isobaric Vapor-Liquid Equilibria for 1-Propanol + Water + Calcium Nitrate. *J. Chem. Eng. Data*. **1999**. 44(6): 1216-1221.
12. Amer Amezaga S., *Anal. Quim.* **1975**. 71: 127-135.
13. Kushner T.M., Tatsievskaya G. I., Serafimov L. A., *Zh. Fiz. Khim.* **1967**. 41(1): 237-243.
14. Mozzhukhin A.S., Serafimov L.A., Mitropolskaya V.A., Sankina L.M., *Liquid - vapour and liquid-liquid phase equilibria in the 1-Propanol-water-propyl propionate system at 760 mmHg*, in *Russ. J. Phys. Chem.* 1967. p. 902-903.
15. Poling B.E.P., O'Connell J. P., *The Properties of Gases and Liquids*. 5th ed, ed. McGraw-Hill. **2001**, New York: McGraw-Hill.
16. Pang F.M., Seng C. E., Teng T. T., Ibrahim M. H., Densities and viscosities of aqueous solutions of 1-propanol and 2-propanol at temperatures from 293. 15 to 333.15 K. *J. Mol. Liq.* **2007**. 136: 71-78.
17. Petrino P.J., Gaston-Bonhomme Y. H., Chevalier J. L. E., Viscosity and Density of Binary Liquid Mixtures of Hydrocarbons, Esters, Ketones, and Normal Chloroalkanes. *J. Chem. Eng. Data*. **1995**. 40: 136-140.
18. Sato H., Uematsu, M., Watanabe K., Saul A., Wagner W., Tables for the Thermodynamic Properties of Ordinary Water Substance. *J. Phys. Chem. Ref. Data*. **1988**. 17: 1439- 1540.
19. Bomshtein A.L., Serafimov L.A., Liquid-Liquid Phase Equilibrium. *J. Appl. Chem. USSR*. **1984**. 57(1): 14-18.
20. Othmer D.F., Tobias P. E., Tie Line Correlation. *Ind. Eng. Chem. Res.* **1942**. 34(6): 693-696.
21. Hayden J.G., O'Connell J. P., A Generalized Method for Predicting Second Virial Coefficients. *Ind. Eng. Chem. Res.* **1975**. 14(3): 209-216.
22. Duarte C. *Production of TAME and n-Propyl Propionate by Reactive Distillation*. Chemical Engineering. **2006**, Universidade do Porto. Porto.



Part II



Conventional Activation

Feasibility Analysis Using Residue Curve Mapping in Reactive Distillation

Reactive distillation design is a complex task. There are several methodologies available in literature that can be used to conceptually design RD processes including graphical, optimization-based and heuristic techniques. In this chapter we have used a practical method called Residue Curve Mapping (RCM) in combination with some heuristic rules to deal with the design problem. To be able to build the RCMs for the test system, the physical properties from Chapter 2 and the thermodynamic model and equilibrium constant expression derived in Chapter 3 are used. The methodology as well as the mathematical expressions is clearly described for two case scenarios. First we address the non-reactive case (only separation is considered) to analyze the topology of the system and to check the existence of distillation boundaries. Then the reactive case is analyzed addressing the changes to the phase behavior of the system and changes in the diagram topology. The results from the RCMs show that it is possible to produce high purity n-propyl propionate using a single column depending on the composition of the feed. With the information gathered from the residual lines and basic heuristic rules a column configuration is proposed for experimentation.

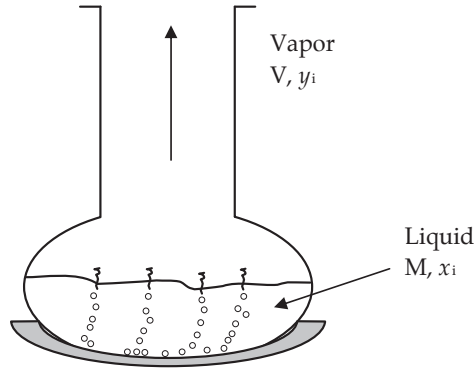
“The first principle is that you must not fool yourself and you are the easiest person to fool”

Richard P. Feynman

4.1 Introduction to Residue Curve Mapping

Residue curve maps (RCMs) are thermodynamic diagrams that cover the whole composition space and give valuable information for the design of separation processes. Their importance lies in the possibility to explicitly see in a visual representation the existence of distillation boundaries (separation constraints) and thus assess the separation feasibility of any given equilibrium-based process. RCMs can be considered as a prerequisite before any attempt is made in reactive distillation experimentation. They are constructed based on phase equilibrium data (vapor-liquid, liquid-liquid, and solid-liquid equilibria) and the system's physical properties thus being suitable for commonly used separation methods. In the case of distillation, the concentration profiles in the liquid phase can be either experimentally determined or theoretically calculated for the ideal situation of equipment operating at infinite reflux conditions with infinite number of stages. This assumption renders small errors for real finite columns that can be neglected at the early stages of design.¹ Soon after the first commercial reactive distillation (RD) process by Eastman Chemical² was disclosed, the first papers on RCMs applied to RD appeared.^{3,4} The original mathematical expressions of non-reactive RCMs were expanded to RD by overlapping the chemical reaction, first assuming chemical equilibrium and later using rate equations and kinetic expressions.⁵⁻⁸ In theory, RCMs for RD can be constructed for successive chemical reactions with n number of components but they can only be represented graphically for up to four, as it becomes difficult to visualize the diagram in a mole fraction coordinate scheme.⁹ As the case system chosen is a four component mixture ProOH/ProAc/ProPro/Water, a three-dimensional tetrahedron is used.

RCMs can be experimentally determined with a simple test following the so called *residue curves* (RC). A liquid with known composition (feed) is placed in a single stage batch still (Fig. 4.1) that is heated up without reflux. The composition of the liquid (residue) is continuously monitored over time until the last drop is vaporized. The resulting plot of the change in liquid composition is the RC.

Figure 4.1 Single stage batch still for experimental determination of RCMs.

RCMs can be generated mathematically as well, by integrating the mass balances and thermodynamic equilibrium relationships that describe the single batch still from Fig. 4.1.

$$\frac{dM}{dt} = -V \quad (4.1)$$

$$\frac{d(x_i M)}{dt} = x_i \frac{dM}{dt} + M \frac{dx_i}{dt} = -y_i V \quad (4.2)$$

The mass balance over the single stage still gives Equations 4.1 and 4.2 with M being the mass of liquid in the system, V the vapor flow, x_i the molar composition of component i in the liquid phase and y_i the molar composition of component i in the vapor phase. For $i=1 \dots n$ number of components present in the system.

$$d\tau = \frac{V}{M} \cdot dt \quad (4.3)$$

Replacing Eq. 4.1 in Eq. 4.2 and introducing a nonlinear time expression from Eq. 4.3 a new RCM equation is obtained where \underline{x} is the composition vector in the liquid phase and \underline{y} is the composition vector in the vapor phase.

$$\frac{d\underline{X}}{d\tau} = \underline{x} - \underline{y} \quad (4.4)$$

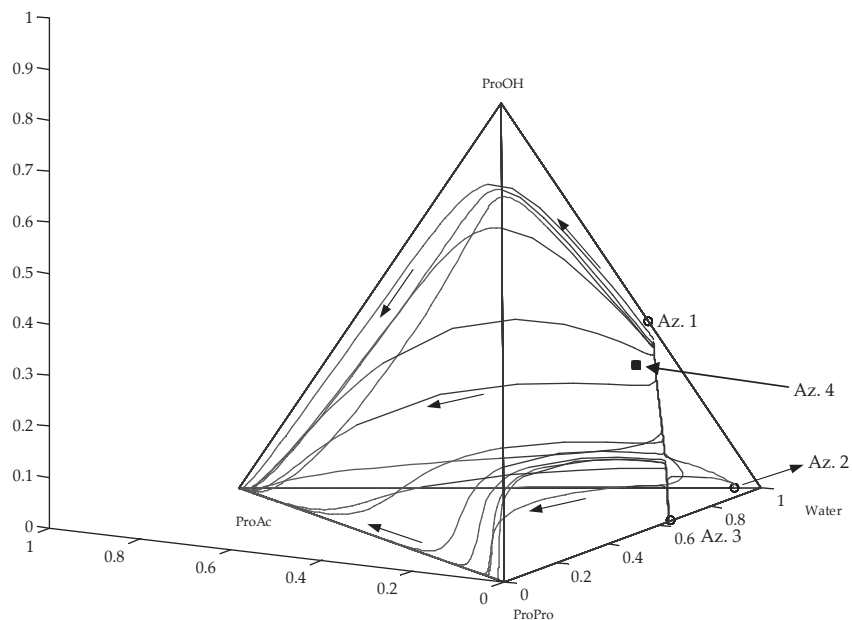
Combining the $n-1$ independent equations using equation 4.4 integrated with the vapor-liquid equilibrium model from *Chapter 3*, the set of equations that construct the RCMs are defined:

$$\frac{dx_i}{d\tau} = x_i - y_i \quad (4.5)$$

$$y_i = f(T, P, x_i) \quad (4.6)$$

$$\sum_{i=1}^n x_i = \sum_{i=1}^n y_i = 1 \quad (4.7)$$

To be able to assess the design of RD via the use of RCMs, two simulation problems have to be solved: the non-reactive and the reactive case. These set of simultaneous differential and nonlinear algebraic equations were programmed using the MATLAB® version 7.5.0 software (MathWorks) in combination with the thermodynamic model using the UNIQUAC activity coefficient model with the Hayden-O'Connell (HOC) equation of state (Eq. 3.1). To solve the algorithm, the built in function ODE45 is used. The integrator gives a numerical solution of the ordinary differential equations based on variable step size Runge-Kutta integration methods. Initial molar compositions in the non-reactive case and transformed variables in the reactive case need to be specified to solve the model and generate RCs that cover completely the composition space. The visual examination of the map gives insight on the behavior of the system.

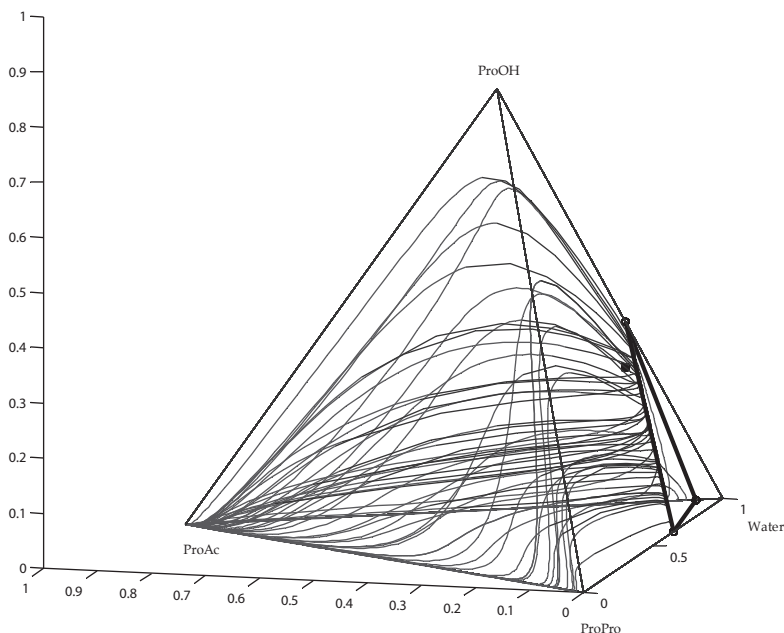
Figure 4.2 Non-reactive RCM for the quaternary system.

4.2 Non-reactive RCMs

By integrating equation 4.5 forward and backward in time from different starting feed compositions, a group of curves is obtained thus building the RCMs. Figure 4.2 depicts the quaternary non-reactive RCM diagram for the case system. The first step in the interpretation of the map is to identify the topology of the RCM. This includes the identification and the location of the azeotropes and determine whether they are *minimum-boiling* (have a lower boiling point than that of any of the components involved) or *maximum-boiling* (have a higher boiling point). For the case system three azeotropes (Az. 1, 3 and 4) are *minimum-boiling*. Besides it is important to identify pure components and azeotropes as stable or unstable *nodes* and *saddles*. As a general rule RCs will always head off towards points with increased temperature. This means that RCs will diverge from low-boiling vertices (pure components or azeotropes) and converge toward high-boiling vertices. *Nodes* are the starting and end points of RCs and can be pure components, or binary or ternary azeotropes. All other vertices are *saddles*. To determine the nature of pure-component vertices, we have followed the procedure from ref. ⁸ drawing arrows on every segment of the ternary faces

from the tetrahedron between pure components and binary azeotropes and let these point toward the segment end with the highest boiling temperature. Stable nodes will only have arrows pointing inward, unstable nodes will have all arrows pointing outward, and saddles will have some arrows pointing inward and some pointing outward.

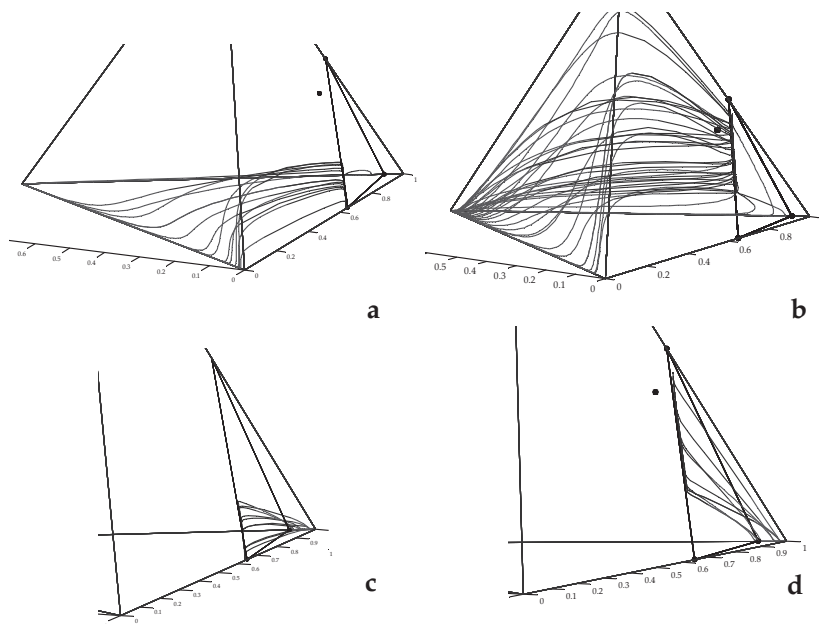
Figure 4.3 Non-reactive RCM for the quaternary system showing the boundary plane.



By looking carefully at Figure 4.2 one can identify two stable nodes, ProAc and Water, two unstable nodes; ProPro and Az. 3 and four saddles; ProOH, Az. 1, Az. 2 and Az. 4. The azeotropic data is resumed in Table 4.1. Once the topology of the RCM has been identified, the distillation boundaries or regions can be outlined. An accurate analysis of the non-reactive RCM reveals that there are two distillation regions. When rotating Figure 4.2, it is possible to identify a nonreactive distillation boundary plane formed by a triangle between the three azeotropes Az. 1, Az. 2 and Az. 3, as depicted in Figure 4.3. This boundary divides the composition space into a region where pure ProPro can be obtained and a region that for practical purposes is not interesting where pure water can be obtained.

Table 4.1 Azeotropic data.

Nr.	Type of azeotrope	Temperature (°C)	Mass fraction (g/g)				Node	Saddle
			ProOH	ProAc	ProPro	Water		
Az. 1	Homo	87.6	0.432		-	0.568		X
Az. 2	Homo	99.9	-	0.050	-	0.950		X
Az. 3	Hetero	90.0	-	-	0.350	0.650	Unstable	
Az. 4	Hetero	86.2	0.350	-	0.130	0.520		X

Figure 4.4 Non-reactive RCM for the quaternary system showing the boundary plane with the four possible trajectories of the RCs.

Besides the saddles and nodes mentioned, there is one composition lying on one side of the boundary plane between Az.1 and Az. 3 that divides each composition space in two parts. The way to identify this point is to draw a family of curves and follow the trajectories. Figure 4.4 shows the four options, two for

each composition space. Figures 4.4.a and 4.4.b describe the composition trajectory that will end in the ProAc vertex but in case *a*, the lines approach the ProPro vertex while in case *b* the lines head towards the ProOH vertex and falling afterwards. Figures 4.4.c and 4.4.d illustrate the lines in the second composition space showing lines that bend at this saddle point and head towards the water vertex.

4.3 RCMs with chemical reactions

The general theory for the construction of RCMs considering multiple chemical reactions and including non-reacting components (inerts) was derived by Ung and Doherty.^{9,10} The equations and procedures for assessing azeotropy, separation feasibility and design in the non-reactive case can be applied to reactive systems by using a set of transformed composition coordinates. When a mixture of n components undergoes n_{rx} simultaneous equilibrium chemical reactions, the RCM expression may be described in terms of transformed molar compositions X_i and Y_i and the reaction non-linear time:

$$\frac{dX_i}{d\tau} = X_i - Y_i \quad i = 1 \dots (n_c - n_{rx} - 1) \quad (4.8)$$

with:

$$X_i = \frac{x_i - v_i^T (v_{ref})^{-1} x_{ref}}{I - v_{total}^T (v_{ref})^{-1} x_{ref}} \quad i = n_c - n_{rx} \quad (4.9)$$

$$Y_i = \frac{y_i - v_i^T (v_{ref})^{-1} y_{ref}}{I - v_{total}^T (v_{ref})^{-1} y_{ref}} \quad i = n_c - n_{rx} \quad (4.10)$$

$$v_{ref} = \begin{pmatrix} v_{(n-n_{rx}+1,1)} & \dots & v_{(n-n_{rx}+1,n_{rx})} \\ \cdot & v_{(i,r)} & \cdot \\ v_{(n,1)} & \dots & v_{(n,n_{rx})} \end{pmatrix} \quad (4.11)$$

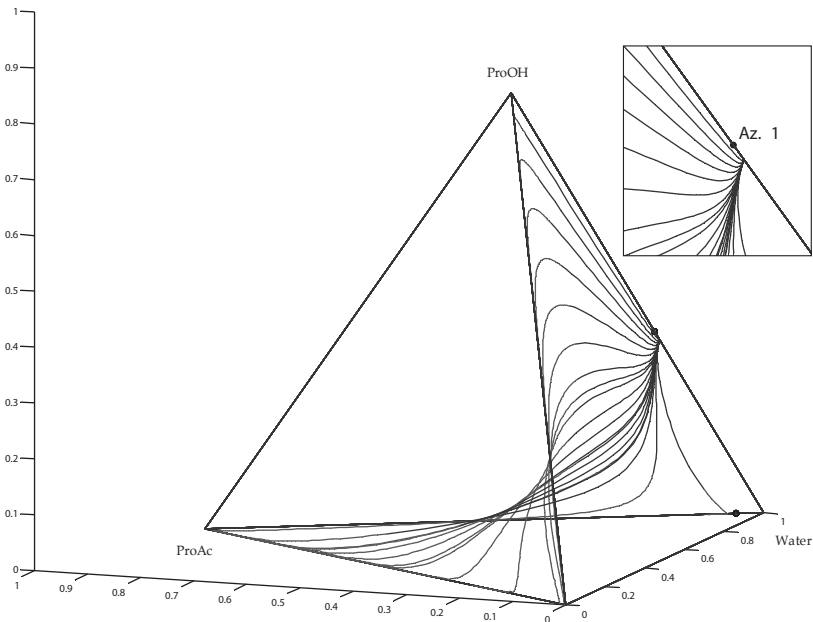
$$d\tau = \left(\frac{I - v_{total}^T (v_{ref})^{-1} y_{ref}}{I - v_{total}^T (v_{ref})^{-1} x_{ref}} \right) \cdot \frac{V}{M} \cdot dt \quad (4.12)$$

Including the calculation of the chemical equilibrium constant for the multi-component vapor-liquid mixture:

$$K_{eq} = \prod_{i=1}^{i=nc} (\gamma_i \cdot x_i)^{v_i} \quad (4.13)$$

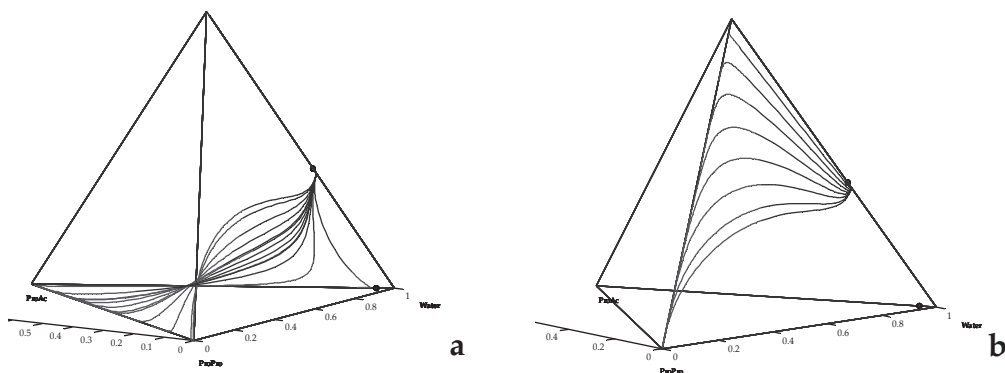
The problem can be solved by specifying one variable (in this case $P=1.023$ bar) and solving simultaneously equations 4.8 to 4.13. The superposition of a chemical reaction on separation can bring important modifications to the phase behavior of a system and changes in the diagram topology.¹¹ These include the formation of so called reactive azeotropes which are not present in the non-reacting system and can limit the separation inside a RD column in the same way that ordinary azeotropes do in conventional distillation. In other cases the reaction eliminates ordinary azeotropes that are present in the non-reacting system thus contributing to the separation.^{3,4} For the test system, ProPro was chosen as the reference component to calculate the transformed composition space. Figure 4.5 shows the RCMs when the chemical reaction takes

Figure 4.5 RCM for the quaternary system with equilibrium reaction.



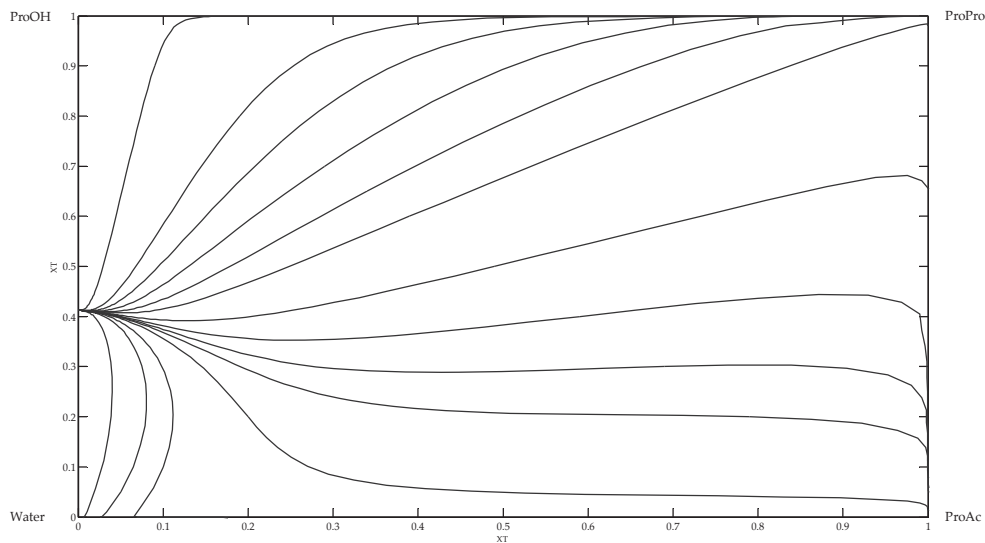
place. All the reactive residue curves start at a new binary reactive azeotrope with a composition very close to that of azeotrope (Az. 1) and end in either the pure ProAc vertex or the pure ProPro vertex. The trajectory of the lines depends on the initial composition of the feed. For feeds close to equimolar conditions (Figure 4.6.a), the RCs will end in pure ProAc. For feeds with an excess of alcohol (Figure 4.6.b), the RCs will end in pure ProPro.

Figure 4.6 RCM for the quaternary system with equilibrium reaction, trajectories ending in pure ProAc (a) and in pure ProPro (b).



Another way to visualize the RCMs with simultaneous chemical reaction and phase equilibrium is to use Doherty's composition transformations and graph the new variables in a 2D plot as shown in Figure 4.7. This transformed composition space shows clearly the reactive azeotrope and the end of the RCs, either in pure ProAc or pure ProPro.

Figure 4.7 RCMs with simultaneous chemical reaction and phase equilibrium using Doherty's composition transformations. ProPro is used as reference component.



4.4 Column configuration

Using the results obtained from the RCMs in combination with some heuristic rules it is possible to propose a feasible process for the synthesis of ProPro in a single RD column. The information gathered from the RCMs show that:

- By using the correct concentration of reagents in the feed composition (e.g. excess of ProOH) the process in a single RD unit will yield pure ProPro at the bottom and an azeotropic mixture of water and ProOH at the column top (Figure 4.6.b). If no excess of alcohol is used, then the bottom product will be a mixture of unreacted ProAc and ProPro.
- The three binary azeotropes are "reacted away" when the chemical reaction occurs. The boundary plane from the non-reactive case is not visualized in the RCMs with chemical reaction.
- The reactive azeotrope is a stable node.
- The ternary azeotrope is likely to occur under certain process conditions and if the concentrations of ProPro/Water/ProOH and temperature are adequate.

It is very important to know the phase split in the ternary diagram (Figure 3.6) and its dependence with temperature to avoid two liquid phases inside the column.

The previous statements are not enough to materialize the concept of a RD process. They determine however the feasibility of the process for a certain range of conditions. By using heuristic rules the conceptual design can be complemented as follow:

- a) Due to the difference in boiling points of the reagents, it is not possible to have only one feed flow to the column. If they were to come together in a single feed, most of the ProOH ($T_b=97.78^\circ\text{C}$) will evaporate and be distilled while most of the ProAc ($T_b=141.16^\circ\text{C}$) will fall down to the bottom. Two feed flows shall mark the reactive section of the column, the acid being fed at the top and the alcohol being fed at the bottom thereby ensuring extensive countercurrent contact of both reactants.
- b) The maximum operating temperature of the ion-exchange resin catalyst is 120°C . Above this temperature the catalyst is inactivated (Chapter 3, section 3.4). In order to protect the catalyst, there should be a safe zone between the reboiler and the reactive section of the column.
- c) The azeotropic mixture obtained at the column top contains valuable ProOH that did not react. A downstream process is needed (e.g. decanter, membrane or distillation column) to recover the alcohol.
- d) Above the reactive section and depending on the column operating conditions a ternary mixture of ProPro/Water/ProOH may exist. The number of stages must be such that mixture is rectified to recover as much as possible ProPro that was distilled.

Collectively, using the RCM approach it is possible to explore the feasibility and the limits of the RD process. We have shown in the information contained herein, that an excess of alcohol is needed to produce high purity ProPro. It must be considered however that the process performance is influenced by many more parameters (e.g. size and location of reactive and non-reactive column sections, reflux ratio, feed stages, number of stages, throughput) affecting the product yield. According to the thermodynamic information gathered in Chapter 3 regarding liquid-liquid equilibrium, it would be possible to recover part of the excess of alcohol in an economic way by using the big immiscibility gap of the ternary mixture ProPro/Water/ProOH using the phase split. Consequently a reactive distillation process in a single column coupled with a decanter on top is proposed for the synthesis of ProPro. To prove experimentally

the concept, the pilot-scale reactive distillation column installed in the laboratory facilities at the Technical University of Dortmund was used. The equipment had the following characteristics:

- a) The glass column had 50mm inner diameter and operating pressure of 1 bar.
- b) Stripping and enrichment sections used conventional structured packing.
- c) The heterogeneous catalyst was immobilized in structured catalytic packing.

In the following chapter, the results of the experiments in the RD column described above are discussed.

4.1 References

1. Fien G.J.A.F., Liu Y. A., Heuristic Synthesis and Shortcut Design of Separation Processes Using Residue Curve Maps: A Review. *Industrial and Engineering Chemistry Research*. **1994**. 33: 2505-2522.
2. Agreda V.H., Partin L. R., *Reactive distillation process for the production of methyl acetate*, in U.S. Patent, U.S. Patent, Editor. 1984: USA.
3. Barbosa D., Doherty M. F., The influence of equilibrium chemical reactions on vapor-liquid phase diagrams. *Chemical Engineering Science*. **1988a**. 43: 529-540.
4. Barbosa D., Doherty M. F., The simple distillation of homogeneous reactive mixtures. *Chemical Engineering Science*. **1988b**. 43: 541-550.
5. Bessling B., Schembecker G., Simmrock K. H., Design of Processes with Reactive Distillation Line Diagrams. *Industrial and Engineering Chemistry Research*. **1997**. 36: 3032-3042.
6. Doherty M.F., Buzad G., Reactive distillation by design. *Trans. IChemE*. **1992**. Part A: 448-458.
7. Song W., Venimadhavan G., Malone M.F., Doherty M.F., Measurement of Residue Curve Maps and Heterogeneous Kinetics in Methyl Acetate Synthesis. *Industrial and Engineering Chemistry Research*. **1998**. 37: 1917-1928.
8. Fien G.-J.A.F., Liu Y. A., Heuristic Synthesis and Shortcut Design of Separation Processes Using Residue Curve Maps: A Review. *Industrial and Engineering Chemistry Research*. **1994**. 33: 2505-2522.
9. Ung S., Doherty M. F., Vapor-Liquid Phase Equilibrium in Systems with Multiple Chemical Reactions. *Chemical Engineering Science*. **1995**. 50: 23-48.
10. Ung S., Doherty M. F., Calculation of residue curve maps for mixture with multiple equilibrium chemical reactions. *Industrial and Engineering Chemistry Research*. **1995**. 34: 3195-3202.
11. Jimenez L., Wanhshafft O. M., Julka V., Analysis of residue curve maps of reactive and extractive distillation units. *Computer and Chemical Engineering*. **2001**. 25: 635-642.

Experimental, Modeling and Simulation of Reactive Distillation

This chapter presents experimental, modeling and simulation results of the heterogeneously catalyzed synthesis of n-propyl propionate (ProPro) performed in a conventional reactive distillation (RD) process that was improved. With the objective to recover product and reactant, an experimental column set-up was equipped with a decanter on top enabling the separation of the distillate product into two main streams. The aqueous phase was discharged and part of the organic phase was refluxed back to the column. Experimental results comprising temperature and composition column profiles were obtained in a pilot-scale column (DN-50), equipped with structured packings (Sulzer BX and Katapak-SP 11 with Amberlyst 46TM for the reactive part). For simulation studies a non-equilibrium stage model (NEQ model) was applied which shows satisfactory agreement with the performed experiments. Further theoretical investigations of relevant operating parameters (total feed, molar feed ratio, reflux ratio and heat duty) and their effect on the overall process performance were realized running model simulations. Studies with the given column configuration showed that product purity in the bottom stream could be increased to $w_{\text{ProPro, bottom}} = 91.0\%$ and maximum ProAc conversions to $X_{\text{ProAc}} = 94.5\%$ obtained. The experimental and theoretical data gathered in this chapter can be used to effectively design an industrial scale process.

The contents of this chapter were adapted from the work published in:

E. Altman, P. Kreis, T. van Gerven, G.D. Stefanidis, A. Stankiewicz, A. Górak
“Pilot plant synthesis of n-propyl propionate via reactive distillation with decanter separator for reactant recovery. Experimental model validation and simulation studies.”

Chem. Eng. Process., **49** (2010) 965-972; DOI:10.1016/j.cep.2010.04.008

© 2010 Elsevier B.V. Reprinted with permission.

“What we have to learn to do, we learn by doing.”

Aristotle

5.1 The relevance of reactive distillation

In today's high demanding energy world and continuously increasing energy prices, the study and advancement in intensified chemical processing operations is a challenge for both academia and industry. The future of many chemical operations depends to a large extent on the innovation capacity of engineers in order to reduce energy consumption, emissions, waste and risk. Process intensification (PI) is a good example of how innovation is driving development in chemical engineering.¹⁻³ One common application of PI is the combination of several unit operations into a multifunctional equipment. Integrated reactive separation processes are becoming gradually more applied by industry due to several reasons: (i) economic benefits such as lower energy consumption, capital investment and operational costs, (ii) reduction of health, safety and environmental risks, and (iii) sufficient progress in the understanding and modeling of such integrated operations allowing for accurate design and scale up. Currently, the most relevant application of the multifunctional reactor concept is reactive distillation (RD).⁴ The concept of RD is not new with the first patent appearing in 1921⁵. Some authors claim that the first undisclosed commercial applications date from the late 1950's⁶ while the best known commercial example being the Eastman process was made public in 1980⁷. Optimal design of RD processes is a complex task. Since both operations are conducted simultaneously, an overlap of the operational window for reaction and distillation exist. Therefore, the temperatures and pressures of both processes are required to match. Good overviews of current and potential applications can be found in the literature.^{6, 8-11} These reviews indicate that reliable models are decisive in the design of RD in order to reduce development time and experimentation costs. Comprehensive models such as the non-equilibrium (NEQ) stage model extended to RD include hardware correlations, accurate calculation of thermodynamic and physical properties, well defined reaction kinetics and consider both multicomponent mass transfer and heat transfer rates. This subject is very well assessed in the review by Taylor and Krishna.¹² Reliable models must be validated with experimental data if they are to be used as decision making tools. Taylor and Krishna have highlighted the

need for experimental column profiles comprising temperature and concentration data, needed for the validation of any process model. Several simulation studies for different applications have been published where predicted values are in good accordance with experimental data. However, when coupling the column with a decanter, only few experimental data are available in literature.¹³⁻¹⁷ Esterification reactions exhibit a good opportunity to couple the column with a liquid-liquid separator since it is ideal to separate the water produced from either the organic product or one of the reactants fed in excess. In this case the 1-propanol (ProOH) fed in excess is separated from the water produced in the reaction and refluxed back (as seen in Fig. 3.1 in Chapter 3). The objective of this experimental work was to evaluate the combination of RD with subsequent separation of water and recovery of ProPro and ProOH that did not react, present a validated consistent model for the synthesis of the ester with a decanter separator and provide simulations for further process optimization. The results presented herein show the difficulties that exist in achieving high product yields in combination with downstream processing of excess reactants. Non-conventional heating techniques like microwaves can be used to try to avoid these hurdles.

5.2 Modeling of reactive distillation

In chemical engineering process development reliable models are often used to reduce time and avoid expensive experimental studies. Extensive literature is available on modeling of reactive distillation processes.^{11, 12, 18, 19} Different modeling depths are available and chosen according to data, parameter availability and how accurate the description of the process should be. In this study, a non-equilibrium stage model (NEQ model) was used. In order to reduce significantly possible model deviations from experimental data, NEQ models necessarily have to account for actual rates of multicomponent mass transport, heat transport and chemical reactions into the equations that describe the process phenomena. Key aspects in NEQ models that should be considered include: (a) accurate thermophysical data of the system, (b) correct reaction kinetics and chemical equilibrium constants and (c) correct correlations for the description of liquid hold-up, pressure drop, mass and heat transfer between the liquid and vapor phases and interfacial area in the structured packings. In addition, the model should be validated with reliable experimental data to guarantee predictability under a broad range of operating conditions. The complete set of equations and the model description can be found in the following references.^{20, 21} The column peripherals are assumed to be ideal and

the heterogeneously catalyzed reaction is modeled using a pseudo-homogenous approach. Specific correlations for the determination of mass transfer coefficients, specific contact area, liquid hold-up and pressure drop for the reactive packing Sulzer Katapak™-SP 11 used in the reactive section of the column were developed in the European research project *INSERT-Integrating Separation and Reaction Technologies*.²² The hydrodynamic properties were calculated using a modified hydraulic model originally proposed for Sulzer Multipak™.²³ Modifications included the adaptation of a more suitable liquid hold-up correlation and the use of a different split factor for the flowing liquid. The following correlations were used; for pressure drop and dynamic liquid hold-up:

$$\frac{\Delta P_{dry}}{\Delta z} = 149.13 \cdot F_v^{1.823} \quad (5.1)$$

$$\frac{\Delta P_{wet}}{\Delta z} = \frac{\Delta P_{dry}}{\Delta z} \cdot (1 + 0.03 \cdot L) \quad (5.2)$$

$$h_d(1h) = 0.0453 \cdot L^{0.274} \quad (5.3)$$

The required binary mass transfer coefficients $\kappa_{i,k}$ can be calculated using Maxwell-Stefan diffusion coefficients and experimental Sherwood correlations.²⁴ For the Sulzer BX packing used in the stripping and rectifying sections, correlations for mass transfer coefficients are from Bravo et al.²⁵ while the correlations to calculate specific contact area, liquid hold-up and pressure drop are from Rocha et al..²⁶ The model equations for RD were validated for a hybrid system of ProPro production.²⁷ The new model including the decanter equations was implemented into the simulation environment ASPEN Custom Modeler™ (ACM) as seen in Figure 5.1.

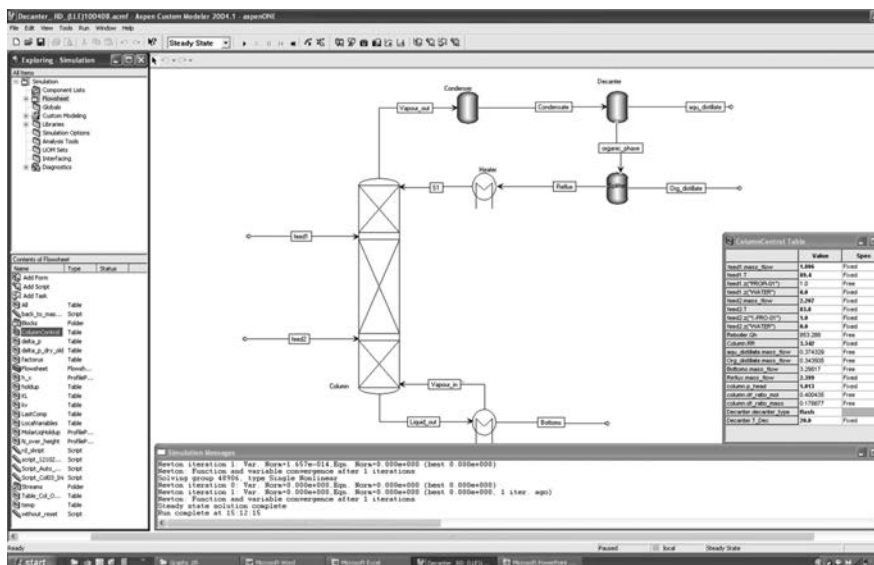
5.2.1 Reaction kinetics

The kinetic study shown in Chapter 3, shows the experimental conditions equations for the determination of the reaction rate and the equilibrium constant in the temperature range of the column operation. In the model of the ProPro synthesis, a pseudo-homogeneous approach formulated in activities is applied for the reaction rate. The temperature dependence of the equilibrium constant K_{eq} and the rate constant k_1 was modeled via the Arrhenius approach (Equations 3.7 to 3.9).

5.2.2 Thermodynamics

For process design, the thermodynamic properties of the quaternary mixture were built on the information of the six binary systems. The complete set of

Figure 5.1 Graphical interface of ASPEN Custom Modeler™.

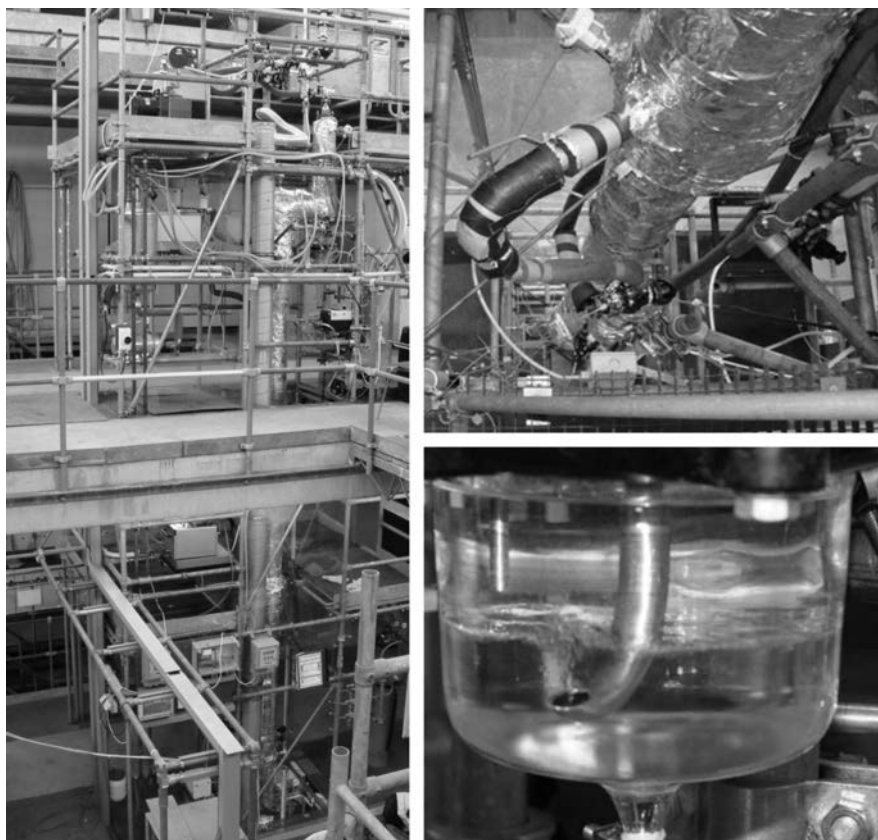


binary interaction parameters for the VLE calculation is presented in Table 3.4 in Chapter 3. To take into account the liquid phase non-idealities the UNIQUAC activity coefficient model was applied. The Hayden-O'Connell equation of state is used to account for the non-idealities of the vapor phase which incorporates the dimerization, necessary due to the presence of ProAc. The system is characterized by strong liquid phase non-idealities with several azeotropes present. The azeotropic data can be found in Table 3.1 in Chapter 3. LLE in the decanter is described by the UNIQUAC approach. The experimental data for the ternary subsystem water/ProOH/ProPro was correlated using the UNIQUAC activity coefficient model to estimate the corresponding binary interaction parameters a_{ij} and $b_{ij}(T)$ presented in Table 3.5 in Chapter 3. Figure 3.6 shows the ternary phase diagram for the subsystem with a large miscibility gap, the mass balance tie lines and the experimental data used.

5.3 Experimental set-up

A series of experiments were performed in a pilot-scale reactive distillation column. The column is made out of glass, has an inner diameter of 50 mm (DN-50) and is equipped with two types of structured packings, Sulzer BX for the stripping and rectifying sections, and Sulzer Katapak™-SP 11 with the ion-exchange resin immobilized in catalyst bags for the reactive part.²⁸ A natural circulating reboiler with a 2 L hold-up and a maximum electrical heat duty of 6.6 kW was used to generate vapor. The column characteristics can be found in Table 5.1.²⁷ Some pictures of the experimental set-up are can be seen in Fig. 5.2 including the column frame, feed inlet and the decanter with the phase split used.

Figure 5.2 Pictures of the pilot-scale reactive distillation column (DN-50) in TU Dortmund.



There are six liquid distributors in-between the packing sections that allow liquid sample collection for product composition analysis and measuring the vapor temperature using calibrated PT-100 thermocouples. In addition three product samples can be collected, one from the bottom stream and two from the top corresponding to the aqueous (dist(w)) and organic (dist(org)) distillates. The schematic view of the column is depicted in Fig. 5.3. All experimental runs were carried out at atmospheric pressure. The column is insulated with an 80 mm thick mineral wool cover. Consequently, temperature gradients between the column and the environment can be neglected and the adiabatic conditions in the process are assumed. The decanter has an internal volume of 0.5 L, is made of glass and is cooled both internally and externally using cold water. Process parameters, such as dist(w), dist(org), bottom product, feeds and reflux mass flows as well as the temperature profile of the vapor along the column were measured continuously. The stream compositions were analyzed off-line using a Shimadzu gas chromatograph (GC-14A) equipped with FID detector. The determination of water content was done with the Karl-Fischer titration method (Mettler Toledo DL 31). In all experiments, ProAc and ProOH were used with purities of minimum 99.9 wt% (BASF). ProAc is fed at the upper part of the reactive section of the column while ProOH is fed in the middle part. As ProAc is the highest boiling component in the mixture and ProOH the lowest, a counter-current like flow of the reactants is established.

The alcohol is fed in excess to maintain a high conversion of the acid. ProPro is the main reaction product and is removed in the bottom stream. To keep constant the flows coming in and out from the column, flow control loops were established in both feeds and level controls for bottom product and dist(org). The reflux mass flow was fixed via a coriolis pump control. The range of the operational parameters were determined under three boundary conditions, (i) to have only one liquid phase inside the column, (ii) to achieve L-L splitting at the top of the column and (iii) not to exceed 120°C in the reactive zone as this causes irreversible damage to the catalyst. The use of accurate data was of paramount importance for later utilization in model validation. Therefore process data were reconciled. This procedure improves data quality by removing random and gross errors that are identified and eliminated. It estimates process variables, adjusting the experimentally measured mass streams and concentrations so that the constraints (mass balance, component balance and reaction rates) are satisfied.

Figure 5.3 Schematic view of the experimental set up column with structured packings.

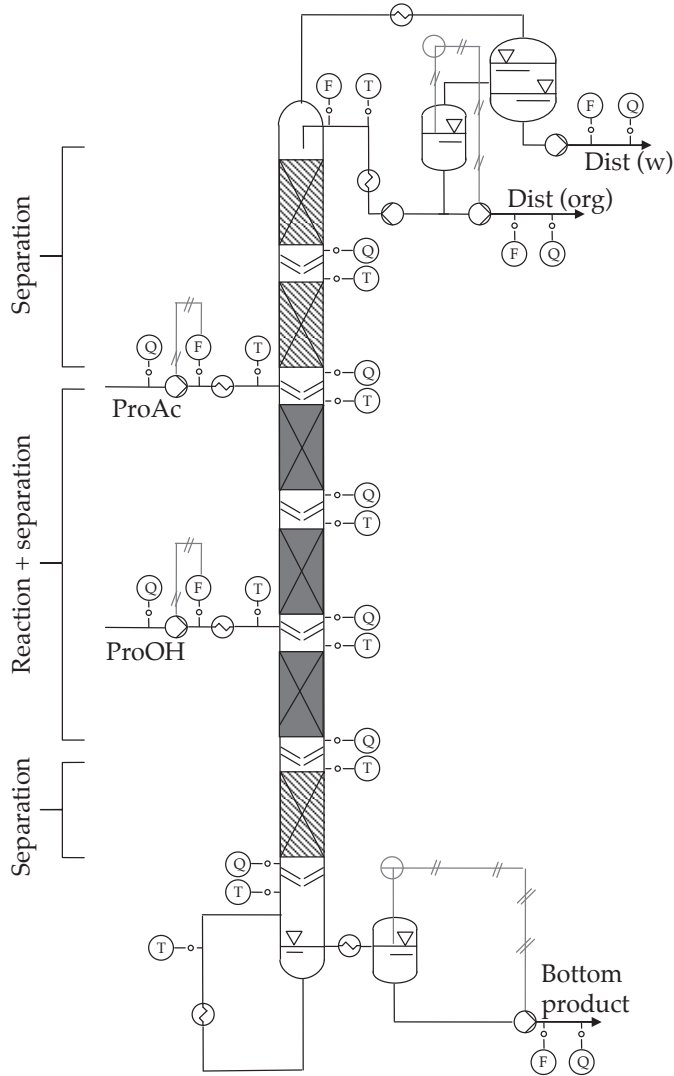


Table 5.1 Pilot-scale reactive distillation column characteristics.

Length reactive zone	2.6 m
Length stripping zone	0.5 m
Length rectifying zone	2.4 m
Total packing height	5.5 m
Condenser type	Total

5.4 Experimental procedure

A defined procedure is followed for each experiment in order to shorten the start-up of the column and the time to reach stable steady state conditions. These procedures have been and are still being studied in order to reduce the amount of energy and product that does not comply with the specifications while operating the column under unsteady conditions. The time span of each experiment can be divided in four stages exemplified in Figure 5.4: (I) column start-up (0 to 2 hrs), (II) online data reconciliation (4 to 8 hrs), (III) steady state operation (8 to 16 hrs) and (IV) column shut-down (after 16 hrs).

The start-up of the column is a demanding task and follows a procedure developed with extensive experimental experience gained in the laboratory with this test system. Inside the reboiler remains a mixture from the previous experiment which contains mostly ProPro and unreacted ProAc with few ProOH. The reboiler is turned on and vapor begins to rise. When the vapor reaches the first column segment the feed pumps are turned on. Following condensation at the column top, liquid enters the empty decanter and phase split occurs. When the decanter is filled, the reflux mass flow is fixed using a coriolis pump control. The total condensate contains a ternary mixture of water, unreacted ProOH and ProPro. No unreacted acid was found in the condensate in any of the experiments. The dist(w) is discharged from the process and part of the dist(org) was refluxed back. The mass flows show high fluctuations and the temperature increases until a value close to the steady conditions.

After the start-up stage both mass flows and temperature profiles stabilize and reach a constant value (stage II in figure 5.4). To determine the existence of a steady state operation of the column, three stationary requirements had to be

Figure 5.4 Monitored temperature profile along the column during experiment. TI 101 is the lowest monitored temperature at column top.

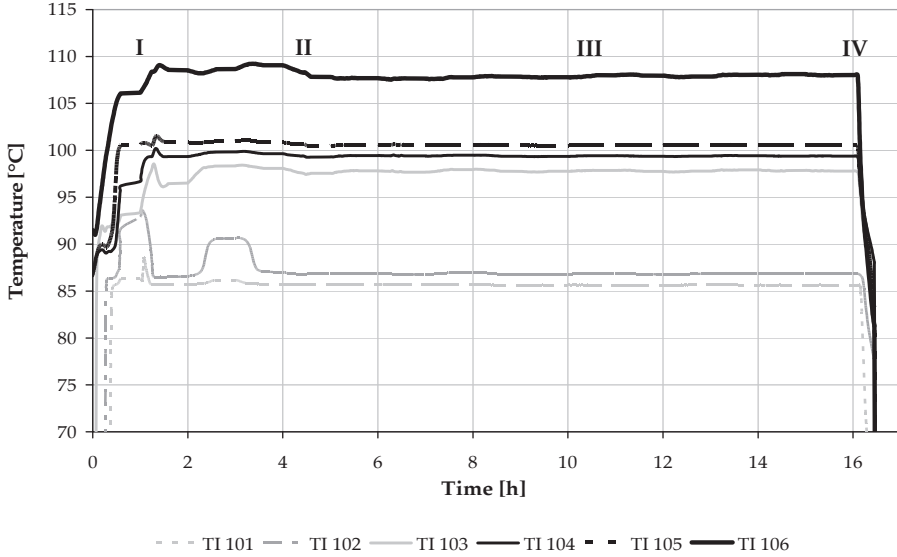
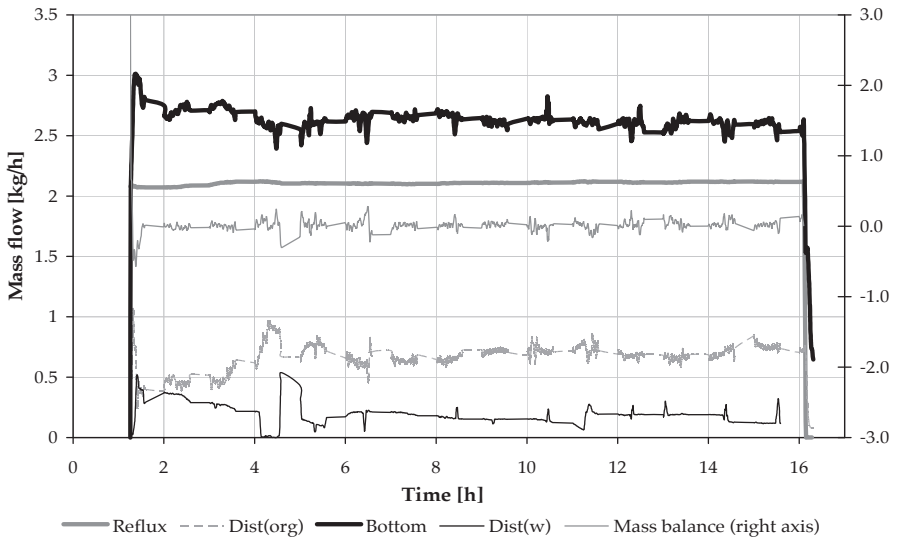


Figure 5.5 Products and reflux mass flows. Vertical lines show the time when samples were taken for data reconciliation and concentration profiles.



fulfilled: (a) minor change over time in the monitored temperature profile of the column ($\pm 0.25^\circ\text{C}$), (b) low change over time in the three product stream mass flows ($\pm 4\%$) and (c) closed mass and component balance of the column streams (maximum $\pm 4 \text{ wt}\%$). When coupling the column with a decanter, this stage may take longer since the concentrations of both phases inside the decanter are changing in time and therefore the reflux concentrations are not constant. When the steady state operating point is reached and identified (stage III in figure 5.4), liquid samples from the 6 distributors, bottom, dist(w) and dist(org) are taken out of the column. These nine samples taken along the column height provide enough detailed data to properly compare experiments with the process model. Three profiles were taken with 90 minute intervals. After all profile samples were collected the column was shut-down.

5.5 Experimental results

In order to validate the model, eight RD experiments with decanter were performed. The goal of these experiments is to illustrate the feasibility of the ProPro synthesis in a reactive distillation column, coupled with a decanter to recover not only product but also unreacted ProOH and reflux them back. By this, detailed process behavior and expertise is generated. The experimental conditions are illustrated in Table 5.2. Operating conditions were chosen according to (i) the time span of the experiments that depended on the total feed in (kg/h) fed to the column, (ii) the heat duty that ensured that the concentrations of the condensate were in the miscibility gap, and (iii) the decanter capacity to handle the distillate flow and its capability to achieve complete phase split.

Experiments were long and lasted on average 17 hours. Table 5.3 shows the experimental results with a comparison between the simulated results for reactants conversion, product purity, organic distillate and bottom flows. Key parameters monitored during the experimental runs are illustrated in Figures 5.4 and 5.5 for experiment E7. Figure 5.4 shows the temperature profile of the vapor along the column during the entire experiment. Temperatures deviated less than 0.5°C after 10 hours when the column had reached steady state conditions. The temperature at the top was $T_{101} = 85.6^\circ\text{C}$ and after condensation immediate phase split was achieved, because the total condensate liquid composition lies inside the miscibility gap. Products and reflux mass flows for experiment E7 are illustrated in Figure 5.5. In all experiments the reflux mass flow was kept constant to a set point value, e.g. for experiment E7 Reflux = 2.118 kg/h. When stationary requirements were met, three independent column

Table 5.2 Operating conditions and experimental results.

Exp. no.	Total feed (kg/h)	ProAc flow (kg/h)	ProOH flow (kg/h)	Molar feed ratio	Reflux ratio	Reflux (kg/h)	Boiler heat duty ^a (W)	Steady state data reconciliation
E1	4.0	1.80	2.20	1.5	1.687	1.948	843	Correct
E2	4.0	1.80	2.20	1.5	1.658	1.880	869	Correct
E3	4.0	1.80	2.20	1.5	2.837	2.488	933	Correct
E4	4.0	1.80	2.20	1.5	2.658	2.250	862	Incorrect
E5	4.0	1.80	2.20	1.5	3.184	2.399	864	Incorrect
E6	3.5	1.50	2.00	1.7	2.156	1.847	757	Incorrect
E7	3.5	1.60	1.90	1.5	2.440	2.118	836	Correct
E8	3.5	1.30	2.20	2.0	2.479	2.024	815	Correct

^a Approximated values

profiles were taken. The sampling only affected slightly the mass flows. A data reconciliation test was performed as a necessary condition for a successful experiment. Experiments E4 to E6 failed to fulfill these requirements, which means that the column was at a state very close to stationary conditions but at least one parameter was not complying with the mass balance and reaction constraints in the reconciliation test.

5.6 Model results

The validation of the non-equilibrium stage model for the column without decanter was performed by Buchaly et al. for this chemical system²⁷. Yet, in this investigation the model is updated including the decanter unit. It was very important to predict correctly the LLE phase behavior because the reflux concentration could change completely the temperature and concentration profiles of the column. Therefore LLE parameters were chosen very carefully from literature and checked against new LLE experiments. It was necessary to keep the temperature in the decanter as low and as constant as possible in order to achieve a good phase separation and to stabilize the column. The decanter temperatures measured were around $T_{\text{Decanter}} = 19.0 \pm 1.0^\circ\text{C}$ with the exception of experiment E1 where the measured temperature was 70°C . Figure 5.6 shows the experimental and modeled results of the concentration profiles of reactants and products and Figure 5.7 shows the experimental and modeled results of the vapor temperature profile taken from experiment E7. A good agreement between the simulated and experimental results was achieved along the entire column, as seen in the graphs and in Table 5.3 where a comparison of the experimental and simulated results for acid and alcohol conversions, product purity, decanter organic flow and bottom flow for all experiments performed are shown. In Figure 5.8, the parity plot depicts a comparison of the simulated and reconciled experimental data of all four components molar fractions in the liquid phase demonstrating the quality of the simulations. Due to the special liquid distributor design, the liquid sampling at the ProAc feed point was very difficult and the sample data at this particular point does not represent the internal liquid column flow. This behaviour was not observed at the alcohol feed point because a different distributor type was used. The biggest error between the simulated and experimental results is observed in Table 5.3 in the dist(org) flows. Consequently, small differences in the concentrations of alcohol, ester and water occur in the reflux stream. Due to design constraints in the decanter, complete separation efficiency was not always achieved although the liquid-liquid equilibrium was reached. The experimental results for the dist(w) flows (data not shown) were always smaller than the ones predicted by the model. Consequently, the difference in mass was leaving the decanter in the dist(org) stream (simulated values were lower than experimental values). Therefore a higher amount of water was fed back which resulted in lower values for acid conversions and lower product concentrations in the bottom stream. The acid being the high boiler ended up in the bottom of the column.

Table 5.3 Experimental and simulated results for reactants conversion, product purity and decanter flows.

Exp. no.	X_{ProAc} conversion (mol/mol)		X_{ProOH} conversion (mol/mol)		Dist(org) (kg/h)		$x_{ProPro, bottom}$ (mol/mol)		Bottom (kg/h)	
	EXP	SIM	EXP	SIM	EXP	SIM	EXP	SIM	EXP	SIM
E1	0.796	0.820	0.528	0.544	1.083	0.959	0.536	0.541	2.841	2.841
E2	0.815	0.819	0.542	0.544	1.004	0.932	0.559	0.582	2.866	2.866
E3	0.774	0.798	0.516	0.531	0.689	0.566	0.485	0.516	3.125	3.125
E4	0.754	0.804	0.500	0.532	0.616	0.512	0.465	0.519	3.152	3.152
E5	0.754	0.798	0.501	0.530	0.550	0.394	0.459	0.502	3.238	3.238
E6	0.833	0.848	0.509	0.518	0.654	0.611	0.520	0.535	2.641	2.642
E7	0.789	0.835	0.526	0.558	0.680	0.610	0.519	0.575	2.629	2.629
E8	0.791	0.849	0.398	0.427	0.725	0.640	0.386	0.446	2.682	2.682

Figure 5.6 Concentration profiles for experiment E7. Experimental data points and simulation. Packing height is measured from bottom to top. Two sections can be distinguished by shaded areas, a negative height part above the reboiler up to the point where the stripping section starts and the reactive section. Feed points are shown as well.

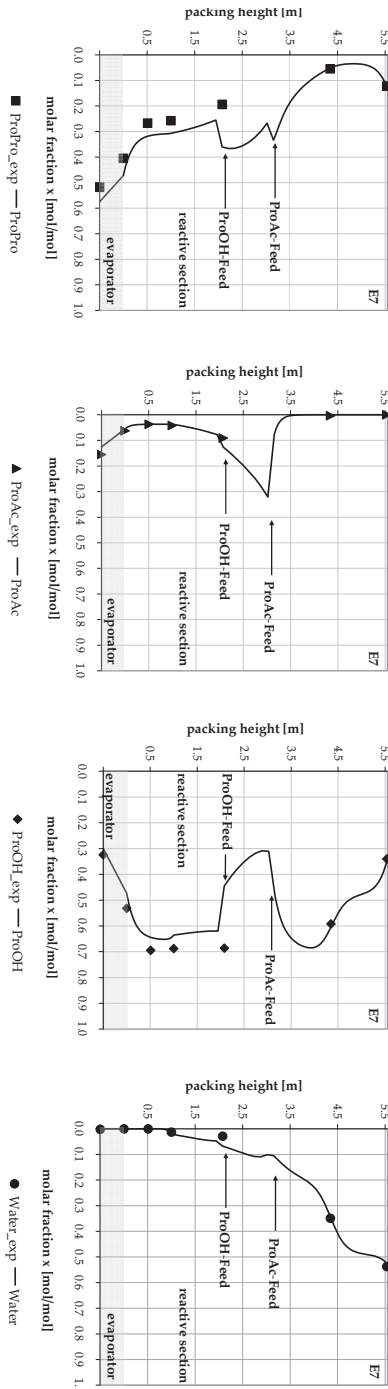


Figure 5.7 Vapor temperature profile for experiment E7. Modeled line vs. experimental temperatures. Maximum temperature inside the column is 120°C.

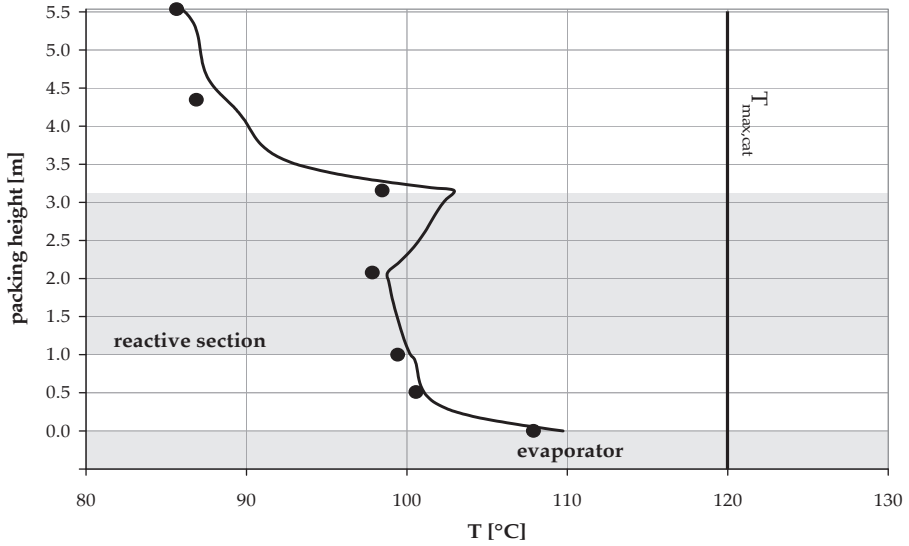
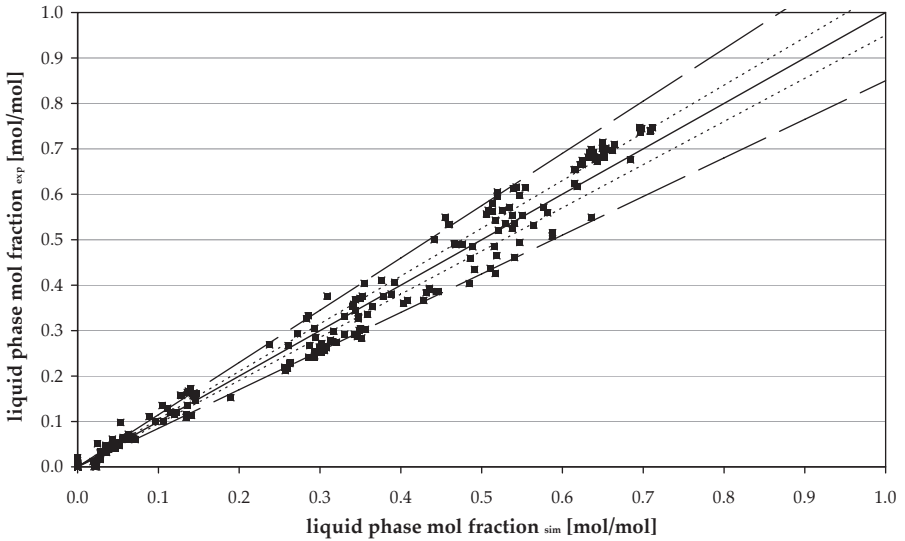


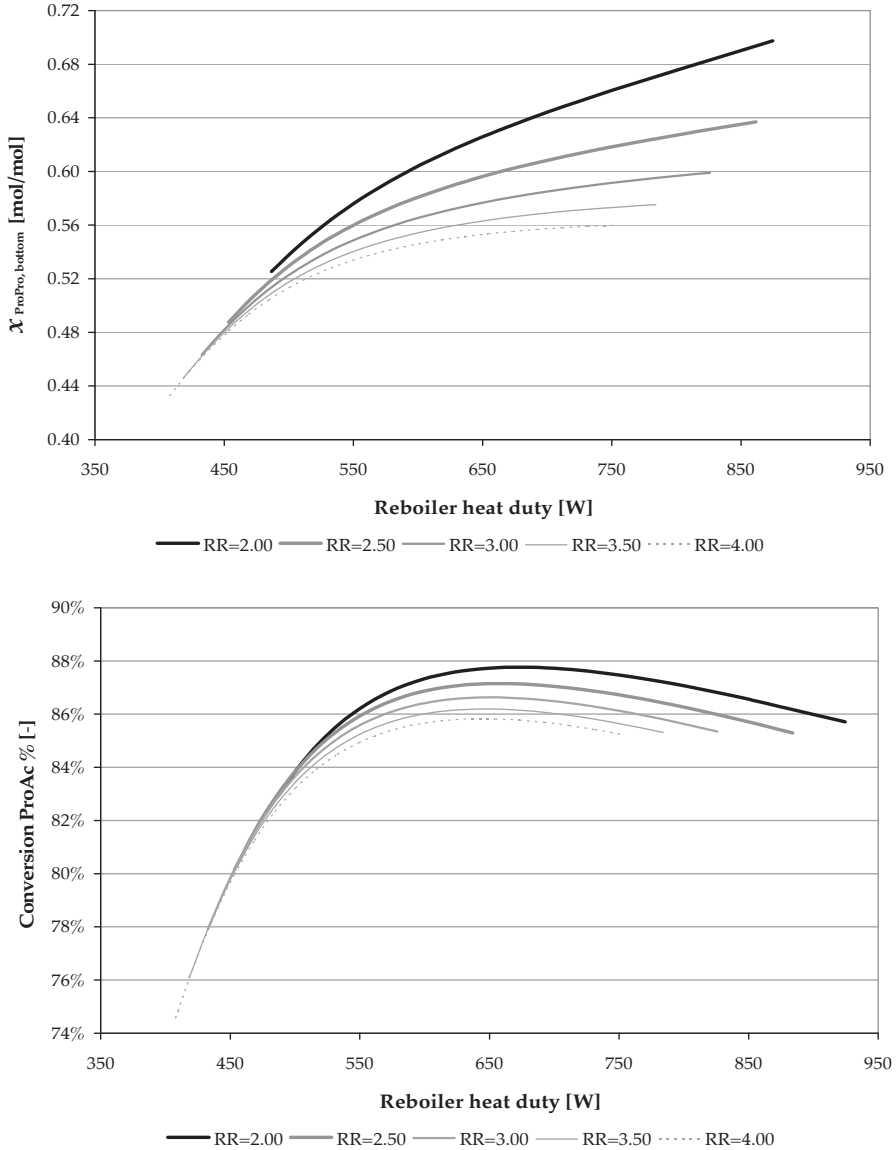
Figure 5.8 Parity plot of simulated and reconciled experimental data.



5.7 Simulation studies

The model was used to study in depth the influence of relevant operating conditions (heat duty and reflux ratio) on the most important process variables (product purity $x_{ProPro, bottom}$ and acid conversion) at different total feeds and reactant molar feed ratios. This is of particular importance since reactive distillation is a process with dual objectives, i.e. reach the highest product purity on the one hand and the highest reactant conversion on the other hand. Column control is usually directed towards the desired product composition neglecting reactant conversion and this could lead to suboptimal column operation²⁹. The total column feed was varied from 2.0 to 4.0 kg/h, the RR was varied from 2.0 to 4.0 while the heat duty was varied from 400 to 1200 W depending on the total feed values. In Figure 5.9 the results from a simulation with a column feed of 3.0 kg/h are illustrated. The results are bound to a minimal reboiler heat duty to attain the required reflux ratio and to a maximum heat duty where no phase split in the decanter occurs. At a given RR an increase in the heat duty augments strongly the acid conversion up to a maximum value. With a further increase of the heat duty, the acid conversion decreases slightly. This is a typical behavior for RD processes because one of the reactants (in this case the low boiler ProOH) is stripped out of the reactive section at high heat duties. Under these conditions, beside the low boiling components water and alcohol, the ester starts to be withdrawn at the top and therefore accumulates in the reactive section. In case of the bottom product purity of the ester, increasing heat duty improves $x_{ProPro, bottom}$ due to increased conversions. Another option is to study the influence of the RR at constant heat duty. In this case a minimal RR should be chosen in order to achieve high bottom product purities and high acid conversions. The composition of the bottom stream changes significantly with deviations in RR while acid conversion changes in a more subtle way. At high reflux ratios reactants accumulate in the bottom lowering the product purity. The resulting effect of the variation of these variables is the same when going to higher feed fluxes. The same outcome could be seen in simulations from a hybrid process when the RD column was coupled with a membrane²⁷. Both, the hybrid process and the column-decanter process can be improved. It is important to notice that due to thermodynamic equilibrium constraints there is unreacted alcohol that is lost in the aqueous stream of the decanter. By coupling this stream to a membrane unit, the total amount of alcohol can be recovered and can be fed back to the column at the alcohol feed point. The overall process performance can be improved for both systems, the energy expenditure can be lower and $x_{ProPro, bottom}$ higher.

Figure 5.9 Influence of reboiler heat duty and reflux ratio on product purity $x_{ProPro, bottom}$ and acid conversion. Simulation conditions total feed of 3.0 kg./h, molar feed ratio ProOH/ProAc of 1.5.



Nomenclature

a_i	activity coefficient of component i (mol/mol)
a_{ij}	temperature-independent binary interaction parameter
c_{act}	concentration of active sites (equiv. kg ⁻¹)
ΔP	pressure drop
F_v	gas load F-factor
h_d	dynamic liquid hold-up
$m_{cat,dry}$	mass of dry catalyst (kg)
n_c	number of components
k_1	rate constant forward reaction (mol eq ⁻¹ s ⁻¹)
K_{eq}	equilibrium constant
L	liquid load (m ³ m ⁻² h ⁻¹)

Greek letters

v_i	stoichiometric coefficient of component i
$\kappa_{i,k}$	binary mass transfer coefficient (m s ⁻¹)

Abbreviations

ProAC	propionic acid
ProOH	1-propanol
ProPro	<i>n</i> -propyl propionate
dist(org)	organic distillate
dist(w)	aqueous distillate

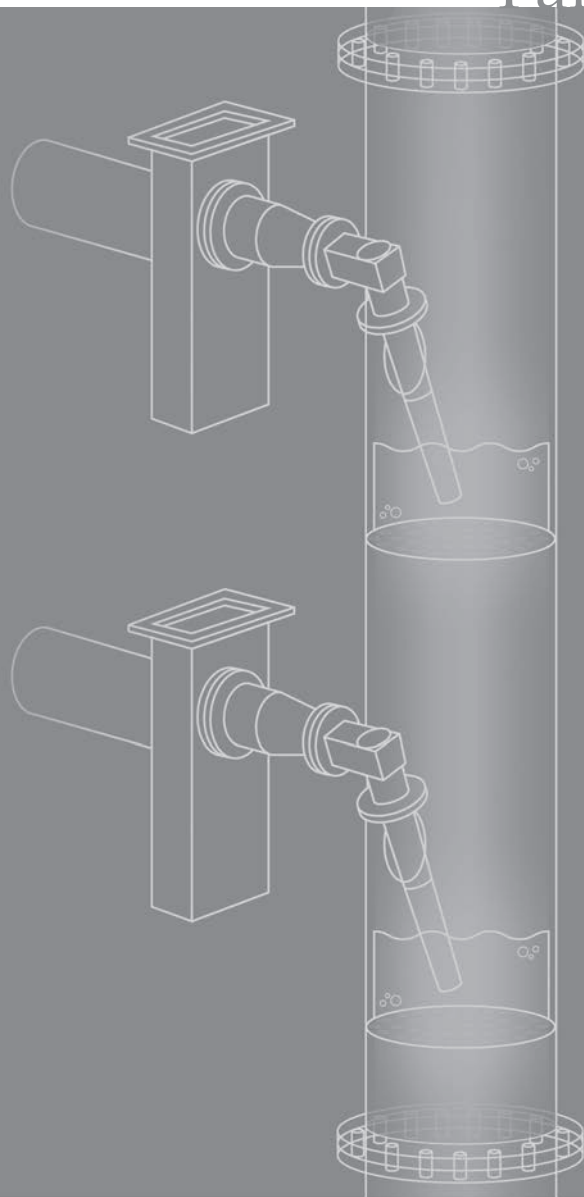
5.8 References

1. Becht S., Franke R., Hahn H., An industrial view of process intensification. *Chemical Engineering and Processing*. **2009**. 48: 329-332.
2. Stankiewicz A., Moulijn J. A., Process Intensification: Transforming Chemical Engineering. *Chemical Engineering Progress*. **2000**. 96(1): 22-34.
3. Van Gerven T., Stankiewicz A., Structure, Energy, Synergy, Time- The Fundamentals of Process Intensification. *Ind. Eng. Chem. Res.* **2009**. 48: 2465-2474.
4. Stankiewicz A., Reactive separations for process intensification: an industrial perspective. *Chemical Engineering and Processing*. **2003**. 42: 137-144.
5. Backhaus A.A., Continuous process for the manufacture of esters. *US Patent 1,400,849*. **1921**.
6. Harmsen G.J., Reactive distillation: The front-runner of industrial process intensification A full review of commercial applications, research, scale-up, design and operation. *Chemical Engineering and Processing*. **2007**. 46: 774-780.
7. Agreda V.H., High-Purity Methyl Acetate via Reactive Distillation. *Chemical Engineering Progress*. **1990**. 86(2): 40-46.
8. Hiwale R.S., Mahajan Y. S., Bhate N. V., Mahajani S. M., Industrial Applications of Reactive Distillation: Recent Trends. *International Journal of Chemical Reactor Engineering*. **2004**. 2: 1-52.
9. Kiss A., Omota F., Dimian A., Rothenberg G., The heterogeneous advantage: biodiesel by catalytic reactive distillation. *Topics in Catalysis*. **2006**. 40(141-150).
10. Srinivas S., Malik R. K., Mahajani S. M., Feasibility of Reactive Distillation for Fischer-Tropsch Synthesis. *Ind. Eng. Chem. Res.* **2008**. 47: 889-899.
11. Sundmacher K., Kienle A., *Reactive Distillation*. **2003**: Wiley-VCH.
12. Taylor R., Krishna R., Modelling reactive distillation. *Chemical Engineering Science*. **2000**. 55: 5183-5229.
13. Forner F., Brehelin D., Repke J.-U., Startup of a reactive distillation process with a decanter. *Chemical Engineering and Processing*. **2008**. 47: 1976-1985.
14. Klöcker M., Kenig E. Y., Schmitt M., Althaus K., Schoenmakers H., Markusse A. P., Kwant, G., Influence of Operating Conditions and Column Configuration on the performance of Reactive Distillation Columns with Liquid-Liquid Separators. *Canadian Journal of Chemical Engineering*. **2003**. 81: 725-732.
15. Lai I.-K., Liu Y-Ch., Yu Ch-Ch., Huang H-P., Production of high-purity ethyl acetate using reactive distillation: Experimental and start-up procedure. *Chemical Engineering and Processing*. **2008**. 47: 1831-1843.
16. Lee H.-Y., Yen L-T., Chien I-L., Reactive Distillation for Esterification of an Alcohol Mixture Containing n-Butanol and n-Amyl Alcohol. *Ind. Eng. Chem. Res.* **2009**. 48: 7186-7204.
17. Schmitt M., Hasse H., Althaus K., Schoenmakers H., Götze L., Moritz P., Synthesis of n-hexyl acetate by reactive distillation. *Chemical Engineering and Processing*. **2004**. 43: 397-409.
18. Noeres C., Kenig E. Y., Górak A., Modelling of reactive separation processes: reactive absorption and reactive distillation. *Chemical Engineering and Processing*. **2003**. 42: 157-178.
19. Peng J., Lextrait S., Edgar T. F., Eldridge R. B., A Comparison of Steady-State Equilibrium and Rate-Based Models for Packed Reactive Distillation Columns. *Ind. Eng. Chem. Res.* **2002**. 41: 2735-2744.
20. Hoffmann A., Górak A., Catalytic Distillation in Structured Packings. *AIChE*. **2001**. 47(5): 1067-1076.
21. Klöcker M., Kenig E.Y., Hoffmann A., Kreis P., Górak A., Rate-based modelling and simulation of reactive separations in gas/vapour-liquid systems. *Chemical Engineering and Processing*. **2005**. 44: 617-629.
22. Brunazzi E. *Mass Transfer Study of Katapak-SP 11 Packing: Experimental Setup, Measurement Procedures, Correlations*. Internal report in the frame of the EU Project "INSERT-Integrating Separation and Reaction Technologies". **2006**.

23. Hoffmann A., Noeres Ch., Górak A., Scale-up of reactive distillation columns with catalytic packings. *Chemical Engineering and Processing*. **2004**. 43(3): 383-395
24. Buchaly C. *Experimental Investigation, Analysis and Optimisation of Hybrid Separation Processes*. Lehrstuhl für Fluidverfahrenstechnik **2008**, Dissertation Technische Universität Dortmund
25. Bravo J.L., Rocha J. A., Fair J. R., Mass transfer in gauze packings. *Hydrocarbon Processing*. **1985**. 64: 91-95.
26. Rocha J.A., Bravo J. L., Fair J. R., Distillation Columns Containing Structured Packings: A Comprehensive Model for Their Performance. 1. Hydraulic Models. *Ind. Eng. Chem. Res.* **1993**. 32: 641-651.
27. Buchaly C., Kreis, P., Górak, A., Hybrid separation processes-Combination of reactive distillation with membrane separation. *Chemical Engineering and Processing*. **2007**. 46: 790-799.
28. Götze L., Bailer O., Moritz P., Scala von C., Reactive distillation with KATAPAK®. *Catalysis Today*. **2001**. 69: 201-208.
29. Sneesby M. G., Tade M. O., Smith T. N., Two-point control of a reactive distillation column for composition and conversion. *Journal of process control*. **1999**. 9: 19-31.



Part III



Microwave Activation

The Effects of Microwave Irradiation on Molecular Separation

An envisioned reactive distillation (RD) process for the esterification reaction of n-propyl propionate (ProPro) from 1-propanol (ProOH) and propionic acid (ProAc) using microwave irradiation (MW) ($f = 2.45$ GHz) as an alternative energy source to heat the column is proposed in this thesis. In order to clearly differentiate between stand-alone operation effects and possible synergistic effects that could be obtained while irradiating the column it was decided to study separately the effects MW may have first on separation and then on reaction. In this chapter the use of MW is explored to study the effects they can exert on molecular separation. Two types of experiments were conducted to produce vapor-liquid equilibrium diagrams with a modified set-up allowing for MW heating. It was found that when the vapor-liquid interface is exposed to microwaves, the system can be disturbed from conventional equilibrium conditions and a positive deviation in phase composition can be achieved, as the vapor phase becomes richer in the component with the lower boiling temperature; the extent of separation improvement depends on the boiling points and the dielectric properties of the mixture components. This finding may have significant practical impact in distillation processes as it implies smaller columns with a lower number of trays, for a given separation efficiency, compared to conventional designs involving heat exchange in the reboiler and the condenser only. It is stressed that the effect was present only when the vapor-liquid interface is exposed to microwaves; no effect is observed when solely the bulk liquid volume was irradiated.

The contents of this chapter were adapted from the work published in:
Ernesto Altman, Georgios D. Stefanidis, Thomas van Gerven, Andrzej I. Stankiewicz

“Process Intensification of Reactive Distillation in the Synthesis of n-Propyl propionate: the Effects of Microwave Radiation on Molecular Separation and Esterification Reaction.”

Ind. Eng. Chem. Res., **49** (2010) 10287-10296; DOI: 10.1021/ie100555h

© 2010 American Chemical Society. Reprinted with permission.

"One thing I have learned in a long life: that all our science, measured against reality, is primitive and childlike- and yet it is the most precious thing we have."

Albert Einstein

6.1 The application of microwaves to vapour-liquid separations

In the last decades, the application of electromagnetic radiation in form of microwaves for chemical syntheses (microwave chemistry) has gathered the attention of the scientific and industrial communities in view of possible process intensification (PI) of commercial operations.¹ Currently, microwave (MW) technology is being successfully applied in industrial operations like metal and ceramic sintering, food thawing and wood drying. In addition to reactions, distillation processes could possibly benefit from MW. Several concepts of microwave-assisted laboratory distillation have been developed.^{2,3} In this thesis, the novel concept of a microwave heated reactive distillation (RD) column is addressed in view of possible PI. When accounting the scale and importance of distillation and reactive distillation in the process industry (Chapter 1), any improvement in the reaction and/or separation functions could have a wide application and direct impact on large scale operations, considering that the main barrier for industrial applications still remains in the scale-up of microwave applicators. In this context one research questions is addressed namely, the effect of microwave irradiation on the physics governing the separation of components. Initially, we have experimentally explored the effect of microwaves on separation of binary mixtures by comparison with conventional thermodynamic equilibrium experiments. Although, the effects of electromagnetic radiation on boiling and evaporation have been studied for more than three decades,^{4,5} the underlying physics are not yet universally agreed upon, as they are difficult to verify experimentally. Different theories have been proposed to explain why the boiling points of polar liquids are higher under MW irradiation; these include surface hydrodynamic instabilities (Marangoni and Hickman),^{6,7} superheating,⁸⁻¹⁰ non-equilibrium conditions at the evaporating interface¹¹ and pressure increase at the interface.¹² In this work, we first performed conventional vapor-liquid equilibrium (VLE) experiments with binary mixtures of components involved in the case esterification reaction (details of the process are given in Chapter 3). Then we executed the same experimental protocol under

microwave heating to investigate potential changes in phase composition as compared to conventional VLE due to selective heating of some compounds that are better MW absorbers than others or due to possible superheating.

6.2 Apparatus

For determination of MW effects on the binary separations, two different setups were used. The main difference between the two is the position of the vapor-liquid interface of the mixture with respect to the cavity where the electromagnetic field is applied. More specifically, in the first set of experiments, a modified glass Fischer LABODEST vapor-liquid equilibrium apparatus model 602/D, (Fischer Labor), shown in Fig. 6.1, was employed to study separation effects using the system ProOH/ProPro. In these experiments, only the bulk liquid was irradiated with the vapor-liquid interface lying outside the MW cavity. The original heating resistance, used for the so-called conventional heating experiments, was removed and, instead, a 50 ml glass flask (containing the liquid binary mixture) was placed in a single-mode microwave oven Discover (CEM corp.) and was connected to the glass body. The apparatus is a dynamic recirculating still equipped with a Cottrell circulation pump; it is inside the Cottrell tube where the phase equilibrium is reached (Fig. 6.1). Two temperatures were measured, one outside the cavity with a digital thermometer placed inside the Cottrell pump and one inside the MW cavity using a microwave transparent fiber optic (FO) temperature probe (FISO Technologies). On-line temperature monitoring was performed using a TMI temperature signal conditioner (FISO Technologies).

A second MW irradiated apparatus, shown in Fig. 6.2, was built to study the effect of MW when not only the bulk liquid but also the vapor-liquid interface is directly irradiated. A 50-mL glass flask with tubing was inserted into a Discover single-mode microwave oven and connected to a custom made distillation head with two valves for condensers connection and a Polytetrafluoroethylene (PTFE) cap from (BOLA). Heating was controlled by a built-in power controller inside the MW. A magnetic stirrer was used to mix the reagents. The distillation head and the reaction flask were insulated with insulation foam to minimize heat losses. Three FO temperature sensors were introduced through the PTFE cap. On-line temperature monitoring was performed using a TMI temperature signal conditioner. The cooling liquid circulation through the two condensers was done using a cooling thermostat.

Figure 6.1 Modified Fischer LABODEST unit used for isobaric vapor-liquid equilibrium experiments of the binary system ProOH/ProPro under microwave heating (only part of the liquid volume is irradiated, whereas the vapor-liquid interface is situated outside of the microwave cavity).

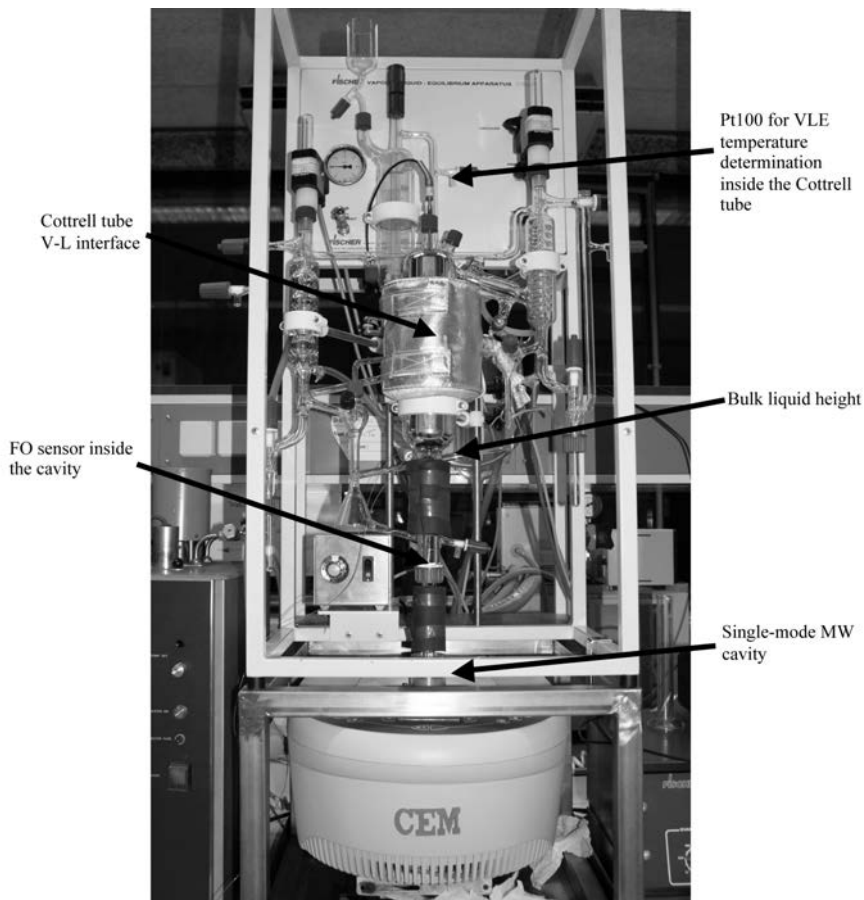
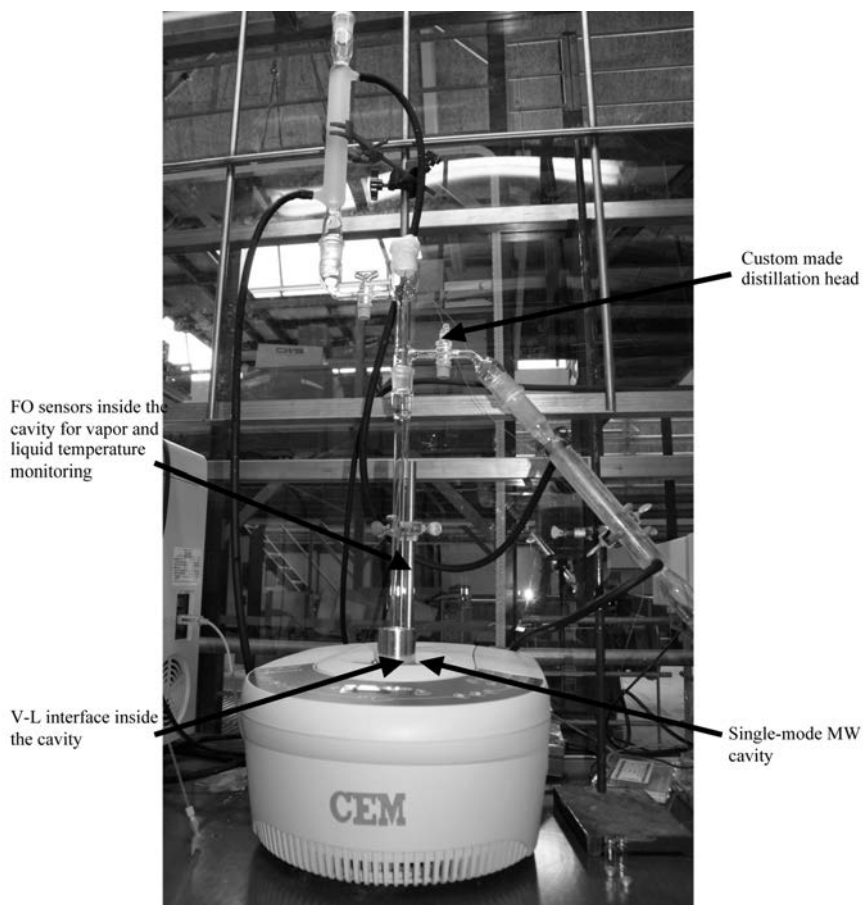


Figure 6.2 Equipment used for vapor-liquid equilibrium experiments of the binary systems ProOH/ProPro, ProOH/ProAc and ProPro/ProAc under microwave heating (Contrary to Fig. 6.1, both the liquid volume and the vapor-liquid interface are irradiated).



6.3 Composition analysis

Vapor and liquid phases formed in the separation experiments as well as products and reactants from the kinetic experiments were measured by gas chromatography with a Varian 3900GC instrument equipped with flame ionization detector. The column was CP-Wax 58 FFAP CB (50m, 0.25mm, 0.2 μ m / CP7727) and helium was used as carrier gas. Injector, detectors and oven temperature were set at 473.15, 503.15 and 423.15 K, respectively. The column temperature profile started at 80 $^{\circ}$ C kept constant for 5 min, followed by a 60 $^{\circ}$ C/min ramp to 130 $^{\circ}$ C, where it remained constant for an additional 1.5 min. Finally, Karl-Fischer titration was used to determine the water content in the product samples from the kinetic experiments.

6.4 Experimental procedure

In the first type of experiments, where only the bulk liquid (and not the interface) is irradiated, 100 ml of the sample mixture were loaded inside the glass body of the modified Fischer LABODEST unit. Isobaric experiments at atmospheric pressure were conducted at a constant MW power of 100 W. Recording of the temperature inside the MW cavity was done with an optical fiber and compared with the temperature reading of the thermometer inside the Cottrell tube. When the temperatures remained constant for 30 min or longer, steady state was assumed; liquid and vapor samples were taken and the experiment was stopped.

For separation experiments using the custom distillation head, 50 ml of the sample mixture were charged in the glass flask inside the MW cavity. Isobaric experiments at atmospheric pressure and total reflux conditions were performed at a constant MW power of 100 W. Two FO temperature sensors were placed inside the cavity, one \sim 0.5 cm below the liquid interface to monitor and record liquid temperature and one \sim 0.5 cm above the interface to monitor and record vapor temperature. When the temperatures remained constant for 20 min or longer, steady state was assumed and liquid samples were collected from the condenser (condensed vapors) and from the bottom of the flask.

6.5 The effects of MW radiation on separation

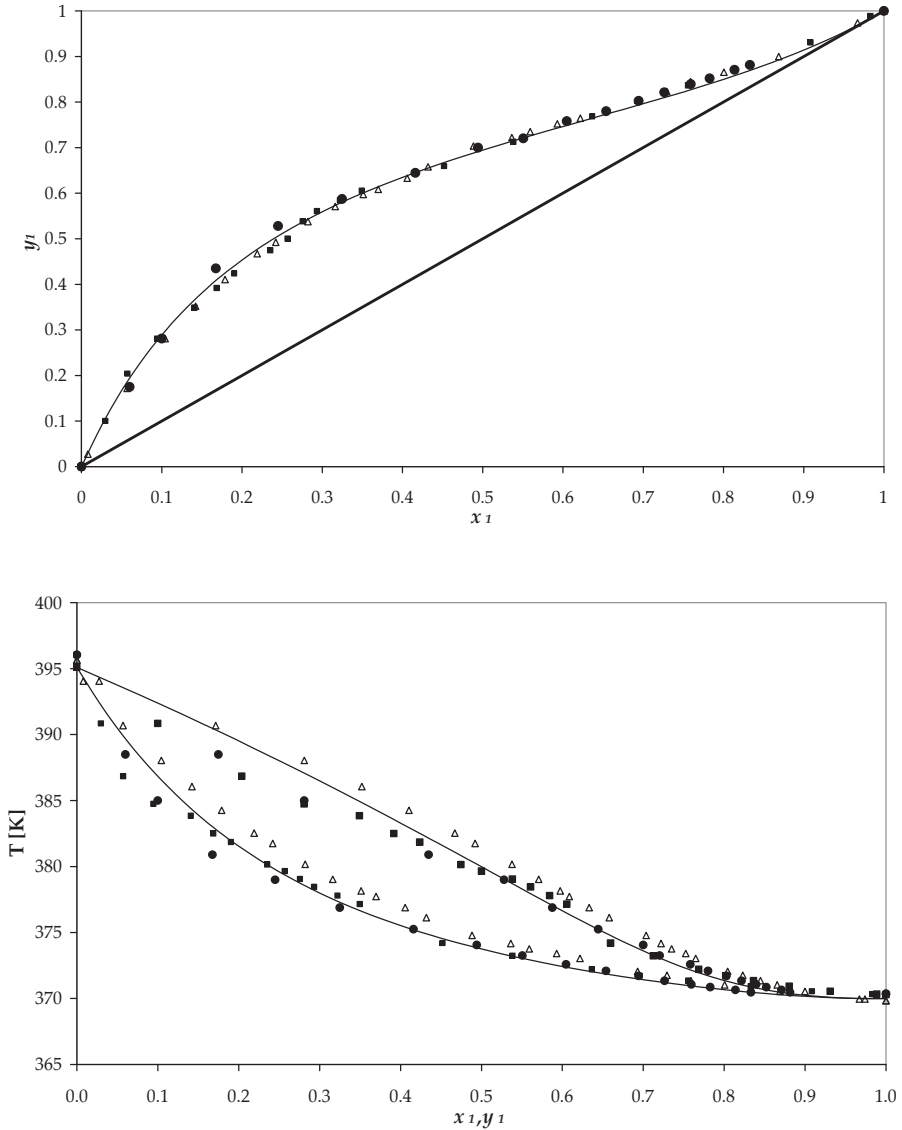
As explained above, two types of experiments were designed and carried out in two different setups. In the first set of experiments, only the bulk liquid was irradiated by MW, whereas in the second set of experiments not only the bulk liquid but also the V-L interface was irradiated.

6.5.1 Part I. Effects when only the bulk liquid is heated

These experiments were designed to resemble what would be the effect of exchanging a conventionally heated reboiler with a MW irradiated one under the motivation of studying the effects electromagnetic radiation on thermodynamic equilibrium. One could expect that if selective heating of molecules in the bulk liquid occurs (according to the difference in dielectric properties), that should reflect in the concentrations of the high MW-absorbing component in the vapor phase. Consequently the same equipment that is normally used for determination of isobaric vapor-liquid equilibrium curves was modified with a mono-mode MW oven. In Fig. 6.3, the experimental results for the system of ProOH/ProPro can be seen.

Initial experiments were performed in the conventional setup with no MW (■). The data obtained was compared with at least one data set from literature¹³ (Δ) and data generated using the UNIFAC group contribution method from ASPEN Properties Plus™ (-); as seen in Fig. 6.3, all these data were found in good agreement. Then, MW experiments were performed and the output (●) was compared with the conventional curves to check how much it deviated. It can be seen that the experimental data obtained using the modified apparatus with the MW heater show no significant difference from the data obtained using the conventional equipment. This is most likely because equilibrium conditions are achieved inside the Cottrell tube (above the microwave cavity), where vapor and liquid have a unique temperature. Moreover, the temperatures monitored with the FO probe inside the 50 ml flask (below the vapor-liquid interface) in the mono-mode cavity were practically the same as the equilibrium temperatures measured with the Pt100 (data not shown). Except the ProOH/ProPro system, the ProOH/Toluene system was also investigated. In the latter one, ProOH is a very good MW absorber ($\epsilon''=15.216$), whereas Toluene almost transparent to MW ($\epsilon''=0.096$). The result was the same as in conventional VLE¹⁴ with the exception that a minimum concentration of ProOH was needed in order to make the mixture boil (the highest power level of 300 W for the Discover microwave oven was used). This shows that MW interaction with selective molecules does exist. However, MW energy is dissipated rapidly into heat and, in combination with

Figure 6.3 Isobaric VLE experimental results for the binary system ProOH (1) / ProPro (2) obtained in the modified glass Fischer LABODEST apparatus (Fig. 6.1) with the Discover single-mode microwave oven at 1 bar. (-) UNIFAC, (Δ) data set from the literature, (\blacksquare) experimental values without MW and (\bullet) experimental values with MW.



stirring, the liquid temperature becomes uniform. The main message from this set of experiments is that molecular separation is not affected when only the bulk liquid is irradiated.

6.5.2 Part II. Effects when the bulk liquid and the V-L interface are heated

A second set of experiments was performed in the custom made distillation head (Fig. 6.2). In this case, not only the bulk liquid but also the vapor-liquid interface can be irradiated by microwaves representing heating conditions of a diabatic column. Experimental results from three binary pairs ProOH/ProPro (System A), ProPro/ProAc (System B) and ProOH/ProAc (System C) were obtained. In Figs. 6.4 through 6.6, xy (above) and the corresponding Txy (below) graphs can be found for each system studied. The following symbol convention is used: (●) for experimental data, (Δ) for reference data and (-) for UNIFAC modeled data. Reference data from ¹³ was also used for comparison in case of system (A). For system (B) no data was published before, but results were compared to own data produced under conventional heating conditions and, finally, for system (C), a data set from ¹⁵ was used. It can be clearly seen that MW irradiation exerts an effect on separation of binary mixtures only when both, the bulk liquid and the V-L interface are irradiated. The experimental data obtained via MW irradiation differ from conventional VLE data in that the vapor phase is richer in the high volatile component for the three systems. It is noted here that the thermodynamic laws governing phase equilibria are well established and hold both for conventional and microwave heating. We believe that the experimental observations presented herein are a consequence of a non-equilibrium state originating from the direct interaction of MW with the VL interface; it is likely that higher temperatures developed locally at the top liquid surface result in enhanced mass transfer from the liquid to the vapor phase (more pronounced for the component with the lower boiling temperature). This qualitative picture, though, is difficult to verify experimentally due to the difficulty in measuring temperature at the interface with the equipment used and due to the liquid being stirred.

The experimental results show that the MW effect is more pronounced in system C followed by systems A and B. This can be related to the difference in boiling points (ΔT_b) of the binary components in each system (A: $\Delta T_b = 25.7^\circ\text{C}$, B: $\Delta T_b = 18.0^\circ\text{C}$ and C: $\Delta T_b = 43.7^\circ\text{C}$). More specifically, the higher the difference in the boiling point, the stronger the separation effect. This indicates a strong thermal effect. Besides, the difference in ΔT_b between systems A and B is not big, whereas the difference in the separation effect is considerable indicating that a secondary dependence on the dielectric properties of the mixture exists. In this frame,

system B (ProPro/ProAc) is of particular importance; except being the least dielectric mixture of the three systems, it also has the low boiling component (ProAc) as the high MW absorber ($\epsilon''= 1.0$ vs. $\epsilon''= 0.2$). If only a thermal effect existed, the separation effect should have been more pronounced meaning that the concentration of ProPro in the vapor phase should have been higher for each measured data point. In contrast, Fig. 6.5 shows that the positive difference in separation when using MW is very little and the MW data are close to the thermodynamic equilibrium curve most likely due to the counter-balancing effect of dielectric properties (i.e. the component with the lower boiling temperature is also the low MW absorber).

The effect of power supplied on separation was studied by heating samples with the same initial concentrations using different power inputs. Fig. 6.7 shows the results of a sample from system B having an initial ProAc concentration of 50% (in volume). The effect on steady state temperatures and x,y concentrations (mentioned in caption) is the same except for the required time to reach the steady-state temperature implying that the effect is not power dependent. Getting more insight into the interaction of MW with the VL interface is needed. Nonetheless, we believe that the reported observations herein are of importance in the field of vapor-liquid separations. In practical terms, the improved separation under MW non-equilibrium conditions may be translated into design of smaller columns with a lower number trays, for a given separation efficiency, compared to conventional designs involving heat exchange in the reboiler and condenser only.

Our experiments show that microwaves can improve binary separation of mixtures only when they interact directly with the vapor-liquid interface. In practical terms, this may be translated into design of smaller columns with a lower number trays, for a given separation efficiency, compared to conventional designs involving heat exchange only in the reboiler and condenser. On the contrary, vapor-liquid equilibrium experiments with microwave-bulk liquid interaction (the interface was not exposed to microwaves) yielded compositions that did not differ from those in conventional vapor-liquid equilibrium experiments.

Figure 6.4 xy and Txy graphs obtained with the Discover single-mode microwave oven and the custom designed distillation head (Fig. 6.2). System ProOH (1) / ProPro (2); (-) UNIFAC, (Δ) data set from the literature and (\bullet) experimental values. Temperature reported is the vapor temperature above the interface.

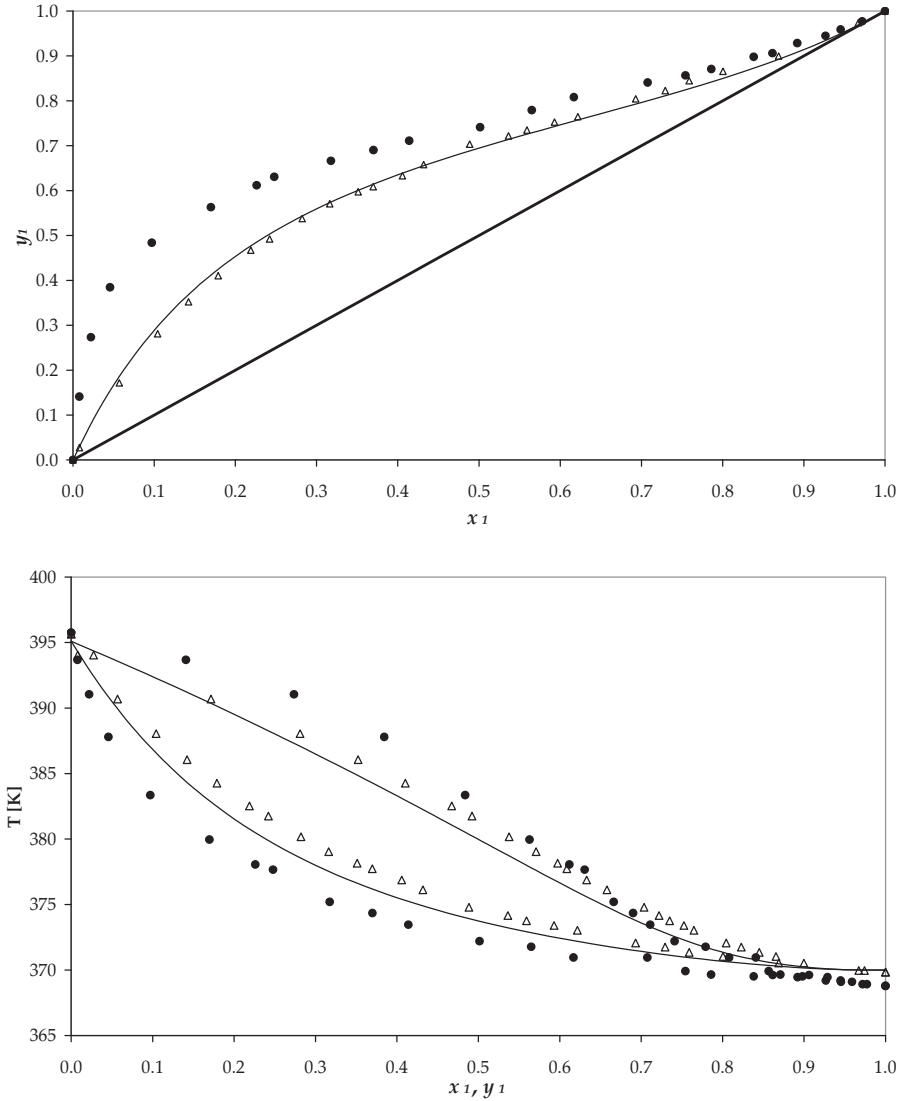


Figure 6.5 xy and Txy graphs obtained with the Discover single-mode microwave oven and the custom designed distillation head (Fig. 6.2). System ProPro (1) / ProAc (2); (-) UNIFAC, (Δ) data set from the literature and (\bullet) experimental values. Temperature reported is the vapor temperature above the interface.

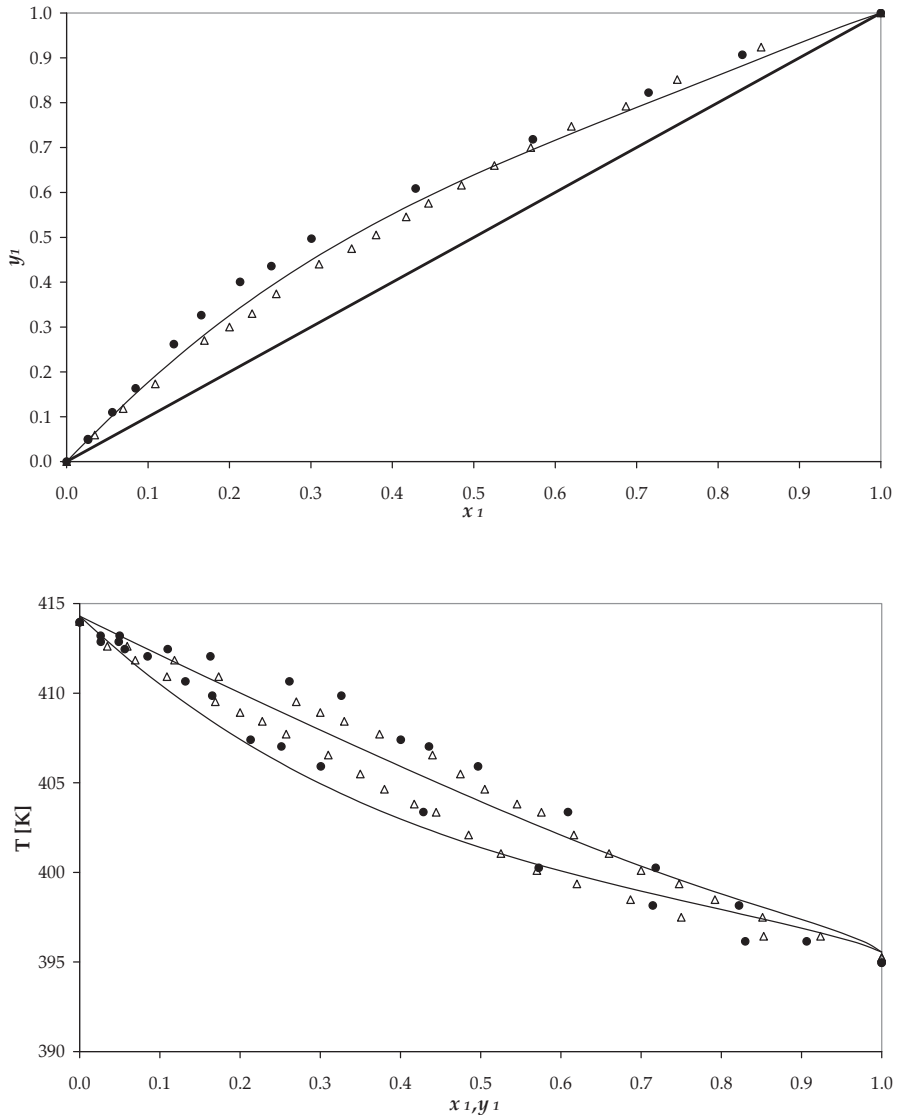


Figure 6.6 xy and Txy graphs obtained with the Discover single-mode microwave oven and the custom designed distillation head (Fig. 6.2). System ProOH (1) / ProAc (2); (-) UNIFAC, (Δ) data set from the literature and (\bullet) experimental values. Temperature reported is the vapor temperature above the interface.

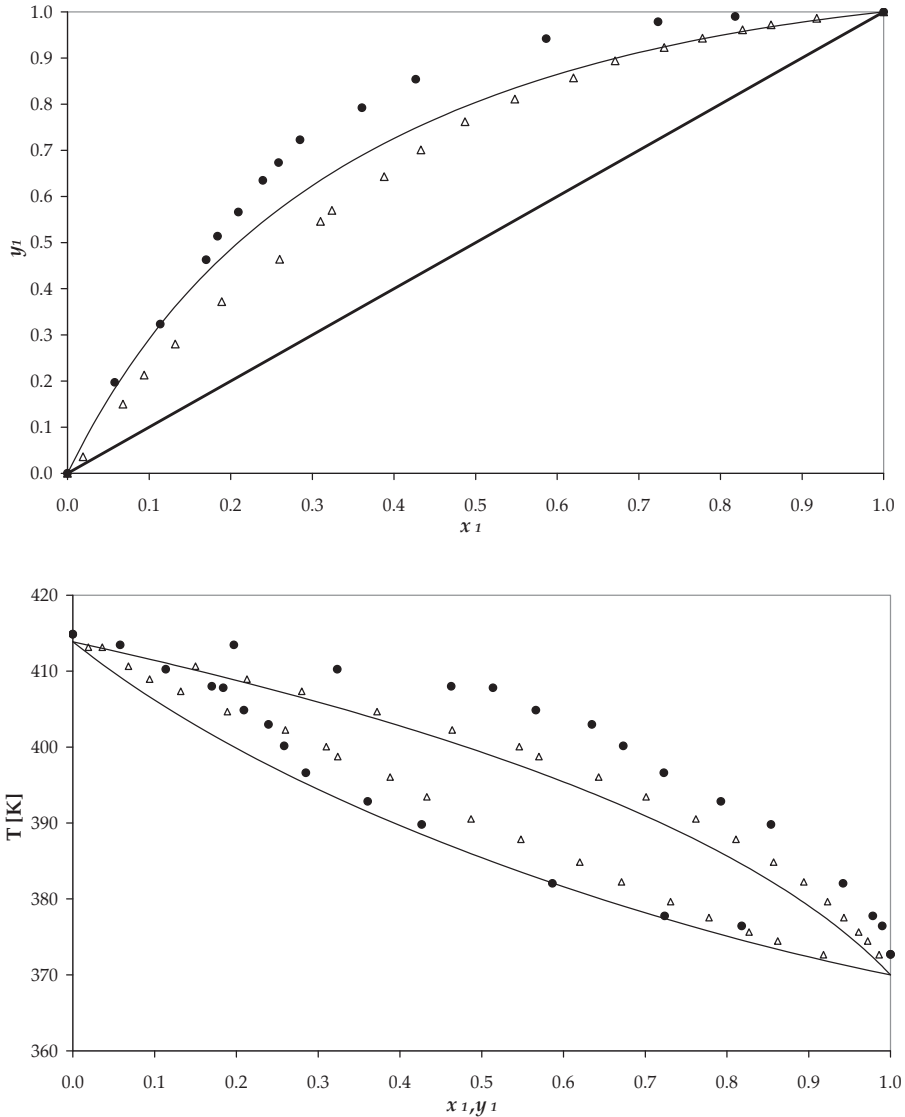
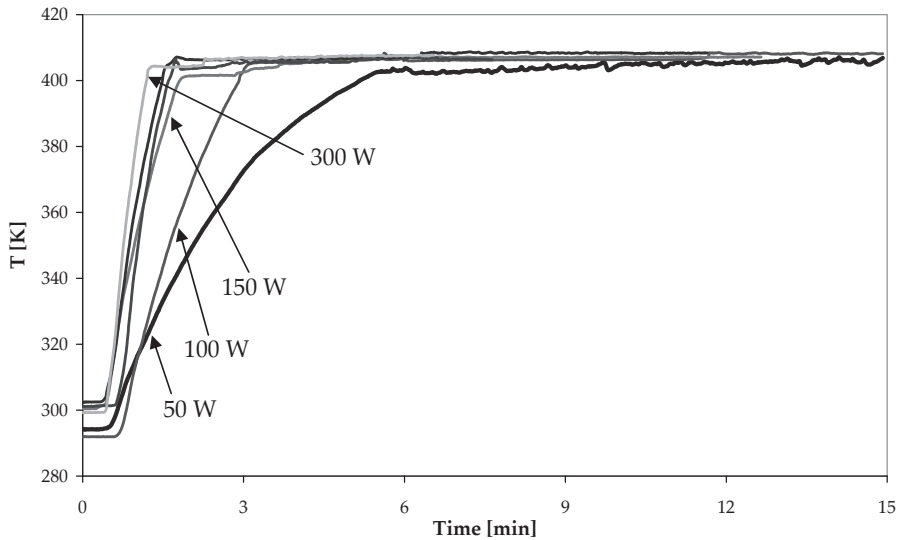


Figure 6.7 Temperature vs. time during heating of system (B): ProPro (1)/ProAc (2) with different MW power inputs. Initial liquid mole fraction: $x_{\text{ProPro}} = 0.36$. Vapor mole fraction: $y_{\text{ProPro}} = 0.58$.



6.6 References

1. Stankiewicz A., Energy Matters Alternative Sources and Forms of Energy for Intensification of Chemical and Biochemical Processes. *Chemical engineering research & design*. **2006**. 84(7): 511-521.
2. Ferhat M.A., Tigrine-Kordjani N., Chemat S., Meklati, B. Y., Rapid Extraction of Volatile Compounds Using a New Simultaneous Microwave Distillation: Solvent Extraction Device *Chromatographia*. **2007**. 65: 217-222.
3. Hao Ye H., Ji J., Deng C., Yao N., Li N., Zhang X., Rapid Analysis of the Essential Oil of *Acorus tatarinowii* Schott by Microwave Distillation, SPME, and GC-MS. *Chromatographia*. **2006**. 63: 591-594.
4. Isom W., Apte P., Holmer A. E., *Method of vaporizing liquids by microwave heating*, U.S. Patent, Editor. 2008, Praxair Technology Inc.: United States.
5. Rajamannan A.H.J., *Microwave distillation*, U.S. Patent, Editor. 1981, Agrohol Systems Inc.: United States.
6. Courville P., Bertrand G., Lallemand A., Stuerger D., The Use of Microwaves to Evaporate Liquids. *Journal of Microwave Power and Electromagnetic Energy*. **1991**. 26(3): 168-177.
7. Stuerger D., Steinchen-Sanfeld A., Lallemand M., *Microwave heating as a tool for coupling Marangoni and Hickman instabilities*, in *Lecture Notes in Physics*. 1996, Springer: Berlin / Heidelberg, p. 227-239.
8. Chemat F., Esveld E., Microwave Super-Heated Boiling of Organic Liquids: Origin, Effect and Application. *Chem. Eng. Technol.* **2001**. 24(7): 735-745.
9. Saillard R., Poux M., Berlan J., Microwave Heating of Organic Solvents : Thermal Effects and Field Modelling. *Tetrahedron*. **1995**. 51(14): 4033-4042.
10. Baghurst D.R., Mingos D. M., Superheating Effects Associated with Microwave Dielectric Heating. *J. Chem. Soc., Chem. Commun.* **1992**. 6: 674-677.
11. Thiebaut J.M., Colin P., Roussy G., Microwave Enhancement of evaporation of a polar Liquid I. *Journal of Thermal Analysis*. **1983**. 28: 37-47.
12. Roussy G., Colin P., Thiebaut J. M., Bertrand G., Wattle G. , Microwave Enhancement of evaporation of a polar Liquid II. *Journal of Thermal Analysis*. **1983**. 28: 49-57.
13. Ortega J., Galvan S. , Vapor-Liquid Equilibria of Propyl Propanoate with 1-Alkanols at 101.32 kPa of Pressure. *J.Chem.Eng.Data*. **1994**. 39(4): 907-910.
14. McDermott C. *Ph.D. Thesis*. Chemical Engineering **1964**, University of Birmingham.
15. Amezcaga A.S., *Anal.Quim.* **1975**. 71: 117-126.

The Effects of Microwave Irradiation on the *n*-Propyl Propionate Esterification Reaction

The experimental results condensed in this chapter evaluate the effects of MW on the reactive test system. The reaction was studied under microwave and conventional heating conditions using a variety of homogeneous and heterogeneous catalysts looking for possible rate enhancement. Special attention was given to zeolite catalysts due the strong interaction that is reported between the microwave field and silanol groups and metal oxides in the framework. Direct evaluation of the heating methods was done by comparing the ester yields after 30 min of equimolar reaction at 100°C. Several catalysts were found to produce more product than the ion-exchange resin Amberlyst 46 under both heating methods and the same catalyst loading. For the test system, the use of microwaves does not improve the conversion of the esterification reaction catalyzed by heterogeneous catalysts possibly because microwaves are dissipated in the liquid phase before they interact with the catalyst particles. From all the catalysts tested, the homogenous Zn triflate proved to be more effective under microwave heating conditions producing 40% more ester compared to the conventionally heated experiment. FT-IR spectra showed that there were no changes in the chemistry of the components and that hydrolysis of Zn triflate into triflic acid, which could promote the reaction, is not likely to occur.

The contents of this chapter were adapted from the work published in:

E. Altman, G. D. Stefanidis, T. van Gerven, A. Stankiewicz
“Microwave-Promoted Synthesis of *n*-Propyl Propionate using Homogeneous Zinc Triflate Catalyst.”

Ind. Eng. Chem. Res., Nigam Issue (2011); DOI: 10.1021/ie200687m
© 2011 American Chemical Society. Reprinted with permission.

"If you're not failing every now and again, it's a sign you're not doing anything very innovative."

Woody Allen

7.1 Esterification reactions and microwaves

The use of alternative forms of energy to improve the yield and selectivity of chemical reactions has been extensively studied by academic researchers in the last decennium. The most important sources investigated include energy from electric, acoustic and electromagnetic (microwaves and light) fields.¹ From these, the application of microwave (dielectric) heating in chemical syntheses has received special attention and is known as microwave chemistry. The state-of-the-art of microwave technology can be covered by the rich amount of literature found in peer reviewed journal publications, as well as many books²⁻⁶ and review articles.⁷⁻¹³ The main benefits that microwave dielectric heating (MW) has shown as compared to conventional heating methods is its capacity to reduce reaction times from several hours to few minutes, increase overall reaction yields and improve selectivity towards a specific product. The main difficulty in the widespread use of MW energy as a heating source is that the fundamental mechanisms by which MW affect reagents and catalysts at molecular scale are still poorly understood.^{4, 14, 15}

Esterification reactions have been studied broadly under conventional heating conditions. Many catalysts including solid acids like ion-exchange resins, zeolites, clays, metal oxides, supported Lewis acids and supported ionic liquids have been investigated.¹⁶⁻¹⁸ Extensive utilization of these catalysts has been hindered by their cost. Simultaneously, esterification reactions have been investigated under MW irradiation in view of possible rate enhancements. Barbosa et al.¹⁹ studied the reaction of acetic acid with 2-methyl-1-butanol using Lewis acids. Reactions were found to occur 30 times faster under MW conditions and ester yields were higher. Pollington et al.²⁰ studied the esterification of 1-propanol with acetic acid using sulfuric acid and Cab-O-Sil catalysts under reflux conditions. The rates of the esterification were found to be identical in both heating modes. Pipuš et al.²¹ studied the esterification reaction of benzoic acid with 2-ethylhexanol in the presence of sulfuric acid, sulfated $ZrO_2 \cdot Fe_2(SO_4)_3$ and montmorillonite KSF as catalysts. The authors concluded that no special

microwave effects were observed under the different heating modes. Shekarriz et al.²² studied several reactions comprising aromatic carboxylic acids with various alcohols using zinc triflate under MW conditions although no experimental comparison with a conventional heating mode was made. The authors obtained shorter reaction times (3 to 5 min) and higher ester yields than in conventional experiments reported in literature. Later, Toukoniitty et al.²³ performed experiments using propionic acid and ethanol over an ion-exchange resin. They concluded that the kinetics and equilibrium of the reaction were unaffected by the method of heating. Recently, Amore et al.²⁴ ran esterification reactions of propionic acid with different alcohols using sulfuric acid. The setup was adjusted so that distillation of water was possible and the reaction equilibrium was shifted. No comparison with conventional heating was presented in this study. Ramesh et al.²⁵ performed butyl ester synthesis using ion-exchanged montmorillonite. The authors claimed that the reactions studied occurred faster with MW irradiation. This literature scan shows the typical outcome of publications in microwave chemistry, where contradictory data are found and results are often not reproducible.

This chapter presents experimental results of the test reaction performed with different types of catalysts (both homogeneous and heterogeneous) comparing both heating methods with special attention given to reaction conditions. The observed phenomena are explained by understanding the dissimilar interactions that exist between the electromagnetic field, reactants and catalysts.

7.2 Experimental Section

7.2.1 Reagents

ProOH, ProAc and ProPro were purchased from Sigma-Aldrich. The reagents were degassed with an ultrasound-bath and dried over molecular sieves from Sigma-Aldrich. The purities of these components were reported by the manufacturer to be more than 99.5% for ProOH and more than 99.0% for ProAc and ProPro.

7.2.2 Catalysts

Homogeneous catalysts: sulfuric acid, zinc (II) trifluoromethanesulfonate (Zn triflate) 98%, copper (II) trifluoromethanesulfonate (Cu triflate) 98%, iron (II) trifluoromethanesulfonate (Fe triflate) 85%, tin (IV) chloride (SnCl_2) 99%, titanium (IV) tert-butoxide ($\text{Ti}(\text{OBu})_4$) 99% and potassium fluoride (KF) 99.99% were purchased from Sigma-Aldrich.

Heterogeneous catalysts: montmorillonite KSF free acid 8-12% was purchased from Sigma-Aldrich; potassium fluoride on alumina oxide 5.5mmol/g of F was purchased from Fluka, and Amberlyst 46 (0.8 - 1.3 eq/kg measured as the concentration of active sites per kilogram of dried catalyst) was purchased from Rohm and Haas. Solid supported catalysts were prepared by wet impregnation following literature methods.¹⁹ Silica (SiO₂) 99% Davisil grade 710, aluminium oxide (Al₂O₃) 98%, zinc chloride (ZnCl₂) puriss Reag. Ph. Eu., ferrous sulfate heptahydrate (FeSO₄ · 7H₂O), and copper sulfate anhydrous 99% (CuSO₄) were purchased from Sigma-Aldrich. For the SiO₂-ZnCl₂ (80%, w/w) catalyst, silica (2.0 g), ZnCl₂ (8.0 g) and ethanol (50 mL) were added to a 100 mL beaker. The slurry was stirred at room temperature for 30 min, dried at 80°C for 3 hours and at 150°C for 15 hours, and then cooled in a desiccator. The same procedure was used for the SiO₂-FeSO₄ (80%, w/w; 2.0g of SiO₂; 8.0g of FeSO₄) and the Al₂O₃-FeSO₄ (80%, w/w; 2.0g of Al₂O₃; 8.0g of FeSO₄) catalysts. For the lower concentrations of acids on the supports the weights were recalculated. The sulfonated MOF was prepared with Basolite A100 (BASF) and H₂SO₄. A solution consisting of 1 g Basolite, 30 g of nitromethane and 0.54 g of trifluoromethanesulfonic anhydride (Fluka) was prepared and stirred for 90 min. Water was used to remove the heat produced. The sulfonated MOF was filtered, washed with ethanol, refluxed in ethanol for 15 hours and then dried in a desiccator for 24 hours. Commercial zeolite catalysts were purchased from Zeolyst International (The Netherlands). The complete list of zeolites with the reported properties by the manufacturer can be found in Table 7.1. Characterization was done using X-ray fluorescence (XRF) for elemental analysis. Crystal size distribution (CSD) was determined using tri-laser diffraction (Microtrac S3500) and the water content was measured by ignition loss using a thermogravimetric analyzer (TGA) with an SDT 2960 thermobalance; the temperature control program set the sample at 120 °C for 1 hour and then ramping to 600 °C for 2 hours. Acidity was measured by ammonia desorption (NH₃-TPD) using a TPD/TPR Micromeritics 2900 setup. Approximately 30 mg of zeolite sample (H⁺) was used for all experiments. For desorption of absorbed water, the sample was heated to 573 K at a rate of 10 K/min under a flow of helium and kept at that temperature for 1 h. The sample was then cooled down to 393 K and three successive pulses of ammonia were injected with subsequent desorption for 30 min at 393 K. TPD was achieved under helium flow by increasing the temperature to 1073 K. Finally, the surface morphology was examined using a Jeol JSM 5400 scanning electron microscope (SEM).

Table 7.1 Zeolite catalysts specifications.

Zeolite type	Commercial Name	SiO ₂ /Al ₂ O ₃ mole ratio*	Nominal cation form	Unit Cell Size* (Å)	Surface Area* (m ² /g)	Crystal size (μm)
FAU	CBV 712	12	Ammonium	24.35	730	1.38
BEA	CP 814C	38	Ammonium	-	710	0.82
BEA	CP 811C	300	Hydrogen	-	620	0.82
FER	CP 914	55	Ammonium	-	400	7.78
FER	CP 914C	20	Ammonium	-	400	4.62
MOR	CBV 21A	20	Ammonium	-	500	0.97

*Data from manufacturer

7.2.3 Composition Analysis

Reacted samples from the kinetic experiments were analyzed by gas chromatography using a Varian 3900GC equipped with a flame ionization detector and a CP-Wax 58 FFAP CB (50m, 0.25mm, 0.2μm / CP7727) column. Helium was used as carrier gas. Injector, detector and oven temperature were at 473.15, 503.15 and 423.15 K, respectively. The column temperature was programmed to rise from 80°C at 20°C/min for 3 min., followed by a 60 °C/min ramp up to 130 °C, and then held constant at 130 °C for an additional 15 min. To determine the water content Karl-Fischer titration was used.

7.2.4 FT-IR Measurements

A ReactIR 15 probe (Mettler-Toledo International Inc.) was used to monitor in situ and in real-time the conventionally heated reaction. Comparison with the MW reaction was done by analyzing the mixture composition at the end of the MW experiment and pairing the IR spectra to find differences in the peak signals. The probe works in a spectral window of 1950 – 650 cm⁻¹ with a resolution of 8 cm⁻¹.

7.2.5 Experimental Procedure

In the experiments for zeolite powder catalyst heating, a 10 ml glass tube containing a catalyst powder bed was inserted into the Discover single-mode microwave oven. Then, power of 10 W was supplied for 35 minutes. Temperature was monitored using one fiber optic (FO) temperature probe placed in the middle of the catalyst bed (with respect to horizontal plane) and introduced 5

cm deep (total height 8 cm). On-line temperature monitoring was performed using the TMI temperature signal conditioner. For the catalyst heating experiments in the solution of reagents the same equipment used to run reactions was employed. The oven was power controlled and set to 100 W. Experiments were carried out for 35 minutes while continuously stirred. For the experiments with zeolites, catalysts with ammonium cations were calcinated to have the H⁺ protonated form and run acidic catalyzed reactions. The zeolites were activated in a conventional oven at 400 °C for 6 hours according to the TGA analysis. Catalysts with already protonated cations were air dried for 24 hours at 100 °C and then used. For catalyst screening experiments a 50 mL glass flask was loaded with the measured amount of acid, alcohol and catalyst (0.9 grams of catalyst, 45 grams of reactants in molar ratio 1:1) and placed inside the Discover MW cavity. (CEM corp.) The mixture was heated at maximum power until the reaction temperature of 100°C was reached. Then, the MW power was controlled to keep the temperature constant. After 30 minutes the reaction was stopped and samples were taken for analysis. For the conventionally heated experiments, the 50 mL glass flask was loaded with the measured amount of acid and catalyst. In a separate flask, the measured amount of alcohol was heated until the reaction temperature. When the reaction temperature was reached in both flasks, the reactants and catalyst were mixed together, and timing was started. Both conventional and MW heated experiments were performed under total reflux conditions for 30 minutes. Every 5 min a sample from the reaction mixture was taken using a syringe for subsequent GC and Karl-Fischer analysis. For reaction experiments, a 500 ml three-neck flask with glass tubing was used. The total amount of reagents was 450g. For experiments under MW conditions a MARS (microwave-accelerated reaction system) multimode cavity (CEM corp.) was used. The microwave was controlled via programmable software SynergyPrep[®] (up to 1600 watts). Temperature feedback control of the microwave cavity is achieved with a microwave transparent FO temperature probe. Temperatures were recorded on-line. Experiments were carried out under open reflux conditions using a condenser with circulating cooling liquid. For experiments under conventional heating conditions the same glass setup was used in combination with a heating mantle equipped with a magnetic stirrer.

7.3 Esterifications and RD

The selection of a catalyst is crucial for the correct operation of an RD column. Pressures and temperatures for reaction and distillation are required to match thus reducing the operational window over which the process is feasible as well as the degrees of freedom to control the process. By the use of MW radiation, this window could be enlarged especially due to selective MW interaction with certain materials. MW heating enables some reactions to occur at much higher rates in the presence of a suitable heterogeneous catalyst thus enabling processes that would otherwise be infeasible due to the low yields or the long time needed to reach high conversions. Consequently, RD technology used so far only in petrochemical and commodities production could be taken to new industrial frontiers in combination with MW radiation. Kappe et al.²⁶ discuss more than 700 reaction schemes performed under MW heating conditions that could serve as suitable reactions for RD processes. As in heterogeneous gas phase reactions, where the use of MW radiation has been demonstrated to enhance reaction rates,²⁷ heterogeneous liquid phase reactions could benefit from the technology in the same way.

7.4 Results and discussion

7.4.1 Dielectric behaviour of the reacting system

Measuring pure component dielectric properties (as seen in Chapter 2) is not enough to fully understand the bulk reaction mixture behavior under microwave irradiation. Although there are many mixing rules reported in literature,^{28, 29} which predict the dielectric behavior of mixtures, we have measured these properties ourselves. In Figure 7.1, the parameters ϵ'' and $\tan \delta$ correspond to 1:1 and 2:1 alcohol to acid molar ratio solutions. The pure alcohol ϵ'' values have been included as reference. It can be seen that the alcohol dictates the dielectric performance of the binary system as there is no much difference between the two concentrations of acid in the mixture. Further, the ϵ'' optimum remains at $T = 50^\circ\text{C}$. When adding a small concentration of catalyst like 2% w/w, the dielectric properties of the mixture remained nearly the same. For equimolar reactions at $T = 100^\circ\text{C}$, the following parameters shall be considered ($\epsilon' = 8.15$, $\epsilon'' = 1.91$, $\tan \delta = 0.235$).

Figure 7.1 Dielectric properties of the reacting binary mixtures of propanol and propionic acid with different molar ratios as a function of temperature.

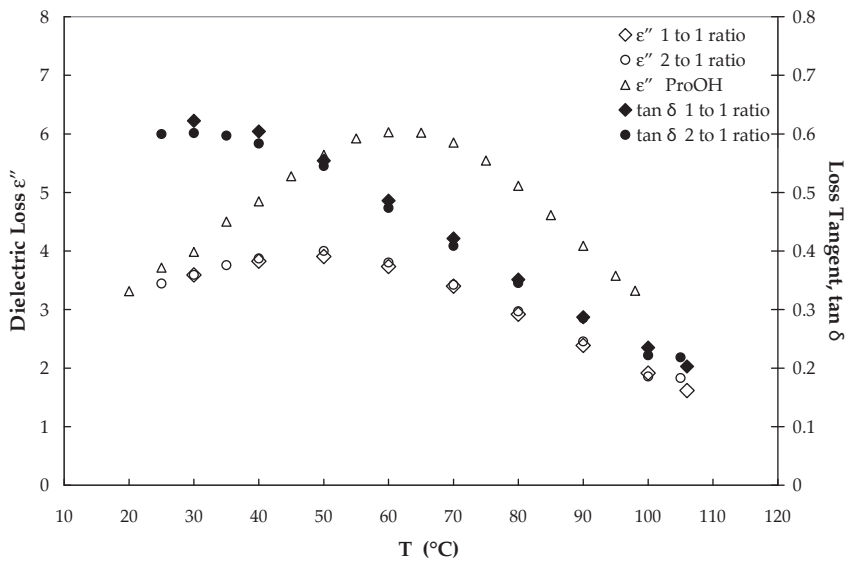


Figure 7.2 Temperature vs. time in different zeolite powder beds irradiated in a Discover mono-mode microwave oven. Power is 10 W.

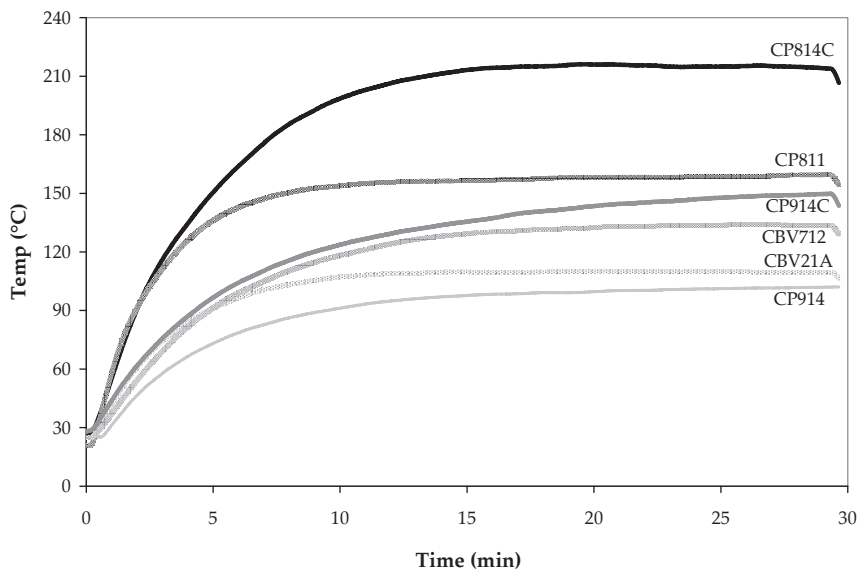


Table 7.2 Zeolite catalysts compositions.

Metal oxide (Wt %)	CP 814C	CP 811C	CP 914	CP 914C	CBV 712	CBV 21A*
SiO ₂	95.4300	99.3100	96.5100	91.4000	87.2000	92.2
Al ₂ O ₃	4.3300	0.4990	3.3300	8.3600	12.6000	7.8
Na ₂ O	0.0217	0.0056	0.0326	0.0299	0.0142	-
P ₂ O ₅	0.0130	0.0106	0.0073	0.0086	0.0074	-
K ₂ O	0.0133	-	0.0064	0.0109	-	-
TiO ₂	0.0182	0.0184	0.0270	0.0306	0.0280	-
Fe ₂ O ₃	0.0727	0.0686	0.0438	0.0567	0.0213	-
ZrO ₂	0.0302	0.0200	0.0063	0.0077	0.0079	-
MgO	0.0360	0.0104	-	-	-	-
CaO	0.0190	0.0096	0.0198	0.0061	-	-
SiO ₂ /Al ₂ O ₃ mole ratio	37.40	337.72	49.18	18.55	11.75	20.0

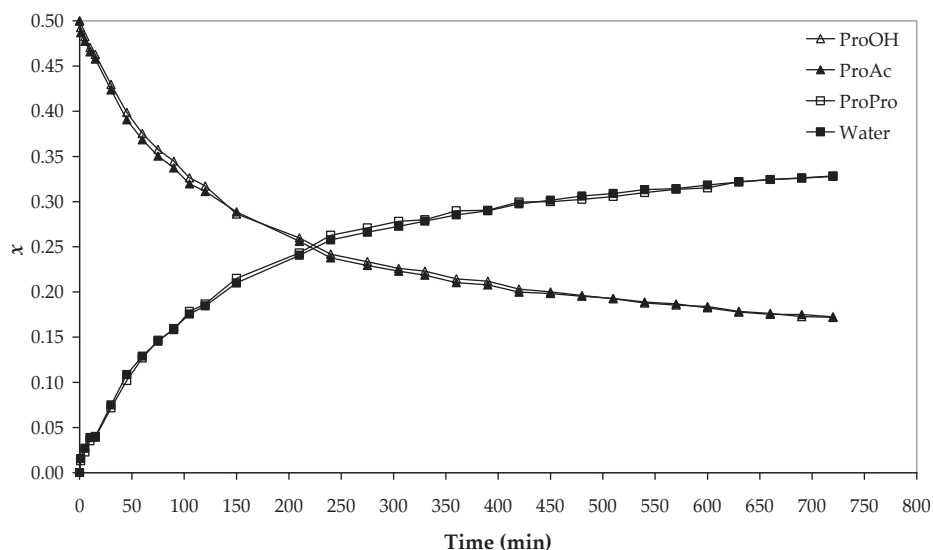
*Ratio calculated

7.4.2 Focus on zeolites

Commercial esterification reactions performed in RD columns are heterogeneously catalyzed using acidic surface-sulfonated ion exchange resins.³⁰⁻³² It has been reported that microwaves cannot enhance heterogeneous reactions using ion-exchange resins because their building block (in this case styrene divinylbenzene copolymers) is transparent to them^{33, 34} and therefore no superheating of catalytic sites can be produced. On the other hand, it has been proven that zeolites can catalyze esterification reactions acting as solid acid catalysts.^{35, 36} Experiments have shown that it is possible to selectively heat catalyst particles and functional groups in zeolites (silanols and other metal oxides present in the framework).³⁷ Furthermore, it has been demonstrated that in heterogeneous gas-solid reaction systems, the use of MW to selectively superheat catalysts may enhance reactions. Following the same approach, a liquid-solid system with the liquid phase being a low MW-absorber could benefit from MW heating in that the bulk liquid temperature remains lower than the solid catalyst temperature ($T_{\text{zeolite/metal/metal oxides}} > T_{\text{bulk liquid}}$). This temperature decoupling would entail energy savings in RD since most of the energy is used to heat the catalyst and not the bulk liquid. Different types of commercial zeolite catalysts, all having a silica/alumina framework in different

morphologies were studied. In Fig. 7.2, the interaction of microwave irradiation with six different commercial zeolites is shown. The catalysts were heated under the same power profile (10 W) showing different heating rates. It was initially expected that selective heating would be dictated by the metal oxide concentrations and the corresponding dielectric properties: Al_2O_3 ($\epsilon'' \approx 9$), TiO_2 ($\epsilon'' \approx 50$), ZrO_2 ($\epsilon'' \approx 25$), Fe_2O_3 ($\epsilon'' \approx 9$). According to this hypothesis and looking to the XRF results quoted in Table 7.2, the best heating catalysts should have been in the order $\text{CBV712} > \text{CP914C} > \text{CBV21A} > \text{CP814C} > \text{CP914} > \text{CP811C}$ following the concentrations of the high dielectric oxides. However, the catalyst rank from the best heated catalyst to the worst one is $\text{CP814C} > \text{CP811C} > \text{CP914C} > \text{CBV21A} > \text{CBV712} > \text{CP914}$. According to these results it can be deduced that it is not only the metal oxides determining the interaction of MW radiation with zeolites but also the silanol groups of the silica. Turner^{37,38} indicates that the concentrations of silanol groups in zeolites may be large. Silanol -OH groups have a substantial dielectric loss thus governing the zeolite heating when exposed to microwave radiation. When the zeolites are heated together with the reaction mixture, the BEA type zeolites perform again better than the rest (results not shown). Overall, the best heated catalysts were the zeolites CP814C and CP811C, which were therefore selected for catalyst screening and comparison experiments.

Figure 7.3 Time_composition plot of a microwave heated equimolar reaction at 373.15 K with 2% w/w of Amberlyst 46.



7.4.3 Catalyst screening and selection

The starting point for the catalyst screening was the reaction performance using the surface sulfonated ion exchange resin Amberlyst 46. This resin and similar counterparts like Amberlyst 15 and Dowex 50 have been extensively studied by Ali¹⁶ and Duarte³⁹, and are currently the preferred catalysts in industrial scale processes. Ion exchange resins are very reliable catalysts in terms of conversion and selectivity but their poor thermal and mechanical resistance hampers them from broader application in industrial processes. It has been demonstrated that MW cannot enhance heterogeneous reactions using ion-exchange resins and consequently other solid acids were considered.²³ Lewis acids are usually preferred over Brønsted acids to avoid byproduct formation and/or to protect acid-labile groups in certain reactions. The problem with this type of reactions, where water is present, is that discrimination between Lewis and Brønsted acids becomes difficult. Various catalysts were selected from reported experiments of esterification reactions performed under microwave irradiation. Equilibrium concentrations were determined after running the reaction for 720 minutes as seen in Figure 7.3. For evaluation, an equimolar solution of alcohol and acid was used with 2% w/w catalyst loading. Catalysts and heating mode comparisons were done by running reactions for 30 minutes and measuring the product yield as compared to the equilibrium concentration ($x_{\text{ProPro}} = 0.33$). In Figure 7.4, the results from the heating mode comparison of the 21 catalysts tested are presented. Several homogeneous and heterogeneous catalysts were found to produce more product than the Amberlyst resin under microwave and conventional conditions with the same catalyst loading and with no by-product formation. In practical applications, only heterogeneous catalysts are used since they are either fixed inside catalytic distillation packings or are easily removed and reused in reactors. The heterogeneous catalysts that were found to yield more ester were the montmorillonite KSF clay, the acidic MOF, the silica supported $\text{Fe}_2(\text{SO}_4)_3$ and the zeolite CP814C. This behavior can be explained since the KSF clay acidity is comparable to that of concentrated nitric and sulfuric acid with a similar surface area⁴⁰ (KSF clay $\sim 40 \text{ m}^2/\text{g}$, Amberlyst 46 (dried) $\sim 50 \text{ m}^2/\text{g}$), while the MOF ($\sim 1500 \text{ m}^2/\text{g}$) and the silica supported iron sulfate ($\sim 500 \text{ m}^2/\text{g}$) have larger areas. Amberlyst 46 sulfonic groups are present only at the catalyst surface, which is disadvantageous in terms of available acidic sites for reaction. The silica supported ferrous sulfate was more effective than the alumina supported iron salt. This may be due to the increased Lewis acidity. In alumina supported catalysts, Brønsted acidity is enhanced as a result of ionic exchange with high valence ions like Fe, which is unfavorable for this reaction. The performance of zeolite CP814C was better, yielding more ester than its counterpart CP811. This can be rationalized by the stronger acidity of this zeolite

reported in Table 7.3. When comparing the heating modes in between zeolites, MW did not yield conversion improvement. Several kinetic studies reported in literature have demonstrated that these catalysts offer a good opportunity in esterification reactions and could potentially replace the actual resins.⁴¹

Table 7.3 Measured acidity for Zeolites CP811 and CP814C.

Zeolite	Acidity (mmol g ⁻¹) NH ₃		
	Weak (A)	Medium (B)	Strong (C)
CP 811C	0.12	0.28	0.41
CP 814	0.47	0.41	0.10

Desorption temperature: (A) 400-650 K; (B) 650-800; (C) 800-1000 K

On the other hand, homogeneous catalysts are still in use in plants with processes designed before the appearance of reactive distillation in the early 1980s. In these processes, concentrated sulfuric acid is still the preferred choice if acid-labile functional groups are not present. The homogeneous catalysts that were found to yield more ester were SnCl₂ and the Cu, Fe and Zn salts of trifluoromethanesulfonic acid (CF₃SO₃H). Lewis acids containing tin metal (particularly SnCl₂) have been investigated in esterification reactions with good results.^{38, 42} The activity of SnCl₂ is comparable to that of sulfuric acid, while SnCl₂ has the advantage of being less corrosive. The other group of catalysts that has received attention for this application includes the metal salts of triflic acid or metal triflates (M(CF₃SO₂)_n or M(OTf)_n). These salts fall into an interesting category of catalysts for green chemistry due to enhanced Lewis acidity, high water tolerance and the possibility to fix them on supports.^{43, 44} From the three metal salts, only Zn triflate proved to be more effective under microwave heating producing 40% more ester than in the event of conventional heating (83% vs. 59%) during the short reaction experiments as seen in detail in Figure 7.5.

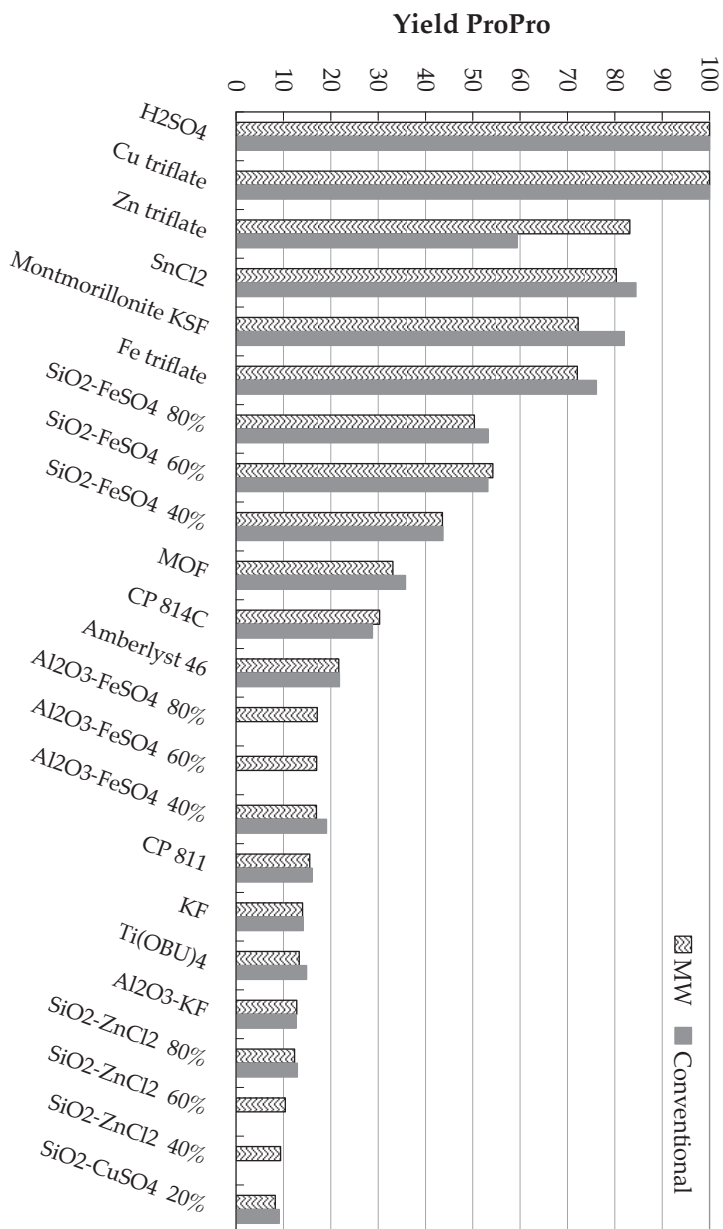


Figure 7.4 Catalysts and heating mode comparison for an equimolar esterification reaction at 373.15 K with 2 wt% catalyst loading. Zn triflate produces 40% more ester under microwave heating (83% vs 59%).

Figure 7.5 Catalysts and heating mode comparison, equimolar reaction at 373.15 K with 2% w/w catalyst loading. (●) reaction with Zn triflate catalyst using MW; (▲) reaction with Zn triflate catalyst conventionally heated; (■) reaction with Amberlyst 46 catalyst using MW.

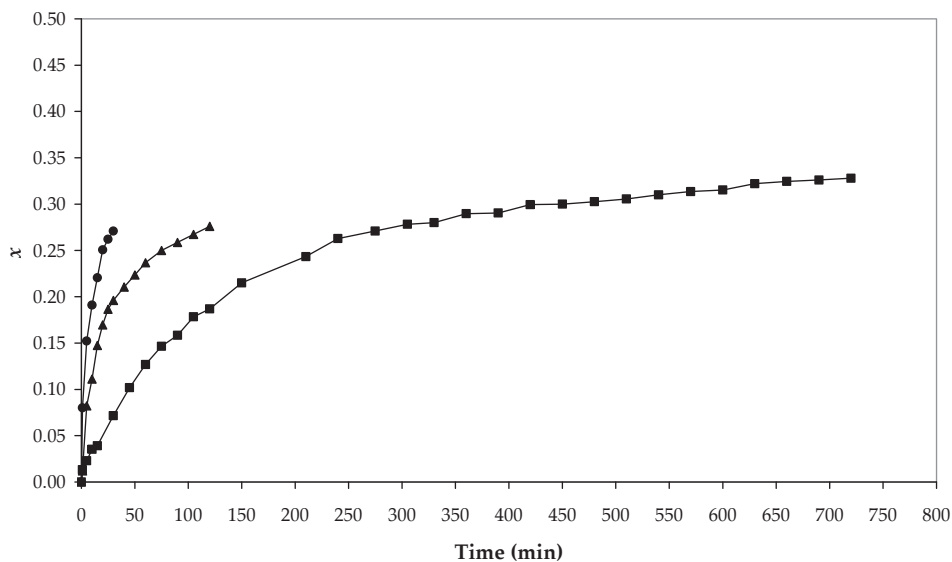


Figure 7.6 FT-IR spectrum of $\text{Zn}(\text{OTf})_2$.

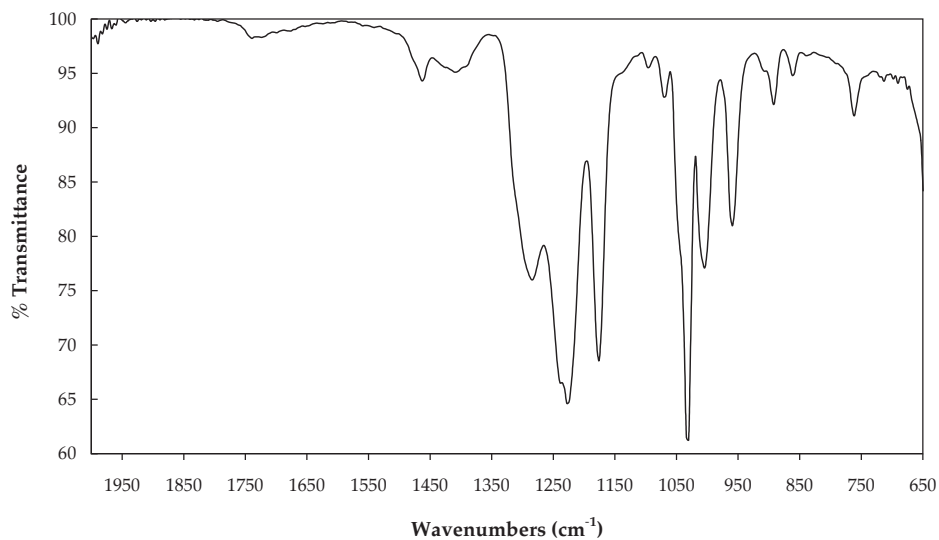


Figure 7.7 Surface plot of the esterification reaction of 1-propanol and propionic acid to produce n-propyl propionate. The characteristic peak for n-propyl propionate is at 1355 cm^{-1} .

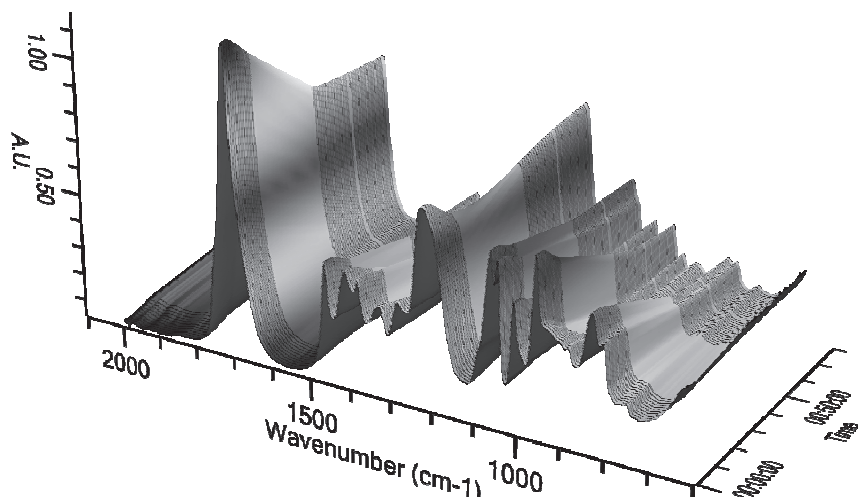
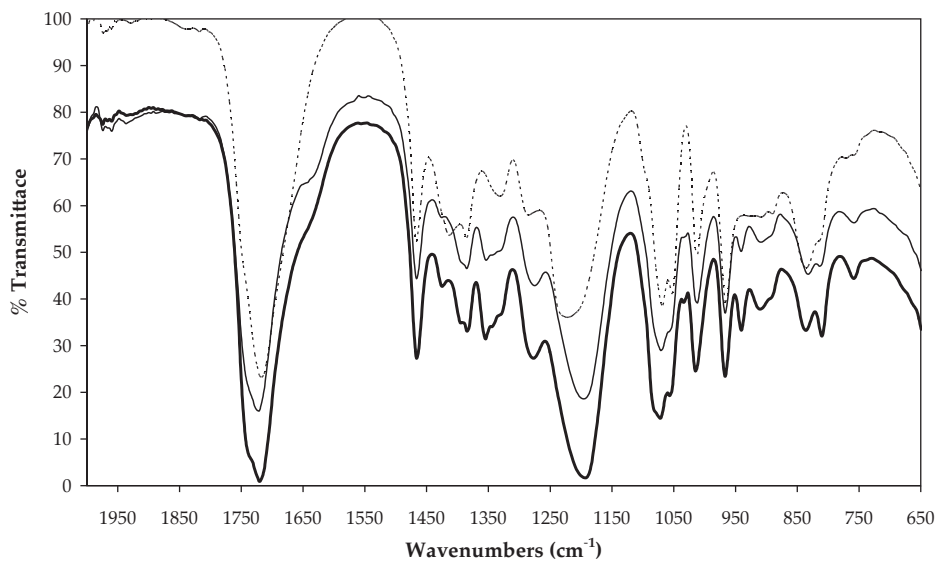


Figure 7.8 FT-IR spectra of the reacting mixtures. --- mixture without catalyst at 100°C , - conventionally heated reaction after 30 min, - MW heated reaction after 30 min.



Elucidation of the phenomena is difficult since the nature of the zinc triflate-MW interaction is actually unknown. In general, rate enhancements are rationalized in three ways; (a) superheating of one of the reactants and/or the catalyst to higher temperatures than the bulk one, associated with increase in the reaction rate constant (pure thermal effect), (b) changes in chemistry due to the superheating effect (e.g. decomposition) and (c) selective interaction of the electromagnetic field with specific molecules in the reacting mixture (known as non-thermal or microwave effect). In the work of Obermayer et al.⁴⁵, a laboratory procedure using SiC vials has been described to easily determine whether the enhancement in the reaction is due to pure thermal effects or not. The limitation, however, lies in the procurement of such vials. Scientists working actively in the field should aim to discriminate the existence of a non-thermal effect. Another way to compare results between conventional and MW heating and discriminate between the above mentioned effects is via in situ spectroscopic techniques. Three methods have been used (yet not extensively) by researchers to follow chemical reactions; X-ray scattering⁴⁶, Raman spectroscopy⁴⁷ and FT-IR spectroscopy.⁴⁸ We have used FT-IR to verify whether there was a change in chemistry particularly in the Zn(OTf)₂ catalyst either by thermal decomposition or other side reactions. Thermal decomposition of triflic groups occurs at 540°C, as measured by Wilson et al.,⁴⁴ which is unlikely to happen under the conditions used in this study and considering the dielectric properties measured. On the contrary, a secondary chemical reaction between hydroxyl groups to form ZnO and CF₃SO₃H (triflic acid) would be more likely to happen and could explain the boost in reaction conversion. Triflic acid is one of the strongest acids known. To determine the Zn(OTf)₂ spectra depicted in Figure 7.6, we used the spectra of a solution of the catalyst in ProOH and subtracted it from the one of pure alcohol. Characteristic peaks for triflic acid as compared to the Zn(OTf)₂ spectra⁴⁹ are found at 1280, 1000 and 959 cm⁻¹. Pure component spectra were obtained and recorded as background. Intense characteristic peaks for ProOH were detected at ca. 967 cm⁻¹, for ProAC at 1414 and 847 cm⁻¹, and for ProPro at 1355 cm⁻¹. We then monitored the conventional reaction in situ. Figure 7.7 shows a surface plot of the ProPro synthesis at 100°C and equimolar alcohol to acid ratio. The progress of the reaction can be followed by the growth of peaks over time. Ester formation can be traced in the peak at 1355 cm⁻¹. In order to compare the two heating modes and verify the possible catalyst reaction, IR spectra obtained from solutions after 30 minutes of reaction along with spectra from the mixture without catalyst are plotted together in Figure 7.8. It can be concluded from the IR spectra that the chemistry of the components in the reaction mixtures is the same for the two heating modes and that hydrolysis of Zn triflate into triflic acid is not likely to occur.

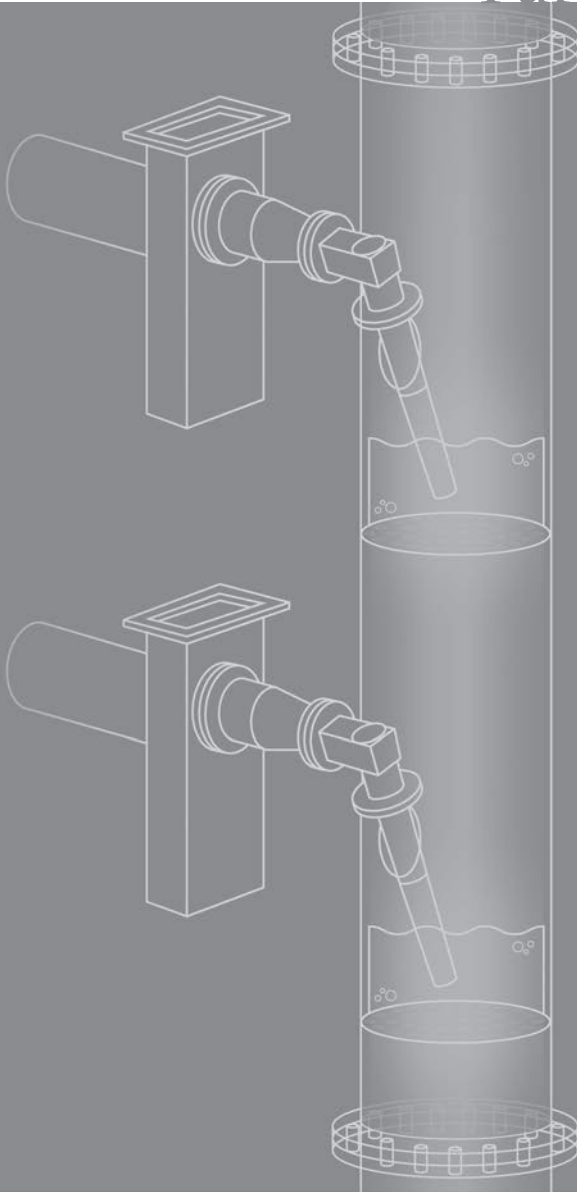
7.5 References

1. Stankiewicz A., Energy Matters Alternative Sources and Forms of Energy for Intensification of Chemical and Biochemical Processes. *Chemical engineering research & design*. **2006**. 84(7): 511-521.
2. Bogdal D., *Microwave-assisted Organic Synthesis, One Hundred Reaction Procedures*. **2005**, Oxford: Elsevier.
3. Kappe C.O.D., Murphree S., *Practical microwave synthesis for organic chemists: strategies, instruments, and protocols*. **2009**, Weinheim: Wiley-VCH.
4. Leadbeater N.E., *Microwave Heating as a Tool for Sustainable Chemistry (Sustainability)*. **2010**, Boca Raton: CRC Press.
5. Roussy G., *Foundations and industrial applications of microwave and radio frequency fields; physical and chemical processes*, ed. Wiley-WCH. **1995**, Sussex: Wiley-WCH.
6. Hayes L.B., *Microwave Synthesis. Chemistry at the Speed of Light*. **2002**, Matthews, NC.: CEM Publishing.
7. De la Hoz A.D.-O., Moreno A., Microwaves in organic synthesis. Thermal and non-thermal microwave effects. *Chem. Soc. Rev.* **2005**. 34: 164–178.
8. Kappe C.O., Controlled Microwave Heating in Modern Organic Synthesis. *Angew. Chem.* **2004**. 43: 6250–6284.
9. Kappe C.O., Controlled microwave heating in modern organic synthesis: highlights from the 2004–2008 literature. *Mol Divers.* **2009**. 13: 71-193.
10. Martínez-Palou R., Microwave-assisted synthesis using ionic liquids. *Mol Divers.* **2010**. 14: 3-25.
11. Nüchter M.O., Bonrath W.; Gumb A., Microwave assisted synthesis – a critical technology overview. *Green Chemistry*. **2004**. 6: 128-141.
12. Strauss C.R.R., Accounting for clean, fast and high yielding reactions under microwave conditions. *Green Chemistry*. **2010**. 12: 1340–1344.
13. Caddick S.F., Microwave enhanced synthesis. *Tetrahedron*. **2009**. 65: 3325–3355.
14. Conner W.C.T., How Could and Do Microwaves Influence Chemistry at Interfaces? *J. Phys. Chem. B*. **2008**. 112: 2110-2118.
15. Perreux L.L., A tentative rationalization of microwave effects in organic synthesis according to the reaction medium, and mechanistic considerations *Tetrahedron*. **2001**. 57(45): 9199-9223
16. Ali S.H.T., Al-Sahhaf T., Synthesis of esters: Development of the rate expression for the Dowex 50 Wx8-400 catalyzed esterification of propionic acid with 1-propanol. *Chemical Engineering Science*. **2007**. 62: 3197-3217.
17. Duarte C., Buchaly C., Kreis P., Loureiro J. M., Esterification of propionic acid with *n*-propanol catalytic and noncatalytic kinetic study. *Inzynieria Chemiczna i Procesowa*. **2006**. 27: 273–286.
18. Lilja J.S., Murzin D. Y., Esterification of propanoic acid with ethanol, 1-propanol and butanol over a heterogeneous fiber catalyst *Chemical Engineering Journal*. **2005**. 115: 1–12.
19. Barbosa S.L.D., Cunha C., Solvent free esterification reactions using Lewis acids in solid phase catalysis. *Applied Catalysis A*. **2006**. 313: 146-150.
20. Pollington S.D.W., Candlin J. P.; Jennings, J. R., The Influence of Microwaves on the Rate of Reaction of Propan-1-ol with Ethanoic Acid. *J. Org. Chem.* **1991**. 56: 1313-1314.
21. Pipuš G.P., Koloini T., Esterification of Benzoic Acid with 2-Ethylhexanol in a Microwave Stirred-Tank Reactor. *Ind. Eng. Chem. Res.* **2002**. 41: 1129-1134.
22. Shekarriz M., Taghipoor S., Jamarani M. S., Esterification of Carboxylic Acids with Alcohols under Microwave Irradiation in the Presence of Zinc Triflate. *J. Chem. Research*. **2003**. 3: 172-173.
23. Toukoniitty B.M., Murzin D. Y., Esterification of propionic acid under microwave irradiation over an ion-exchange resin. *Catalysis Today*. **2005**. 100: 431–435.
24. Amore K.M.L., Microwave-Promoted Esterification Reactions: Optimization and Scale-Up. *Macromol. Rapid Commun.* **2007**. 28: 473–477.
25. Ramesh S. P., Bhat Y. S., Enhancing Brønsted acid site activity of ion exchanged montmorillonite by microwave irradiation for ester synthesis. *Applied Clay Science*. **2010**. 48: 159-163.

26. Kappe C.O., Dallinger D., Controlled microwave heating in modern organic synthesis: highlights from the 2004–2008 literature. *Mol. Divers.* **2009**. 13: 71-123.
27. Durka T., Van Gerven T., Stankiewicz A., Microwaves in Heterogeneous Gas-Phase Catalysis: Experimental and Numerical Approaches. *Chem. Eng. Technol.* **2009**. 32(9): 1301-1312.
28. Harvey A.H., Prausnitz J. M., Dielectric Constants of Fluid Mixtures over a Wide Range of Temperature and Density. *Journal of Solution Chemistry*. **1987**. 16: 857-869.
29. Lou J., Hatton T. A., Laibinis P. E., Effective Dielectric Properties of Solvent Mixtures at Microwave Frequencies. *J. Phys. Chem. A*. **1997**. 101: 5262-5268.
30. Duarte C., Buchaly C., Kreis P., Loureiro J. M., Esterification of propionic acid with *n*-propanol catalytic and noncatalytic kinetic study. *Inżynieria Chemiczna i Procesowa*. **2006**. 27: 273-286.
31. Lundquist E., *Catalyzed esterification process*. 1995: US Patent
32. Schmitt M., von Scala C., Moritz P., Hasse H., *n*-Hexyl acetate pilot plant reactive distillation with modified internals. *Chemical Engineering and Processing*. **2003**. 44: 677-685.
33. Toukoniitty B.M., Esterification of propionic acid under microwave irradiation over an ion-exchange resin. *Catalysis Today*. **2005**. 100(3-4): 431-435.
34. Kabza K.G., Chapados B. R., Gestwicki J. E., McGrath, J. L., Microwave-Induced Esterification Using Heterogeneous Acid Catalyst in a Low Dielectric Constant Medium *J. Org. Chem.* **2000**. 65(4): 1210-1214.
35. Peters T.A., Benes N. E., Comparison of commercial solid acid catalysts for the esterification of acetic acid with butanol. *Applied Catalysis A: General*. **2006**. 297: 182-188.
36. Kirumakki R.S., Nagaraju N., Narayanan S., A comparative esterification of benzyl alcohol with acetic acid over zeolites H β , HY and HZSM5. *Applied Catalysis A: General*. **2004**. 273: 1-9.
37. Turner M.D.L., Microwave Radiation's Influence on Sorption and Competitive Sorption in Zeolites. *AIChE Journal*. **2000**. 46(4): 758-768.
38. Cho C.S.K., Choi H. J., Catalytic activity of tin(II) chloride in esterification of carboxylic acids with alcohols. *Bull. Kor. Chem. Soc.* **2002**. 23: 539-540
39. Duarte C. *Production of TAME and n-Propyl Propionate by Reactive Distillation*. Department of Chemical Engineering. **2006**, University of Porto.
40. Liu Y.X.Z., Deng N. S., Photodegradation of Bisphenol A in the Montmorillonite KSF Suspended Solutions. *Ind. Eng. Chem. Res.* **2008**. 47: 7141-7146.
41. Otera J.N., *Esterification*, ed. Wiley-WCH. **2010**, Weinheim: Wiley-WCH.
42. Cardoso A.L.N., da Silva M. J., Kinetic Study of Alcoholysis of the Fatty Acids Catalyzed by Tin Chloride(II): An Alternative Catalyst for Biodiesel Production. *Energy & Fuels*. **2009**. 23: 1718-1722
43. Clark J.H., Catalysis for green chemistry. *Pure Appl. Chem.* **2001**. 73(1): 103-111.
44. Wilson K. R., Clark J. H., Novel heterogeneous zinc triflate catalysts for the rearrangement of α -pinene oxide. *Catalysis Letters*. **1999**. 61: 51-55.
45. Obermayer D. G., Kappe C. O., Microwave Chemistry in Silicon Carbide Reaction Vials: Separating Thermal from Nonthermal Effects. *Angew. Chem. Int. Ed.* **2009**. 48: 832-8324.
46. Robb G.R.H., Whittaker A. G., Temperature-resolved, in-situ powder X-ray diffraction of silver iodide under microwave irradiation. *Phys. Chem. Comm.* **2002**. 5: 135-137.
47. Leadbeater N.E.S., Barnard T. M., Using *in situ* Raman monitoring as a tool for rapid optimisation and scale-up of microwave-promoted organic synthesis: esterification as an example. *Organic & Biomolecular Chemistry*. **2007**. 5: 822-825.
48. Leadbeater N.E., *In situ* reaction monitoring of microwave-mediated reactions using IR spectroscopy. *Chem. Comm.* **2010**. 46: 6693-6695.
49. Varetti E.L., The infrared spectra of trifluoromethanesulphonic acid in different states of aggregation. *Spectrochimica Acta Part A: Molecular Spectroscopy* **1988**. 44: 733-738.



Part IV



**Microwave Enhanced Reactive Distillation
(MWeRD)**

Technology Integration: The Concept of Microwave Enhanced Reactive Distillation (MWeRD)

As shown in previous chapters, microwave (MW) radiation can affect the molecular separation of components (Chapter 6) and reaction kinetics (Chapter 7) when applied to each of the processes separately. This chapter discusses the application of MW to a RD unit. The engineering problem of introducing MW energy into a RD column is initially addressed. Several potential MW technologies are then explained along with their effect on conventional column design and operation, based on test system characteristics. Scaling-up and energy conversion issues are also discussed. Finally, the concept of a new technology—Microwave Enhanced Reactive Distillation—is explained in detail.

“I want to retire knowing I did everything I could”

Michael Phelps

8.1 Reactive Distillation meets Microwaves

Because of its unique heat transfer characteristics, microwave (MW) heating has been used at large scales in diverse applications. Examples include processes like drying (wood, textiles, paper), food defrosting, tempering, baking and pasteurization, polymer synthesis (rubber curing and vulcanization) and material sciences (sintering, melting, gluing). In chemical manufacturing, however, its utilization is reduced to small-scale niche applications, mostly in the fields of pharmaceuticals and drug discovery and in biomedical, environmental, analytical and biochemistry. Technology integration and the benefits of combining a conventional reactive distillation process with MW heating are discussed in this chapter. It is always important to keep in mind that process technology aims at reaching pilot-scale and ultimately full-scale production. If the new combined technology is ever to become a reality, there are a number of technical questions that need to be addressed before a fully integrated *Microwave Enhanced Reactive Distillation* (MEeRD) column is built.

Although the technical principles and engineering aspects of MW hardware are beyond the scope of this thesis, an understanding of the basics of MW operation, especially its main technological drawbacks, is necessary before advances can be made in equipment integration. The main barriers to the large-scale use of MW technology in chemical processing are extensively discussed in books and articles, and include the following: (i) the design of microwave applicators that could fit conventional chemical apparatuses,¹⁻⁶ (ii) the reliable scale-up of laboratory results⁷⁻⁹, and (iii) the energy efficiency of the magnetrons.¹⁰⁻¹² Each barrier will be discussed separately taking into consideration the test system, the pilot-scale DN-50 column used for RD experimentation (described in Chapter 5) and the experimental results given in Chapters 6 and 7. Specific conditions for separation and reaction have to be met to fully benefit from the MWeRD technology integration. The experiments detailed in Chapter 6 have shown that MW can improve the separation of binary mixtures only when they interact directly with the vapour-liquid interface. This means that the MW equipment must radiate as much vapour-liquid contacting

area as possible. In principle, all the packing inside the column (structured or random) or the entire number of trays used should be effectively radiated. Another condition derived from experiments about the reaction front and discussed in Chapter 7 is that the original heterogeneous catalyst Amberlyst 46, used in conventional RD for the synthesis of ProPro, has to be replaced by the homogenous Zn triflate—the only catalyst that was found to promote the reaction using MW, yielding 40% more ester. Therefore the column configuration described in Chapter 5 has to be modified, considering the low liquid holdup of the structured packing used, the position of the feeds and where and how the catalyst will be loaded.

8.1.1 Microwave cavities for RD

MW equipment consists of three basic parts: a *magnetron* that produces the electromagnetic waves; a *waveguide* (hollow metal pipe) that conveys electromagnetic waves between its endpoints and an *applicator* or *cavity* that holds the volume required to perform chemical processes. There are some additional components including the *power transducer*, a *tuner* to adjust the equipment so that most of the emitted energy ends up inside the sample and not reflected back, *controllers* and *MW leakage sensors*. This discussion will only focus on the applicator, which plays a key role in coupling the MW hardware to the RD column.

Two types of MW applicators, manufactured by many different suppliers, are available on the market for chemists and engineers to perform MW chemistry at laboratory¹³⁻¹⁶ and industrial¹⁷⁻²² scales: the so-called mono-mode or single-mode applicator and the multi-mode applicator (Figure 8.1). Both have widespread uses, are heavily used by researchers in the field and have advantages and disadvantages depending on the intended application. For the work undertaken in this study, both types of applicator were used, being provided by the CEM Corporation, a partner of this project. The multi-mode applicator is perhaps more popular because of historical and economical reasons as the first ovens employed for laboratory applications were domestic MV apparatuses. The main difference between a domestic oven and a laboratory multi-mode oven is that the latter is built to survive laboratory conditions, including corrosion-resistant materials with several health and safety features. These applicators feature large cavity geometries (up to 3L) and allow multiple samples to be treated simultaneously.

The operation principle of these ovens is quite simple. Once the waves are emitted from the magnetron (the same used in ordinary domestic models at a frequency of 2.45 GHz) and after being conducted through the waveguide, they are scattered throughout the cavity with a mode stirrer or field diffuser (a rotating metal plate). This induces stochastic field behaviour as the waves reflect against the cavity walls, interacting among themselves constructively and destructively, and hitting the sample at different positions. Different levels of energy intensity are generated at different locations in the cavity volume, recognized as hot and cold spots, as a result of the coexistence of many resonant modes. One way to avoid this random behaviour is to average the field exposure across the cavity, for example by rotating the samples or stirring in multi-phase mixtures.

Figure 8.1 Microwave ovens from CEM Corporation. On the left the mono-mode Discover™ unit and on the right the multi-mode MARST™ unit.



Another difficulty encountered when using multi-mode instruments is the low power density that is applied due to the large volume of the cavity. The DN-50 column geometry and size allows a stack of multi-mode cavities to be used along the length of the column (only where the packing sections or trays are located). The continuous movement of the vapour rising and liquid falling inside the column may be enough to continuously change the field and avoid hot and cold spots inside the cavity, producing well scattered waves along the radiated section. With this configuration, however, scale-up will only be possible with column diameters up to DN-100 due to the penetration depth of the waves inside the sample (as will be explained in section 8.1.2). The changing field poses serious challenges for experimental reproducibility as well.

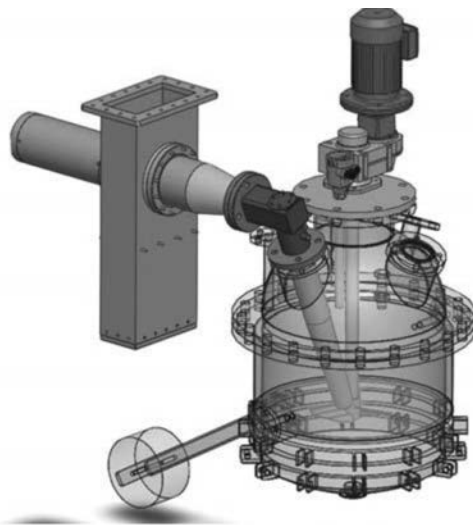
A different option is to use single-mode cavities, which have a more consistent and predictable field distribution achieved by using a well-defined cavity geometry specially designed and tuned for a specific vessel, size and position. These single-mode applicators use ordinary magnetrons and support only one resonant mode, therefore resulting in highly localized heating. Contrary to multi-mode applicators, they can efficiently provide high field strength at mode-specific locations. The limitation of mono-mode applicators is the lack of proper scale-up concepts for columns with diameters larger than the DN-100 column. A stack of single-mode cavities that irradiate the column length can be used in the case of the DN-50 column. The superior performance in reproducibility, field predictability and energy optimization comes at a higher capital cost as the number of units and the price per unit will be higher as compared with the counter-current counterparts. As described above, both cavities can be properly used for MWeRD experimentation at pilot scales up to DN-100. Nonetheless, two more requirements should be taken into account: (1) the position of the column inside the cavity, which forces the MW apparatus to completely surround the column, and (2) the material of the column, which should be MW transparent (e.g. normal glass, quartz or PTFE) so that all the MW energy can reach the reaction mixture and ultimately be absorbed by it.

Recently, a rather new and innovative way to introduce MW to conventional column apparatuses in terms of size and materials has become available. The French MV equipment manufacturer Sairem¹⁷ has developed a technology called Internal Transmission Line (INTLI). This technology does not make use of a formal cavity. Instead, the waveguide is connected to an antenna that can be inserted inside conventional apparatuses, “leaking” MW radiation along the length and at the tip of the tube as seen in Figure 8.2. In the case of this figure, the antenna is inserted inside a conventional chemical reactor, resulting in more effective MW-load coupling and process intensification in terms of volume reduction. Further scale-up issues, besides the MW-column hardware integration, are highlighted in section 8.1.2.

8.1.2 Scale-up

In recent years, the scaling up of MW reactions has received considerable attention from researchers and the number of equipment options offered by MW assembling companies has also increased. However, despite these efforts, not a single large-scale commercial chemical production process has been disclosed due to the factors mentioned in Chapter 1, thus hindering the widespread use of MW in bulk chemical manufacturing.^{23, 24} Scale-up has accordingly received most of the attention. There are many ways to scale-up

Figure 8.2 Microwave ovens from CEM Corporation. On the left the mono-mode Discover™ unit and on the right the multi-mode MARS™ unit.

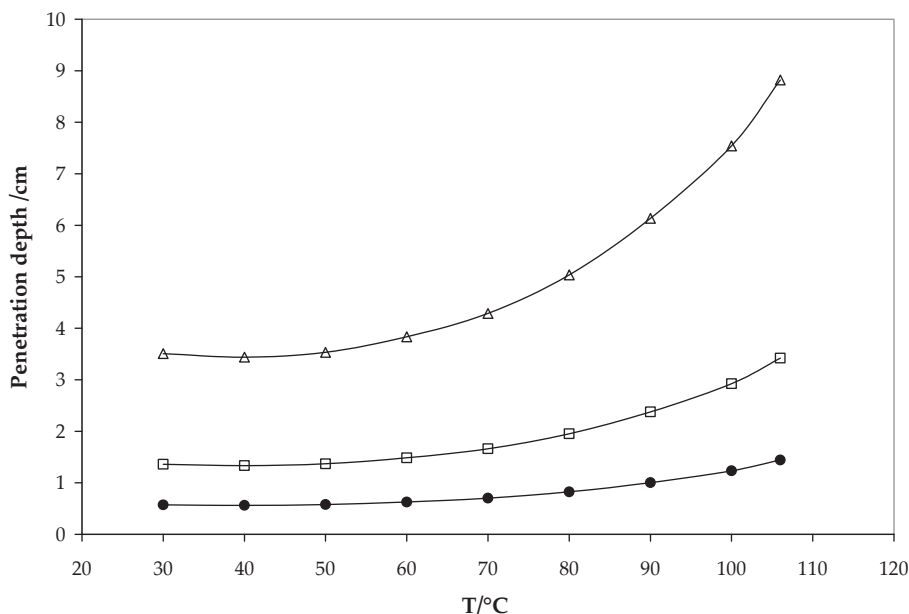


MW reactions depending on process conditions. Although not all of them are pertinent to the intended application of a MWeRD column, the following two should be mentioned: (i) scale-up in parallel, where multiple vessels are treated simultaneously (numbering-up approach), typically used for sealed vessels in multi-mode cavities, and (ii) scale-up using semi-continuous and continuous flow, which has recently received considerable interest.

The principle here is to heat the reaction mixture as it passes through a radiation zone. The throughput depends on flow rate, which in turn determines the residence time that corresponds to the RD column case. Another issue with scaling-up MW is the non-linearity of several parameters. Power density falls dramatically at larger scales, which can result in temperatures and heating rates that are lower than those obtained at laboratory scales, which can, in turn, hamper the desired MW effect. However, the scale-up issue is actually of intrinsic nature. Physically, the penetration depth (d_p) of MW cannot be manipulated in the sense that the d_p is fixed at a given frequency, temperature and dielectric properties of the reacting components. This poses a physical boundary to the process, limiting the application of the technology to column sizes that are far from the usual manufacturing scales in distillation and RD. For the test system, the d_p has been calculated using Equation 2.9 in Chapter 2. Figure 8.3 shows its dependency on temperature for three different frequencies

(5.8, 2.45 and 0.95 GHz). Since d_p is defined as the maximum distance that a wave can penetrate into a sample when its power has dropped to 37% of its original transmitted value, the d_p is just 2.5 to 3.5 cm under the reaction conditions used in the ProPro synthesis (equimolar, 90–110°C).

Figure 8.3 Penetration depth d_p as a function of temperature for an equimolar solution of ProOH and ProAc at 3 different frequencies; •, 5.8 GHz; □, 2.45 GHz; Δ, 0.95 GHz.



8.1.3 Energy efficiency of magnetrons

Although MW systems operating at 2.45 GHz are more expensive than the usual conventional heating methods^{10, 25} many industries use the technology at large commercial scales, proving its economic viability.²⁶ The fundamental limitation lies, however, in the efficiency of conversion of electrical power into MV by the magnetron. Magnetron efficiency may range from 60% to 90% depending on the operation frequency (e.g. 2.45 vs. 0.95 GHz), the power level applied, the operation mode (stationary vs. pulsing mode) and the process duration. In addition, depending on other process factors such as system dielectrics, equipment configuration and cavity design, the electromagnetic

power is partially converted into heat in the targeted sample/process fluid. In principle, up to 100% efficiency of electromagnetic energy dissipation in the process fluid can be achieved with proper MW engineering. The question then is whether the above mentioned inefficiencies can be overcome with the benefits MW bring to chemical processes. This question remains unanswered and is case-specific in the MW chemistry field, where several studies have been published on the overall efficiency of MW heating^{26,27} in reference to small-scale experiments that may not be economically significant (and will possibly differ) at pilot or large scales; then conventional heating has proven to be more efficient. Along this line, several authors argue that MW energy can only be applied to cases of high value per unit of product mass or when MW give unique processing conditions that are unachievable by conventional methods, as in several food processing and biochemistry applications (e.g. peptide and nanotube synthesis). In the specific case of a MW-heated RD column, the question to be addressed is whether the accelerated reaction rate and the enhanced molecular separation account for sufficient energy savings to compensate for the extra MW cost so that the overall process becomes more energy efficient. This question can only be definitively answered if a conventionally heated process is compared with a MW-heated process at a pilot scale.

8.2 The concept of microwave enhanced reactive distillation (MWeRD)

8.2.1 Design operation features applied to pilot scale RD production of ProPro

The new concept of a microwave-heated column for the synthesis of *n*-propyl propionate differs significantly from the conventional reactive distillation system described in Chapter 5 in the following important aspects:

1. One suitable way to integrate the RD and the MW hardware is to use a stack of mono-mode microwave ovens with a custom-designed circular waveguide that efficiently fits the DN-50 column. Using single-mode cavities will ensure field homogeneity and improved experimental reproducibility.
2. The number of MW ovens should be calculated based on the maximum column height that the custom-designed waveguide can irradiate, plus the safety length to prevent wave leakage outside the cavity. This means that there will be column parts that will not be radiated.
3. Because the column will use heat input along its height, diabatic conditions must be considered and accounted for in the energy balances.

4. The catalysis of reaction conditions will shift from heterogeneous to homogeneous. The ion-exchange resin inside the column and ultimately the Katapack-SP packing should be removed from the column and replaced by a new structured or random packing.
5. The catalyst will be dissolved in the propionic acid and fed to the column at an equivalent location to the conventional process. Both feeds will remain in locations featuring counter-current flow. Reaction should be considered in all column sections starting from the acid feed to the bottom of the column, including the liquid distributors and the reboiler.
6. The catalyst will sink to the bottom of the column and accumulate in the reboiler. The intended product ProPro will contain dissolved catalyst that will have to be removed downstream.
7. An alternative solution to the downstream separation of the homogenous catalyst could be to fix the Zn triflate on a support, but without losing the effect observed using the homogenous catalyst. In this way, the complexity arising from the homogenous catalyst manipulation described in points 4 to 6 can be avoided.
8. In the case of a MW-heated column section, the interaction of the electromagnetic radiation with the materials of the packings employed must be investigated. To avoid MW reflection and improve penetration, more suitable MW-transparent materials should be identified.

Figure 8.4 illustrates the new MWeRD process using mono-mode cavities.

8.2.1 MWeRD at large scale

In order to go to larger column diameters and make use of conventional distillation and reactive distillation equipment above DN-100, the best available option of microwave equipment in the market at the moment is Sairem's Internal Transmission Line (INTLI). A possible way to couple this technology with RD hardware is to insert a number of antennas to the column and connect them to a MW generator using a conventional waveguide. Since the use of packings may cause difficulties in radiating the largest possible interfacial area between vapor and liquid, a necessary condition to enhance molecular separation as explained in Chapter 6, a more suitable option could be the use of distillation trays. In that way, the liquid that holds-up over the trays can be efficiently radiated. In between trays, structured packing can be used as a way to increase separation and/or reaction efficiency and make use of all the column volume. The INTLI hardware features operating parameters like: maximum microwave power of 30kW and 915 MHz, control of the forward and reflected power and high attainable microwave power densities. Figure 8.5 illustrates the new MWeRD process using Sairem's Internal Transmission Line (INTLI).

Figure 8.4 Concept of the MWeRD column radiated using a stack of mono-mode cavities.

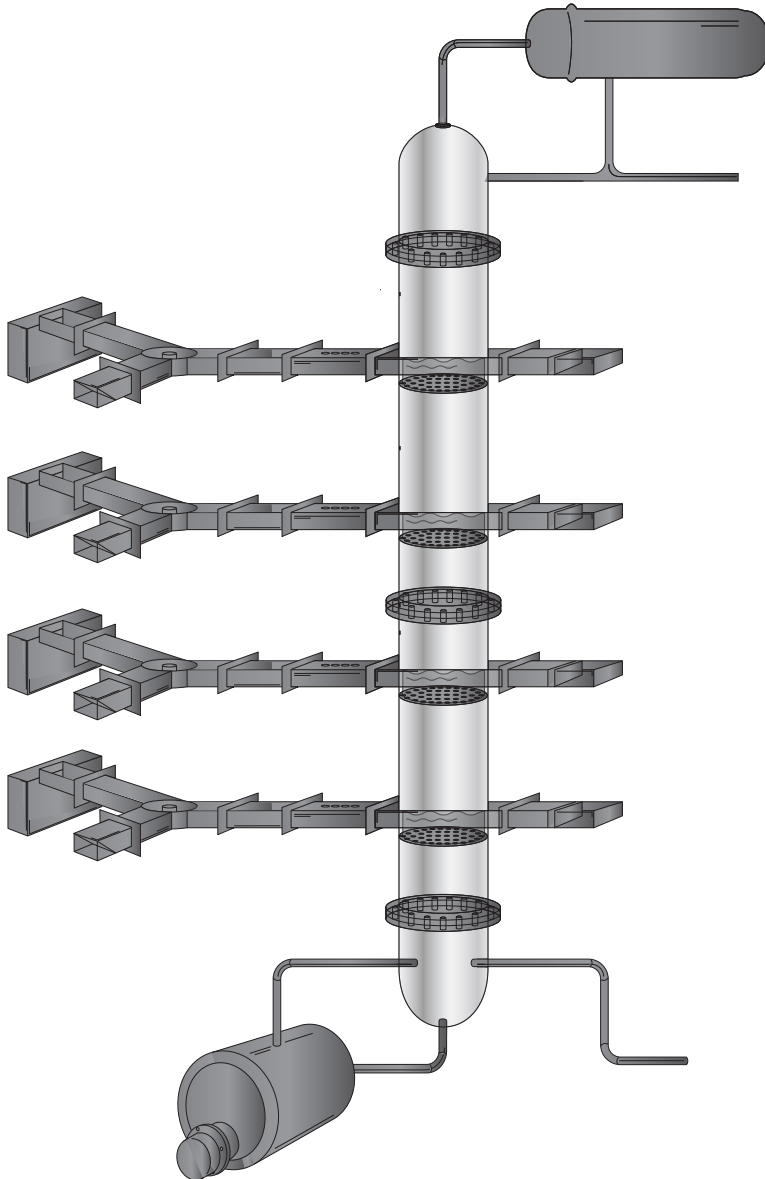
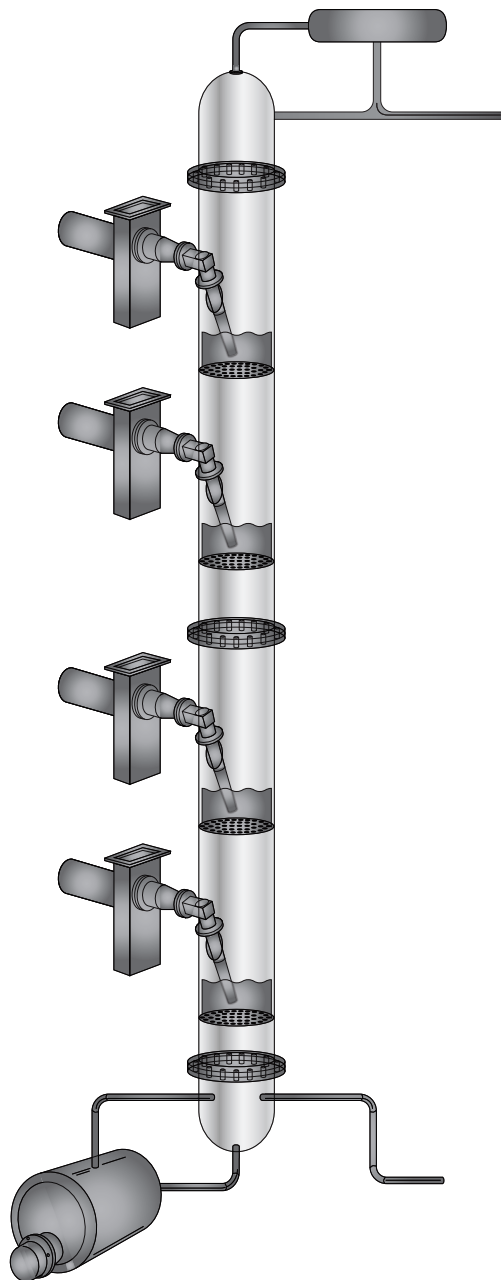


Figure 8.5 Concept of the MWeRD column radiated using Sairem's Internal Transmission Line (INTLI).



8.3 References

1. Forner F., Brehelin D., Repke J.-U., Startup of a reactive distillation process with a decanter. *Chemical Engineering and Processing*. **2008**. 47: 1976-1985.
2. Lee H.-Y., Yen L.-T., Chien I.-L., Reactive Distillation for Esterification of an Alcohol Mixture Containing n-Butanol and n-Amyl Alcohol. *Ind. Eng. Chem. Res.* **2009**. 48: 7186-7204.
3. Lai I.-K., Liu, Y.-Ch., Yu,, Ch-Ch., Huang, H.-P., Production of high-purity ethyl acetate using reactive distillation: Experimental and start-up procedure. *Chemical Engineering and Processing*. **2008**. 47: 1831-1843.
4. Backhaus A. A., Continuous process for the manufacture of esters. *US Patent 1,400,849*. **1921**.
5. Charpentier J. C., McKennab T. F., Managing complex systems: some trends for the future of chemical and process engineering. *Chemical Engineering Science*. **2004**. 59: 1617-1640.
6. Turner M.D.L., Microwave Radiation's Influence on Sorption and Competitive Sorption in Zeolites. *AIChE Journal*. **2000**. 46(4): 758-768.
7. Damm M.G., Kappe C. O., Translating High-Temperature Microwave Chemistry to Scalable Continuous Flow Processes. *Organic Process Research & Development*. **2010**. 14: 215-224.
8. Leonelli C.M., Microwave and ultrasonic processing: Now a realistic option for industry. *Chemical Engineering and Processing*. **2010**. 49: 885-900.
9. Strauss C.R., On Scale Up of Organic Reactions in Closed Vessel Microwave Systems. *Organic Process Research & Development*. **2009**. 13: 915-923.
10. Moseley J.D., Kappe C. O., A critical assessment of the greenness and energy efficiency of microwave-assisted organic synthesis. *Green Chemistry*. **2011**. 13: 794-806.
11. Razzaq T., Kappe C. O., On the Energy Efficiency of Microwave-Assisted Organic Reactions. *ChemSusChem*. **2008**. 1: 123-132.
12. Gronnow M.J., Clark J. H., Macquarrie D. J., Energy Efficiency in Chemical Reactions: A Comparative Study of Different Reaction Techniques. *Organic Process Research & Development*. **2005**. 9: 516-518.
13. *CEM corporation*. Available from: www.cem.com.
14. *Biotage*. Available from: www.biotage.com.
15. *Milestone Inc.*; Available from: www.milestonesci.com.
16. *Anton Paar*. Available from: www.anton-paar.com.
17. *Sairem*. Available from: www.sairem.com.
18. *Fricke und Mallah*. Available from: www.microwaveheating.net.
19. *Microwave TM*. Available from: www.radiofrequency.com.
20. *Industrial Microwave Systems, L.L.C.*; Available from: www.industrialmicrowave.com.
21. *C-Tech Innovation*. Available from: www.ctechinnovation.com.
22. *Püschner*. Available from: www.pueschner.com.
23. Conner W.C., Tompsett G. A., How Could and Do Microwaves Influence Chemistry at Interfaces? *J. Phys. Chem. B*. **2008**. 112: 2110-2118.
24. Perreux L.L., A tentative rationalization of microwave effects in organic synthesis according to the reaction medium, and mechanistic considerations *Tetrahedron*. **2001**. 57(45): 9199-9223
25. Nüchter M.M., Ondruschka B., Tied A., Microwave-Assisted Chemical Reactions. *Chem. Eng. Technol.* **2003**. 26: 1207-1216.
26. Metaxas A.C., Meredith R. J., *Industrial microwave heating*. **1993**, London: Peter Peregrinus.
27. Komorowska M., Stefanidis G. D., Van Gerven T., Stankiewicz A. I., Influence of microwave irradiation on a polyesterification reaction. *Chem. Eng. J.* **2009**. 155: 859-866.

9

Overview and Conclusions

“This is the end of what should rightfully be called the beginning”

Anonymous

Overview and conclusions:

In recent years the chemical industry has had to address the growing global concern regarding energy availability, climate change, materials sourcing, safety and sustainability. Companies are forced to re-engineer the way they operate at different levels, striving to develop processes that are substantially more efficient. One possible way to achieve these developments is to apply a fundamental approach that can deliver innovative, radically different and avant-garde technologies, often with demonstrated feasibility at the pilot and industrial scales. The latter approach has been categorized by modern chemical engineering as process intensification (PI). Perhaps one of the top examples of PI and one of the most relevant applications of the multifunctional reactor concept is reactive distillation (RD), also known as catalytic distillation where reaction, separation and enthalpy exchange take place in a single processing unit. Nonetheless, the widespread application of RD is hindered by a number of identified barriers that could be overcome if PI principles and approaches were used.

This thesis explores the use of microwave radiation ($f=2.45$ GHz) in the frame of PI as an alternative energy source to expand the operational feasibility window of an esterification reaction performed in a conventional RD process. In this context, a new integrated concept of a microwave enhanced reactive distillation (MWeRD) unit is proposed by separately researching (i) a conventional RD process, (ii) the effects of MW on a model homogenous and heterogeneous esterification reaction and (iii) the effects of MW on molecular separation for application in vapour-liquid contactors. The esterification reaction for the synthesis of *n*-propyl propionate (ProPro) was chosen to illustrate the proposed system. The ester can be obtained from the reaction of propionic acid (ProAc) with 1-propanol (ProOH) catalyzed under acidic conditions. The state-of-the-art industrial scale production of ProPro involves the use of a RD process as the system core, with two downstream units for reactant recovery and product purification.

In the first part, the introductory guidelines and basic thermo-physical data needed for the feasibility analysis and accurate process design of conventional RD processes as well as the relevant data needed for MW dielectric heating were presented. The dielectric properties ϵ' , ϵ'' and $\tan \delta$ of reagents, products and the reacting system were measured in the frequency range 200 MHz to 20 GHz and in the temperature range 20°C to 140°C. The importance of considering the dielectric parameters at reaction temperature was elucidated as well as the relevance of the dielectric loss (ϵ'') parameter as a measurement of the capacity of a substance to transform electromagnetic energy into heat, regardless of process efficiency. In the test system, alcohol—as the highest MW absorber—dictates the dielectric behaviour in the mixture. In the thermodynamic domain, the lack of pertinent literature made it necessary to recur to outdated experimental data published for several of the six constituent binary pairs that could build the quaternary mixture model. Accordingly, isobaric experimental vapour-liquid equilibrium (VLE) data were measured for the binary systems ProOH/ProAc, ProOH/ProPro, ProPro/ProAc, and water/ProPro as well as liquid-liquid equilibrium (LLE) data for the ternary system ProOH/water/ProPro. Binary parameters were then regressed for a UNIQUAC-HOC model. Based on these results, the model obtained was able to accurately fit VLE experimental data and therefore predict the phase behaviour of the mixture. The ProOH/water/ProPro system presented a large immiscibility gap that could be favourably used to separate an aqueous (water/ProOH) and an organic phase (ProPro/ProOH). To predict the phase split, experimental LLE data were regressed and binary parameters determined for a UNIQUAC model. Once a consistent thermodynamic model was available, a pseudo-homogenous model was then developed for the reaction kinetics based on activities. The parameters of both equilibrium and reaction constants were fitted using kinetic data obtained from the literature.

In the second part of this research, the set of parameters obtained from the thermodynamic and kinetic models was used to assess the feasibility of the process first using the residue curve mapping (RCM) technique and then performing pilot-scale RD experimentation. The RCM methodology and the mathematical expressions were described for two case scenarios: non-reactive and reactive. The non-reactive case (where only separation is considered) was assessed and system topology identified. Two stable nodes (ProAc and water), two unstable nodes (ProPro and the heterogeneous azeotrope from ProPro/water), and four saddles (ProOH, the homogeneous azeotrope from ProOH/water, the homogeneous azeotrope from ProAc/water and the heterogeneous ternary azeotrope) were categorized. A nonreactive distillation boundary plane,

formed by a triangle between the three binary azeotropes, was documented. The boundary divides the composition space into one region in which pure ProPro can be obtained and another in which pure water can be produced but, for practical purposes, is irrelevant. The reactive case was analyzed by addressing the changes to the phase behavior of the system as well as the changes in the topology diagram generated by the superposition of the reaction on separation. The results of the reactive RCMs revealed the formation of a reactive azeotrope and the disappearance of the three binary ones, along with the possibility of producing high purity ProPro using a single column depending on feed composition. For feeds with excess alcohol, the RCMs end in pure ProPro. The feasibility of producing a pure product was hindered by the difficulty of separating the azeotropic mixture distillate formed by non-reactive alcohol and water. An economic way of performing this separation was by using a decanter coupled to the RD column, thereby recovering part of the distillate stream. To prove the feasibility of this concept, experiments were conducted using a glass column (DN50) equipped with two types of structured packings: Sulzer BX for stripping and rectifying sections, and Katapak-SP 11 with the ion-exchange resin Amberlyst 46TM immobilized for the reactive part. A non-equilibrium stage model was applied. This model took into account reaction kinetics via the derived pseudo-homogeneous approach. A series of experiments were carried out to determine the accurate operating conditions that guaranteed the compositions for phase split in the distillate stream. Experimental data was compared with simulated results, showing that the model was highly capable of predicting process operation (composition profiles, temperature profiles and mass flows). A detailed analysis of experimental and simulated results showed that high product purities ($w_{ProPro, bottom} = 0.91$ (kg/kg)) and acid conversions ($\pm 94\%$) can be obtained by this process, along the entire range of operating conditions studied, and that part of the distillate stream can be recovered in an inexpensive way. This detailed investigation on the conventional process gave valuable insight about the process, which served as basis to develop the MW heated column concept.

Experimentation with MW heating outlined the third part of this thesis and the results presented herein set the base ground for the development of a MW-RD integrated experimental set-up. The aim of the conducted experiments was to investigate the possible effects that MW radiation had on the two fundamental processes carried out inside a reactive distillation column. Consequently it was decided to investigate separately the effects on molecular separation and then on the chemical reaction so that they could be clearly differentiated. One of the most interesting outcomes of this thesis was the

discovery that MW could improve molecular separation of mixtures while being irradiated. Our experiments have shown that molecular separation of certain binary mixtures can be enhanced only when microwaves interact directly with the vapour-liquid interface that is exposed. On the other hand, VLE experiments with MW-bulk liquid interaction (the interface was not exposed to MW) yielded compositions that did not differ from those in conventional VLE experiments. Regarding distillation, this may be translated, in practical terms, into the design of smaller columns with fewer trays for a given separation efficiency, compared with conventional designs involving heat exchange only in the reboiler and condenser. The mechanisms involved in this process are still unknown, and further research is required to gain additional insight into the interactions between MW and the vapour-liquid interface. Nonetheless, the reported observations are of key importance in the field of vapour-liquid separations. On the reaction front, the synthesis of ProPro was investigated using various homogeneous and heterogeneous catalysts that could possibly enhance the reaction rate under microwave heating conditions as compared with conventional heating methods. Catalysts were evaluated by running equimolar reactions with 2% w/w catalyst, loading for 30 minutes and then measuring the product yield as compared to the equilibrium concentration. The baseline for catalyst screening was the reaction using the ion exchange resin Amberlyst 46, one of the best performing catalysts used for the test system. Several catalysts, including zeolite CP814C, montmorillonite KSF, sulfonated Basolite MOF, $\text{SiO}_2\text{-Fe}_2\text{SO}_4$, SnCl_2 and Cu, Fe and Zn triflates, were found to yield more ester under both heating methods with no by-product formation. Only the homogenous reaction using Zn triflate as catalyst was enhanced with the use of MW heating, producing 40% more ester. Once again, the mechanisms facilitating the reaction were not completely elucidated. FT-IR spectra revealed that there were no changes in the chemistry of the components and that the hydrolysis of Zn triflate into triflic acid, which could have enhanced the reaction, did not occur.

By taking into consideration all the experimental work from this research, the concept of a fully integrated MWeRD column for the synthesis of ProPro was accordingly developed. Key aspects for technology integration, such as cavity design, scale-up and energy efficiency of magnetrons, were introduced and extensively discussed. The differences between the new and the conventional process were also clearly described. MWeRD has the potential to be much more efficient, not only because of the proven independent effects of MW on molecular separation and chemical reaction, but also because it takes advantage of the synergistic effects generated inside the column.

In conclusion, the main research questions put forth in Chapter 1 of this thesis were addressed and answered. MW can potentially enlarge the operational feasibility window of a RD process by enhancing the molecular separation of components in a mixture, accelerating the chemical reaction and by using equipment materials that can interact with the electromagnetic field (e.g. structured packings made of silicon carbide thus heating surfaces to temperatures higher than the surrounding liquid). The limited overlap between the reaction and the separation windows can then be magnified so that the required match in process conditions occur. As clearly evidenced by the work conducted, to establish whether a given system can benefit from MW heating, extensive experimentation have to be performed determining if enhanced molecular separation and increased reaction yields take place prior to conducting experiments in the integrated MWeRD system.

Recommendations for further research:

Although many of the experimental results presented herein along with the MWeRD concept are important for the academia and the process industry, there are still several ideas that could broaden the knowledge in the field and should be considered in future research.

- (i) The fundamental mechanisms of how MW work at the molecular level is still an open question for scientists. Future research could take two different approaches. The first would be to use in-situ analysis techniques like Raman spectroscopy or FT-IR, tools that have already been applied by other research groups with relative success and have been found to allow on-line monitoring of ongoing chemical processes. The second approach would be to use modeling tools to understand MW chemistry at the molecular level, which differs considerably from standard chemical engineering and relates more to the fields of molecular dynamics and quantum chemistry. Nonetheless, simulations of ensembles under conditions of MW heating could improve the understanding of mechanisms that occur other than those that just report the effects, which is what has been traditionally done so far.
- (ii) Building a MW irradiated RD column set-up could confirm the partial effects demonstrated in this thesis and be used to give a definitive answer regarding the energy efficiency of the proposed concept. The design of such an apparatus is economically viable if a conventional pilot-scale column is already in place and operating like the one used for experimentation during this research.

(iii) The MWeRD concept could be applied to different reactions currently of great economic interest. Reactions following green chemistry principles, such as ethyl lactate, succinate esters, malate esters, acetals from glycerol or second-generation biodiesel production, are worth exploring using this novel technology.

Curriculum Vitae
Publications and Oral Presentations
Acknowledgements



Ernesto Altman was born in Santiago de Cali, Colombia on February 9th 1977. He followed Chemical Engineering studies at the Universidad del Valle in Colombia obtaining his bachelor degree in 2000. During his studies he spent one semester at Kansas State University in the USA. From 2000 to 2002 he worked for Johnson & Johnson consumer company as a process engineer in Santiago de Cali. In the fall 2002 Ernesto joined Wageningen University in The Netherlands to pursue studies in Food Science with specialization in Process Design. He obtained his Master of Science degree in 2004 after completing his thesis on a novel process to produce meat analogues from vegetable proteins. After that he returned to Colombia where he married his wife Natalia and joined his family's chemical business B. Altman S.A.S. as Operations Manager. During this time he gained experience in the production of food and pharmaceutical grade chemical specialties including minerals, natural extracts and natural flavorings. In 2007 he decided to become a researcher and university lecturer and was appointed as PhD student in the Intensified Reaction and Separation Systems group under the supervision of Prof. Andrzej Stankiewicz at the Process & Energy Laboratory in Delft University of Technology. In 2008 Ernesto spent 5 months as a visiting scholar at the laboratory of Fluid Separations, Department of Biochemical and Chemical Engineering in the Technical University of Dortmund in Germany under the supervision of Prof. Andrzej Górak where he gained hands-on experience working in reactive distillation. The results of his research have been presented in internationally renowned conferences and published in peer reviewed scientific journals. Upon completion of his Ph.D thesis he will return to Colombia to work in his company and join his old university as a part time lecturer and researcher focusing on the application of process intensification approaches to food processes and the production of multifunctional ingredients. Ernesto is a keen athlete practicing Under Water Rugby for more that 20 years and has participated in competitions with different teams around the world. His hobbies include scuba diving, squash and photography. In 2009 he became the father of Alejandro and next year the family expects the second baby boy Nicolas.

Publications

1. Altman E., Kreis P., van Gerven T., Stefanidis G.D., Stankiewicz A., Górak A., Pilot plant synthesis of *n*-propyl propionate via reactive distillation with decanter separator for reactant recovery. Experimental model validation and simulation studies. *Chem. Eng. Process.*, **2010**. 49: 965-972.
2. Altman E., van Gerven T., Stefanidis G.D., Stankiewicz A., Process intensification of reactive distillation in the synthesis of *n*-propyl propionate: the effects of microwave radiation on molecular separation and esterification reaction. *Ind. Eng. Chem. Res.*, **2010**. 49: 10287-10296.
3. Altman E., van Gerven T., Stefanidis G.D., Stankiewicz A., Phase equilibria for reactive distillation of propyl propionate. Pure component property data, vapor-liquid equilibria and liquid-liquid equilibria. *J. Chem. Eng. Data*, **2011**. 56: 2322-2328.
4. Altman E., van Gerven T., Stefanidis G.D., Stankiewicz A., Microwave-promoted synthesis of *n*-propyl propionate using homogeneous zinc triflate catalyst. *Ind. Eng. Chem. Res.*, **2011**. Nigam Issue.

Oral Presentations

1. Synthesis of *n*-propyl propionate via reactive distillation. Netherlands Process Technology Symposium 2008 (NPS8), Veldhoven, The Netherlands, October **2008**.
2. Pilot plant synthesis of *n*-propyl propionate via reactive distillation with decanter separator for reactant recovery. International Green Process Engineering Congress and European Process Intensification Conference (GPE-EPIC), Venice, Italy, June **2009**.
3. Conceptual design of reactive distillation processes heated with microwaves. 8th World Congress of Chemical Engineering (WCCE8), Montreal, Canada, August **2009**.
4. Process intensification of reactive distillation: Effects of microwaves in the synthesis of *n*-propyl propionate. CAPE Forum, Aachen, Germany, March **2010**.
5. Process Intensification of Reactive Distillation for the Synthesis of *n*-Propyl propionate: The Effects of Microwave Radiation on Molecular Separation and Esterification Reaction. 21st International Symposium on Chemical Reaction Engineering (ISCRE 21), Philadelphia, USA, June **2010**.
6. Microwaves as intensification tool for the production of esters in reactive distillation processes. Netherlands Process Technology Symposium 2010 (NPS10), Veldhoven, The Netherlands, October **2010**.

Aknowledgements

I think every Ph.D. student that has come to the point of writing this part of the thesis feels a great joy. Not only because it is the end of almost five years of hard work but also because it is the time to turn back and remember all those moments and people that made these years worth living and especially made this work possible. I would like to begin saying thank you to my promotror Prof. Andrzej Stankiewicz. The unique opportunity that you have given me by taking part in this innovative project has shaped my academic career and personal life in ways you cannot imagine. I hope that your ideas and opinions with process intensification resonate with greater echo in academia and industry and spread faster around the world. At least in Colombia you can be sure they will. The same words follow to Dr. Georgios Stefanidis my copromotor and direct supervisor for almost 3 years. I must say that I learned a lot from you in so many different ways. The conclusions from our discussions on Ph.D. life, science, microwaves and chemical engineering will stay with me for a long time. Thanks for the big push, today I can tell it paid back. Dr. Tom van Gerven gave the kick-off in this project and supervised me during the first year. You were always there to help, support and guide me during the complete project. I appreciated very much all your comments and corrections when needed. Thank you very much. You were my mentors during this journey and hope to see you along the way in the years to come.

Special thanks go to all the people at the P&E department starting with all the administration assistance that I needed numerous times, Leslie, Helma and Ilona thank you. I have to express a great appreciation to my colleague Michel van Brink. You were always there to help me in the analytical lab with all the problems we experienced. Thank you for all the help. Teus, you gave me a big hand with Aspen. Professor Theo de Loos must be mentioned as well. Without your permission to work in the thermo lab a great part of this thesis would have not been possible and thanks for the wonderful opportunity you gave me in taking part in the European course in supercritical fluids and green solvents. Last but not least, thanks to all the guys in the workshop (Thanks Jan) who always helped me to fix something in the set-up.

A full paragraph has to be dedicated to the laboratory of fluid separations at the Technical University of Dortmund in Germany under the direction of Prof. Andrzej Górak. I feel very fortunate to have the chance to work in what is perhaps, the best laboratory scale reactive distillation column in the world operating at a university. Prof., you received me as one of your own students

and always had an open door to my questions and requests. I recall the time that I spent in your lab as one of the most challenging and fruitful of my Ph.D. studies. I hope that the day when somebody can couple your DN-50 column with a microwave is not so far. Sincere and special words go for many people in Dortmund starting with Dr. Peter Kreis; thanks for all the time dedicated to me, my experiments and the patience to teach me ACM, Dr. Carsten Buchaly; Dr. Peter van Beijeren; Poland was great man but be aware of Russians, Tobias Keller; at least we tried, and of course can't forget the long days in the lab shared with Katrin and Siggy. Martín, para ti también va un saludo especial en México y un abrazo muy grande de agradecimiento.

A chapter apart should have been written for my colleagues at P&E. Tomek and Magda, we walked a long way together in these years. I wish you all the best as a couple and hope that very soon I can read both your theses. To my office mates, Aylin; don't cry you will find your prince charming, Xiaohua; I think you still have my thermo book, Guido; I should have worked using your schedule, Stephanie; good choice Delft is prettier than Aachen. Thanks for everything guys, the room looks odd without all of you. I remember a time when it was easier to learn Italian than Dutch at P&E, I should have given that a try. Gianluca, Mattia, Jacopo, Martina and all the Italians that came on and off, you are all right; pizza, pasta and espresso should only be sold in Italy. The Nespresso machine improved things a bit though. Ryan, Marcin, Bart and John good luck with your projects and careers wherever they take you. Kamarza, Somayeh and Alondra; we had a great time in Istanbul. Christian and Khalik maybe we have the chance to play squash again, be aware I will be training. And to all the ones that were once there: Jelán, Richard, Marta, Widya, I think we had a great time and to the ones that follow hang-on and good luck. Marloes, Henk and Guido many thanks with the Dutch translation. Emile, Eleonora, Gianluca, Diana, Winand, Marjolein, Bram, Cerial, Claudia, friendship took a wonderful meaning after meeting you guys. We really miss you in Colombia. Alvarito, vos también mereces un agradecimiento enorme, Calamaro y birras nunca harán falta.

Finalmente, gracias Nati por estar siempre ahí, incondicional para apoyarme en todo.

Ernesto
Delft, November 2011